Density Model for Beaked Whales (*Mesoplodon spp. and Ziphius cavirostris*) for the U.S. East Coast: Supplementary Report

Duke University Marine Geospatial Ecology Lab*

Model Version 4.4 - 2016-03-09

Citation

When referencing our methodology or results generally, please cite our open-access article:

Roberts JJ, Best BD, Mannocci L, Fujioka E, Halpin PN, Palka DL, Garrison LP, Mullin KD, Cole TVN, Khan CB, McLellan WM, Pabst DA, Lockhart GG (2016) Habitat-based cetacean density models for the U.S. Atlantic and Gulf of Mexico. Scientific Reports 6: 22615. doi: 10.1038/srep22615

To reference this specific model or Supplementary Report, please cite:

Roberts JJ, Best BD, Mannocci L, Fujioka E, Halpin PN, Palka DL, Garrison LP, Mullin KD, Cole TVN, Khan CB, McLellan WM, Pabst DA, Lockhart GG (2016) Density Model for Beaked Whales (*Mesoplodon spp. and Ziphius cavirostris*) for the U.S. East Coast Version 4.4, 2016-03-09, and Supplementary Report. Marine Geospatial Ecology Lab, Duke University, Durham, North Carolina.

Copyright and License

Revision History

Version	Date	Description of changes
1	2014-10-20	Initial version.
2	2014-11-21	Reconfigured detection hierarchy and adjusted NARWSS detection functions based on additional information from Tim Cole. Updated documentation.
3	2015-01-17	Removed CumVGPM180 predictor and refitted models. This was supposed to be version 2 but I left it in by mistake.
4	2015-01-18	Switched from DistToCanyon predictor to DistToCanyonOrSeamount and refitted models, to reduce edge effects with AFTT model.
4.1	2015-03-06	Updated the documentation. No changes to the model.
4.2	2015-05-14	Updated calculation of CVs. Switched density rasters to logarithmic breaks. No changes to the model.
4.3	2015-09-08	Updated the documentation. No changes to the model.
4.4	2016-03-09	Changed document title to clarify that Ziphius cavirostris is included in this model. No changes to the model or other parts of the documentation.

*For questions, or to offer feedback about this model or report, please contact Jason Roberts (jason.roberts@duke.edu)

Survey Data

Survey	Period	Length (1000 km)	Hours	Sightings
NEFSC Aerial Surveys	1995-2008	70	412	16
NEFSC NARWSS Harbor Porpoise Survey	1999-1999	6	36	0
NEFSC North Atlantic Right Whale Sighting Survey	1999-2013	432	2330	7
NEFSC Shipboard Surveys	1995-2004	16	1143	128
NJDEP Aerial Surveys	2008-2009	11	60	0
NJDEP Shipboard Surveys	2008-2009	14	836	0
SEFSC Atlantic Shipboard Surveys	1992-2005	28	1731	32
SEFSC Mid Atlantic Tursiops Aerial Surveys	1995-2005	35	196	0
SEFSC Southeast Cetacean Aerial Surveys	1992-1995	8	42	1
UNCW Cape Hatteras Navy Surveys	2011-2013	19	125	38
UNCW Early Marine Mammal Surveys	2002-2002	18	98	0
UNCW Jacksonville Navy Surveys	2009-2013	66	402	0
UNCW Onslow Navy Surveys	2007-2011	49	282	2
UNCW Right Whale Surveys	2005-2008	114	586	2
Virginia Aquarium Aerial Surveys	2012-2014	9	53	0
Total		895	8332	226

Table 2: Survey effort and sightings used in this model. Effort is tallied as the cumulative length of on-effort transects and hours the survey team was on effort. Sightings are the number of on-effort encounters of the modeled species for which a perpendicular sighting distance (PSD) was available. Off effort sightings and those without PSDs were omitted from the analysis.

Season	Months	Length (1000 km)	Hours	Sightings
All_Year	All	897	8332	226

Table 3: Survey effort and on-effort sightings having perpendicular sighting distances.

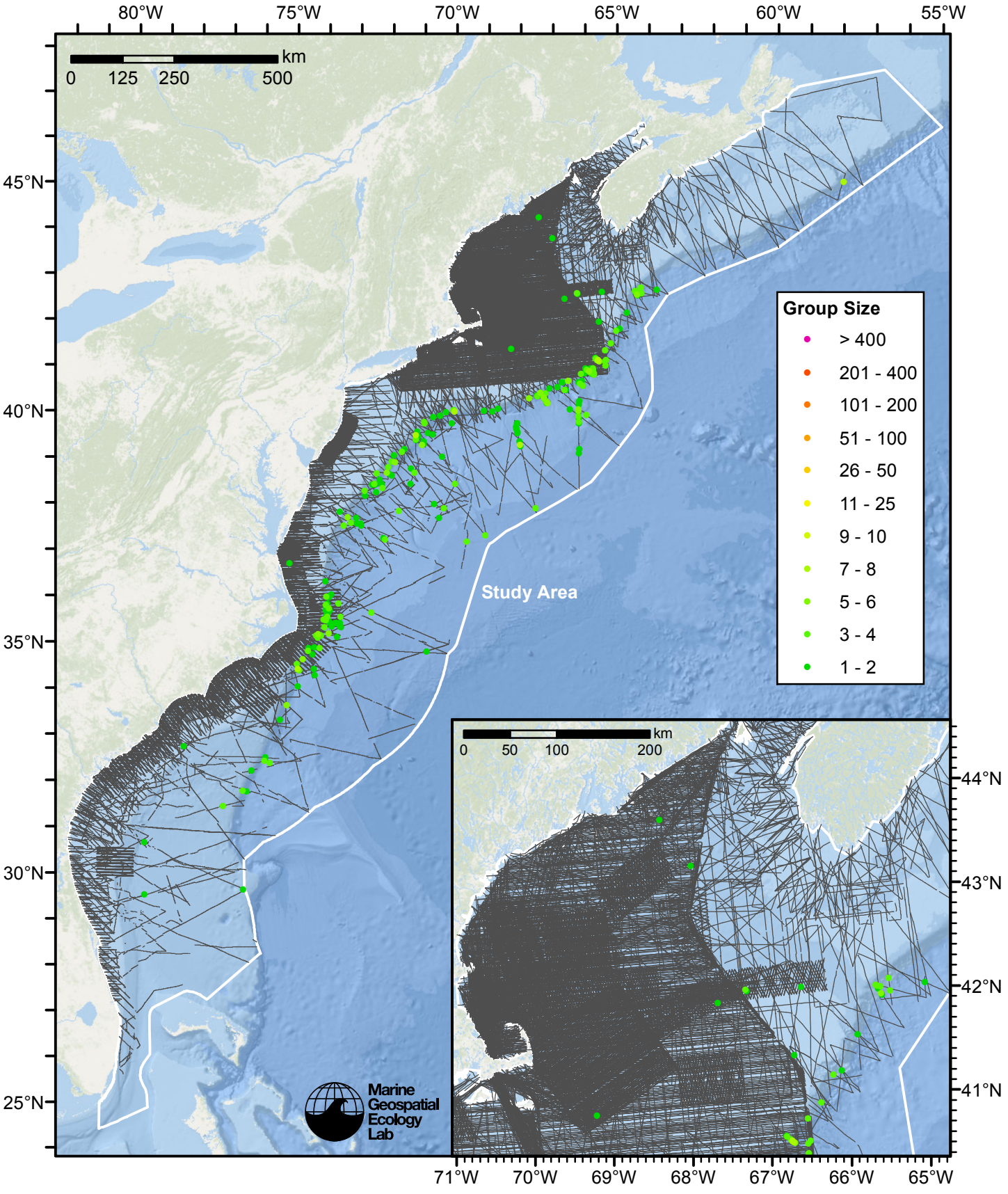

Figure 1: Beaked whales sightings and survey tracklines.

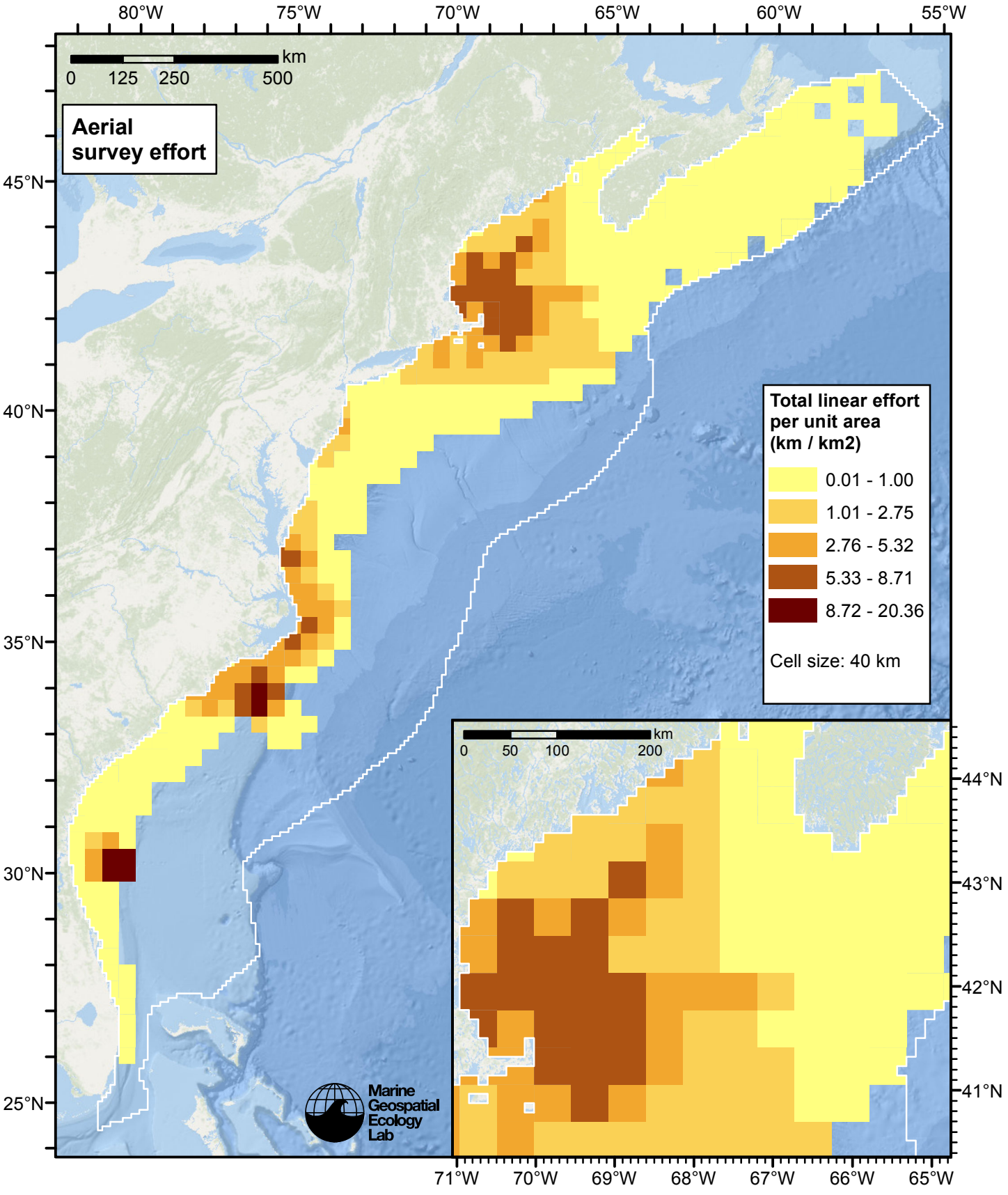

Figure 2: Aerial linear survey effort per unit area.

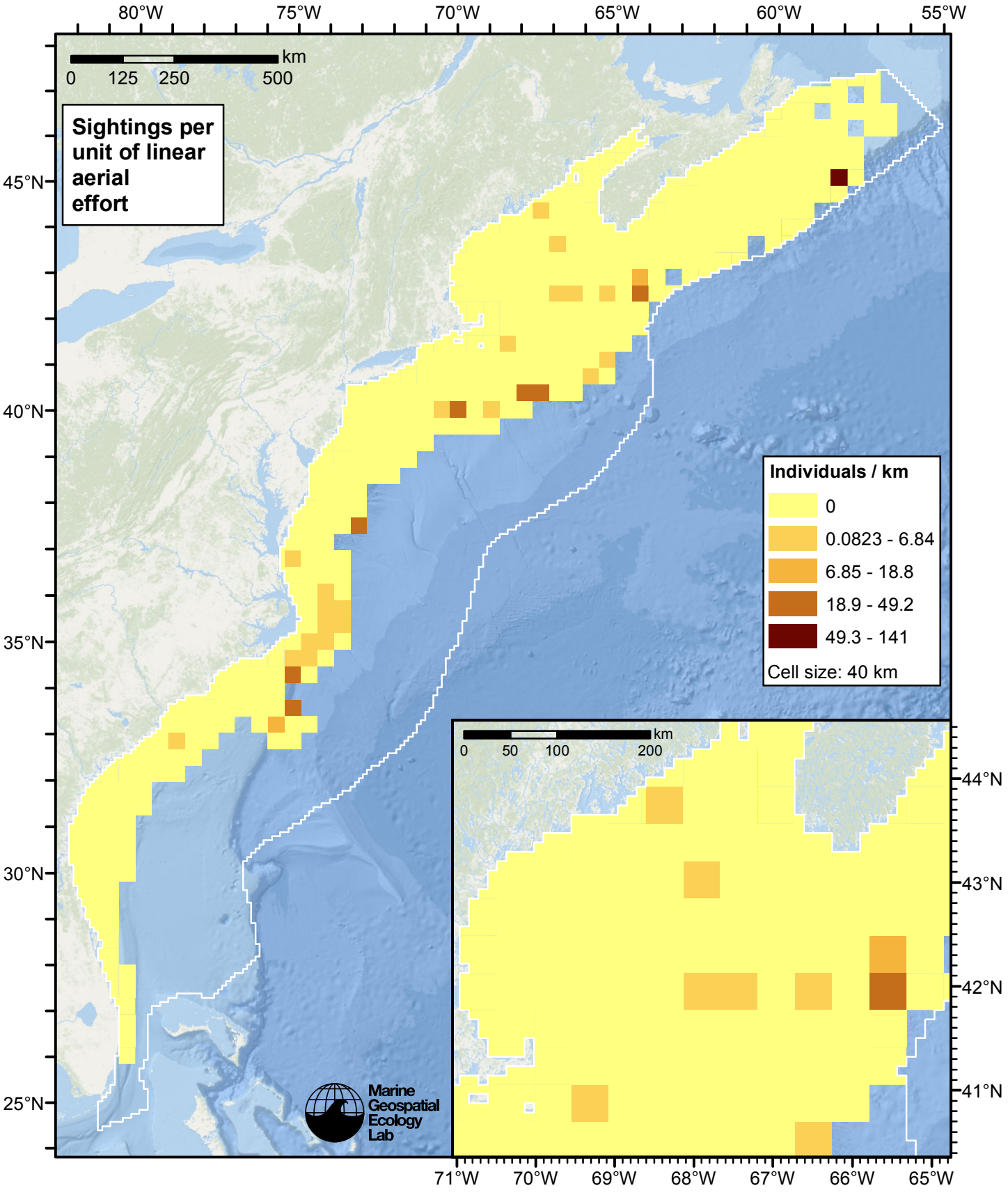

Figure 3: Beaked whales sightings per unit aerial linear survey effort.

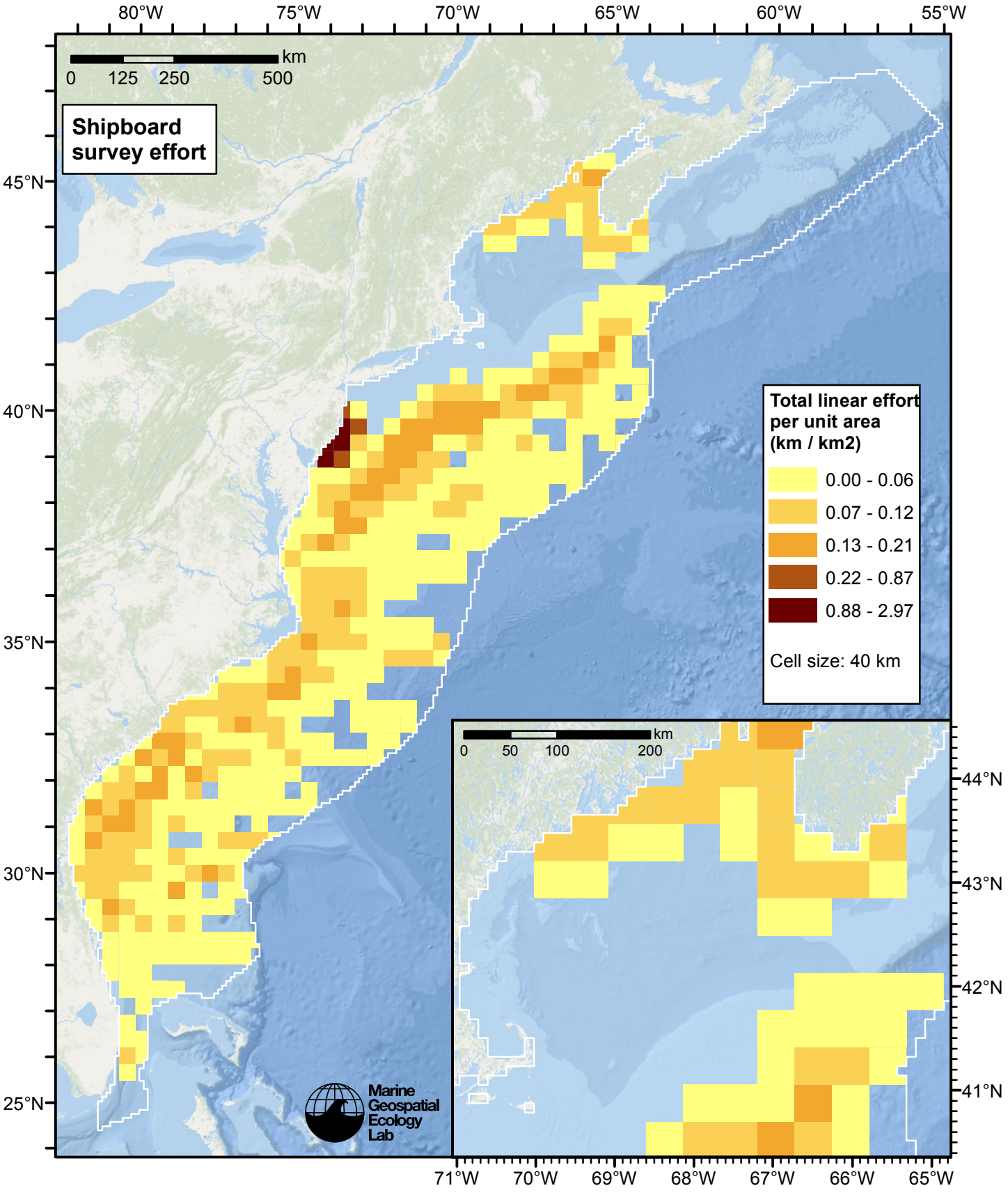

Figure 4: Shipboard linear survey effort per unit area.

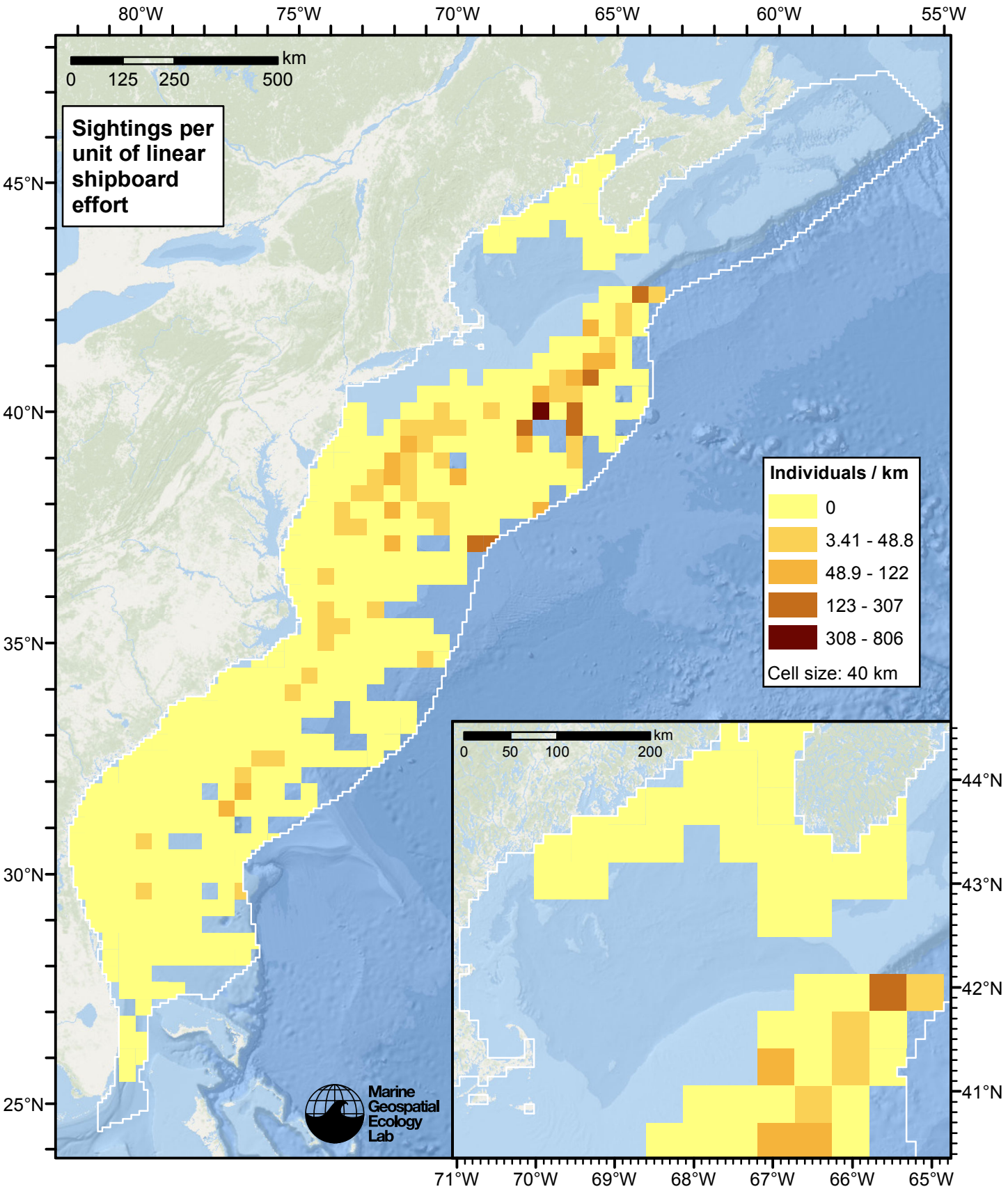

Figure 5: Beaked whales sightings per unit shipboard linear survey effort.

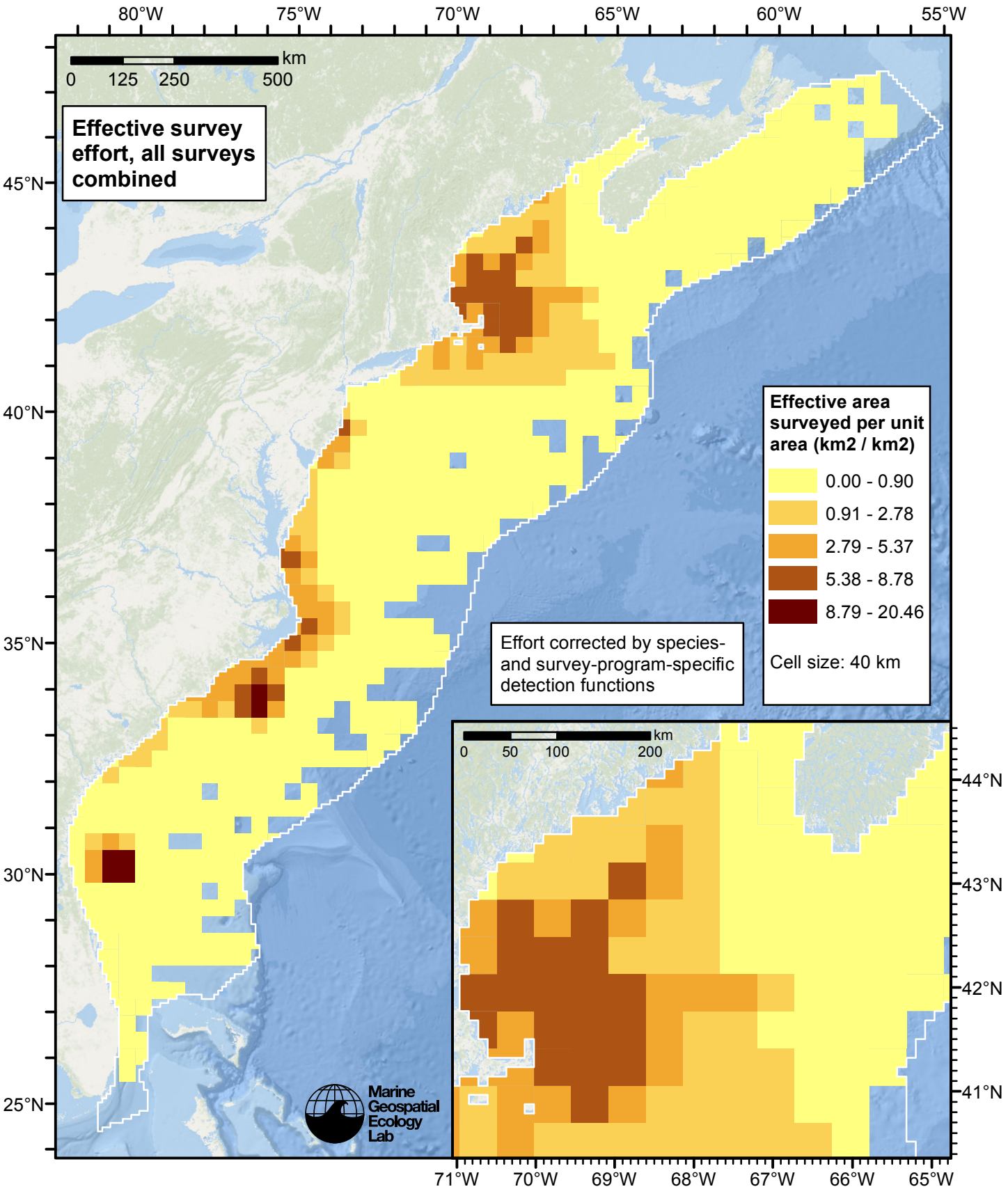

Figure 6: Effective survey effort per unit area, for all surveys combined. Here, effort is corrected by the species- and survey-program-specific detection functions used in fitting the density models.

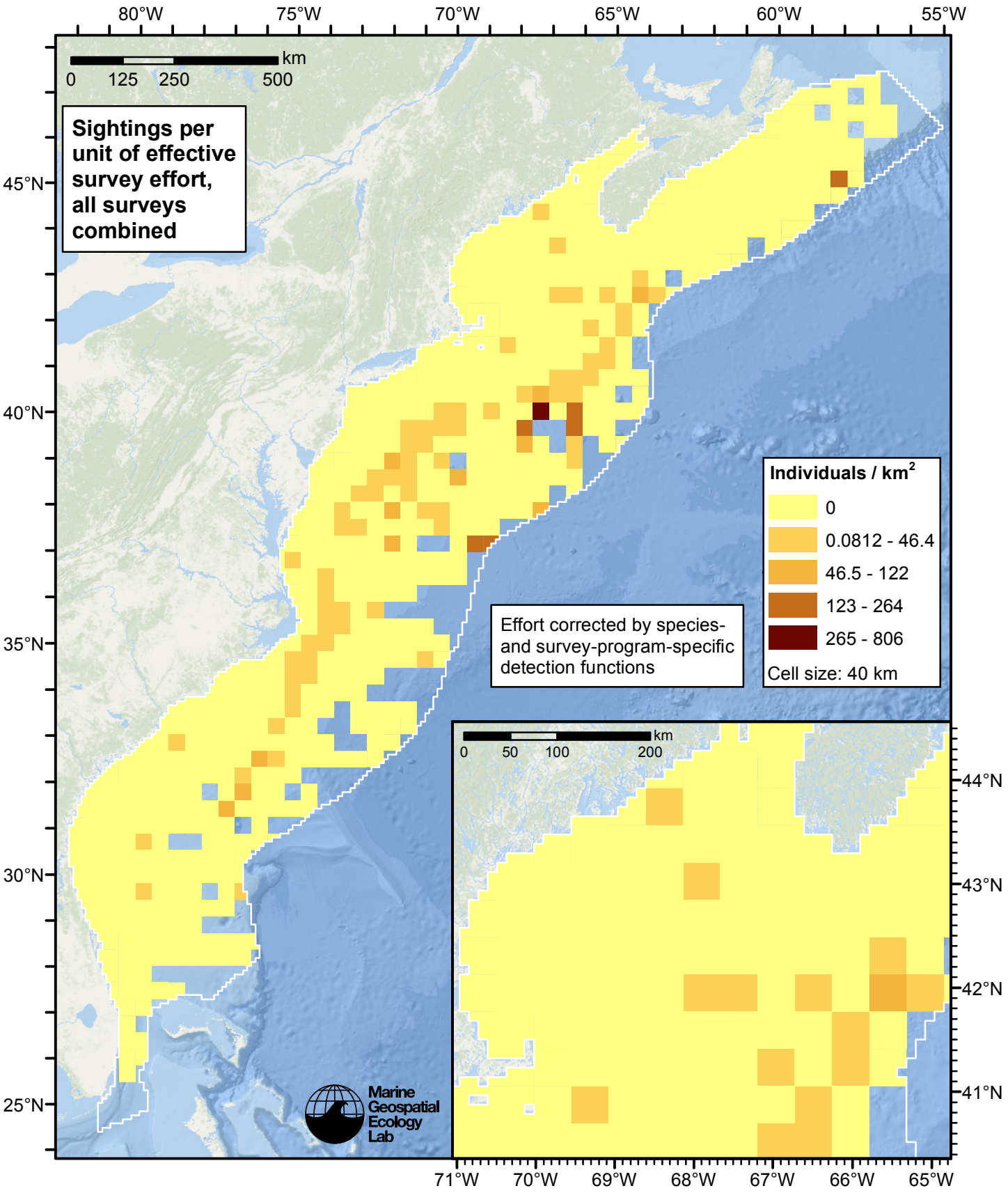

Figure 7: Beaked whales sightings per unit of effective survey effort, for all surveys combined. Here, effort is corrected by the species- and survey-program-specific detection functions used in fitting the density models.

Detection Functions

The detection hierarchy figures below show how sightings from multiple surveys were pooled to try to achieve Buckland et. al's (2001) recommendation that at least 60-80 sightings be used to fit a detection function. Leaf nodes, on the right, usually represent individual surveys, while the hierarchy to the left shows how they have been grouped according to how similar we believed the surveys were to each other in their detection performance.

At each node, the red or green number indicates the total number of sightings below that node in the hierarchy, and is colored green if 70 or more sightings were available, and red otherwise. If a grouping node has zero sightings–i.e. all of the surveys within it had zero sightings–it may be collapsed and shown as a leaf to save space.

Each histogram in the figure indicates a node where a detection function was fitted. The actual detection functions do not appear in this figure; they are presented in subsequent sections. The histogram shows the frequency of sightings by perpendicular sighting distance for all surveys contained by that node. Each survey (leaf node) recieves the detection function that is closest to it up the hierarchy. Thus, for common species, sufficient sightings may be available to fit detection functions deep in the hierarchy, with each function applying to only a few surveys, thereby allowing variability in detection performance between surveys to be addressed relatively finely. For rare species, so few sightings may be available that we have to pool many surveys together to try to meet Buckland's recommendation, and fit only a few coarse detection functions high in the hierarchy.

A blue Proxy Species tag indicates that so few sightings were available that, rather than ascend higher in the hierarchy to a point that we would pool grossly-incompatible surveys together, (e.g. shipboard surveys that used big-eye binoculars with those that used only naked eyes) we pooled sightings of similar species together instead. The list of species pooled is given in following sections.

Shipboard Surveys

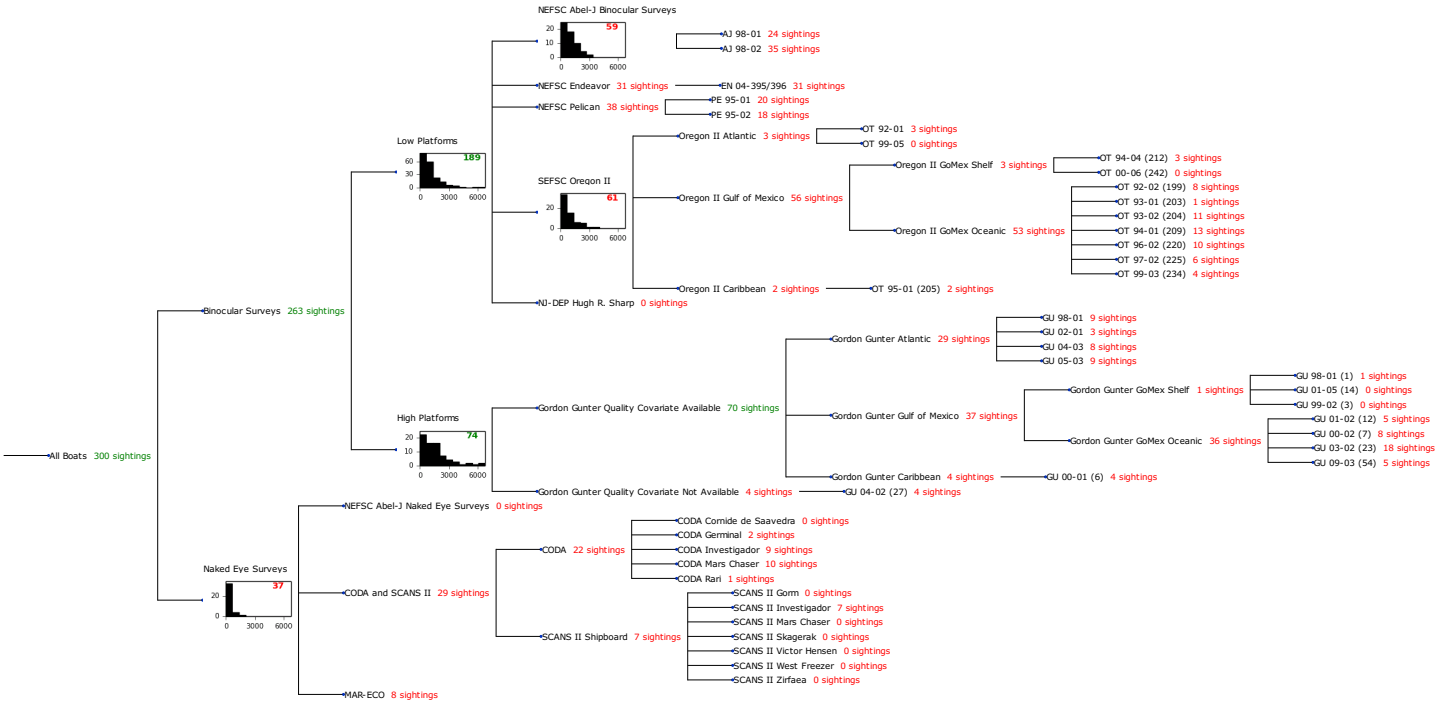

Figure 8: Detection hierarchy for shipboard surveys

Low Platforms

The sightings were right truncated at 4000m.

Covariate	Description

beaufort	Beaufort sea state.
size	Estimated size (number of individuals) of the sighted group.

Table 4: Covariates tested in candidate "multi-covariate distance sampling" (MCDS) detection functions.

Key	Adjustment	Order	Covariates	Succeeded	Δ AIC	Mean ESHW (m)
hr			beaufort	Yes	0.00	1587
hr			beaufort, size	Yes	1.19	1597
hn			beaufort	Yes	5.57	1604
hn			beaufort, size	Yes	5.88	1610
hr			size	Yes	9.64	1547
hn	cos	2		Yes	9.99	1348
hr				Yes	10.33	1503
hr	poly	4		Yes	12.30	1497
hr	poly	2		Yes	12.31	1492
hn	cos	3		Yes	14.69	1349
hn				Yes	16.57	1616
hn			size	Yes	16.57	1617
hn	herm	4		Yes	18.29	1613

Table 5: Candidate detection functions for Low Platforms. The first one listed was selected for the density model.

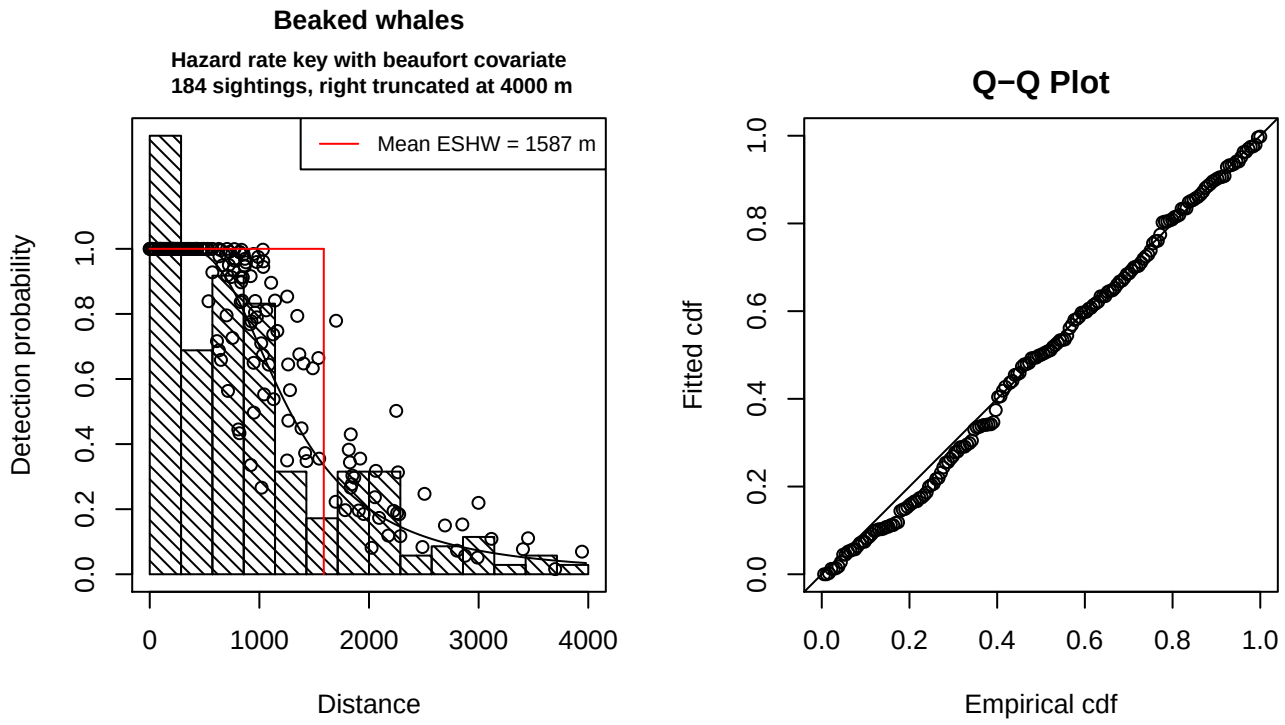

Figure 9: Detection function for Low Platforms that was selected for the density model

Statistical output for this detection function:

```
Summary for ds object
Number of observations :  184
Distance range         :  0  -  4000
AIC                    :  2884.38

Detection function:
 Hazard-rate key function

Detection function parameters
Scale Coefficients:
             estimate         se
(Intercept)  7.587412 0.19712999
beaufort    -0.216970 0.06683021

Shape parameters:
            estimate        se
(Intercept) 1.015423 0.1506178

                       Estimate          SE         CV
Average p             0.3768315  0.02955767 0.07843737
N in covered region 488.2819513 47.96111310 0.09822422
```

Additional diagnostic plots:

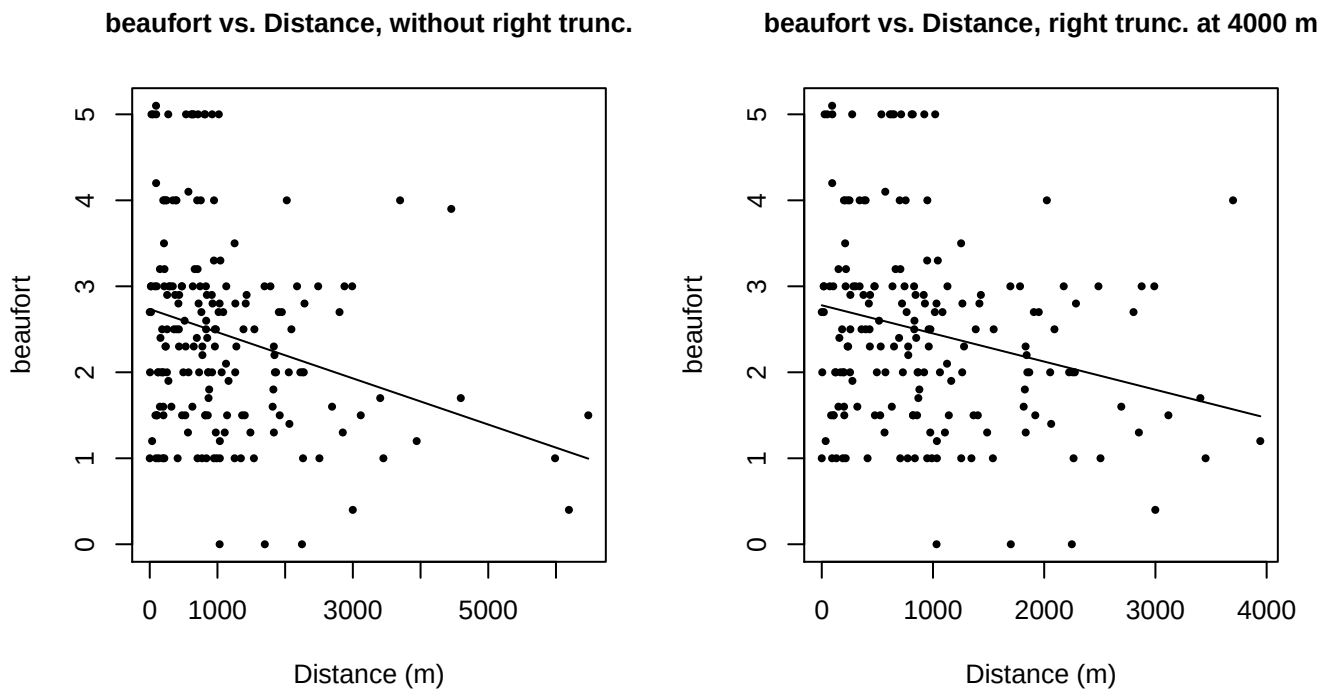

Figure 10: Scatterplots showing the relationship between Beaufort sea state and perpendicular sighting distance, for all sightings (left) and only those not right truncated (right). The line is a simple linear regression.

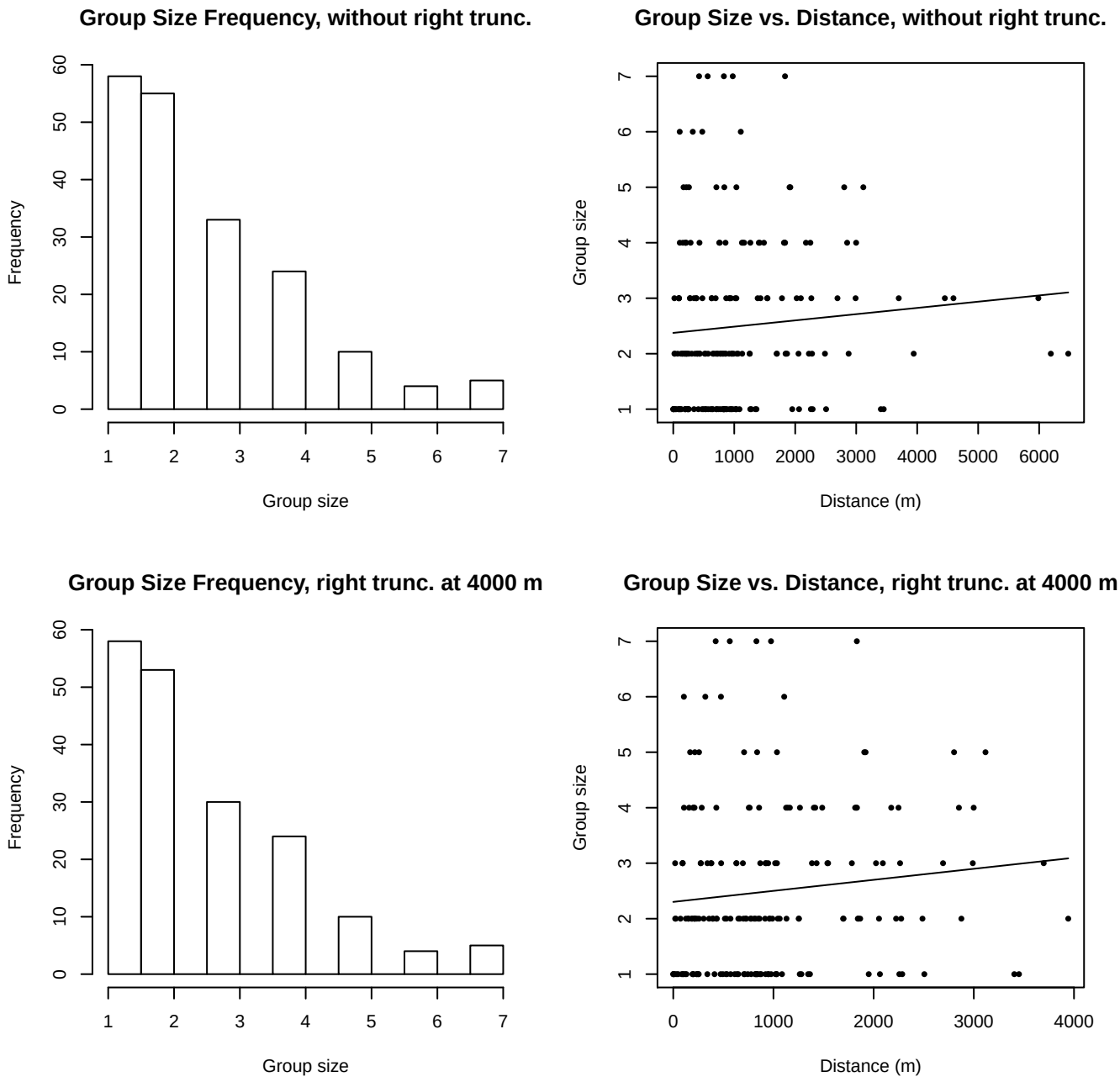

Figure 11: Histograms showing group size frequency and scatterplots showing the relationship between group size and perpendicular sighting distance, for all sightings (top row) and only those not right truncated (bottom row). In the scatterplot, the line is a simple linear regression.

NEFSC Abel-J Binocular Surveys

The sightings were right truncated at 3000m.

Covariate	Description
beaufort	Beaufort sea state.
quality	Survey-specific index of the quality of observation conditions, utilizing relevant factors other than Beaufort sea state (see methods).
size	Estimated size (number of individuals) of the sighted group.

Table 6: Covariates tested in candidate "multi-covariate distance sampling" (MCDS) detection functions.

Key	Adjustment	Order	Covariates	Succeeded	Δ AIC	Mean ESHW (m)
hn				Yes	0.00	1593
hr				Yes	1.40	1620
hr			beaufort	Yes	1.43	1533
hn			beaufort	Yes	1.50	1601
hn	cos	2		Yes	1.77	1480
hn	herm	4		Yes	1.93	1587
hn	cos	3		Yes	1.99	1625
hr			quality	Yes	3.31	1622
hr			size	Yes	3.36	1627
hr	poly	4		Yes	3.40	1620
hr	poly	2		Yes	3.40	1620
hr			quality, size	Yes	5.27	1628
hn			quality	No		
hn			size	No		
hr			beaufort, quality	No		
hn			beaufort, quality	No		
hr			beaufort, size	No		
hn			beaufort, size	No		
hn			quality, size	No		
hr			beaufort, quality, size	No		
hn			beaufort, quality, size	No		

Table 7: Candidate detection functions for NEFSC Abel-J Binocular Surveys. The first one listed was selected for the density model.

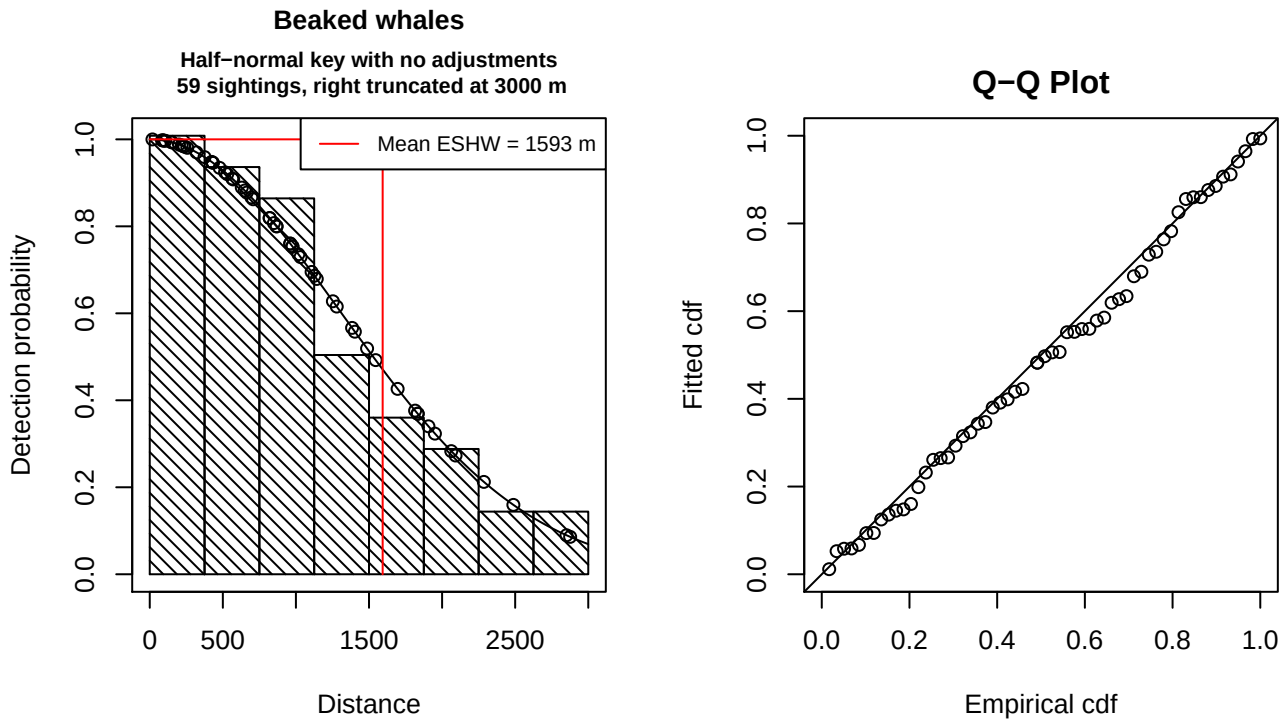

Figure 12: Detection function for NEFSC Abel-J Binocular Surveys that was selected for the density model

Statistical output for this detection function:

```
Summary for ds object
Number of observations :  59
Distance range         :  0  -  3000
AIC                    :  923.3904

Detection function:
 Half-normal key function

Detection function parameters
Scale Coefficients:
            estimate        se
(Intercept) 7.168947 0.1142126

                       Estimate          SE         CV
Average p             0.5311446  0.05276048 0.09933355
N in covered region 111.0808717 14.82580443 0.13346856
```

Additional diagnostic plots:

Figure 13: Scatterplots showing the relationship between Beaufort sea state and perpendicular sighting distance, for all sightings (left) and only those not right truncated (right). The line is a simple linear regression.

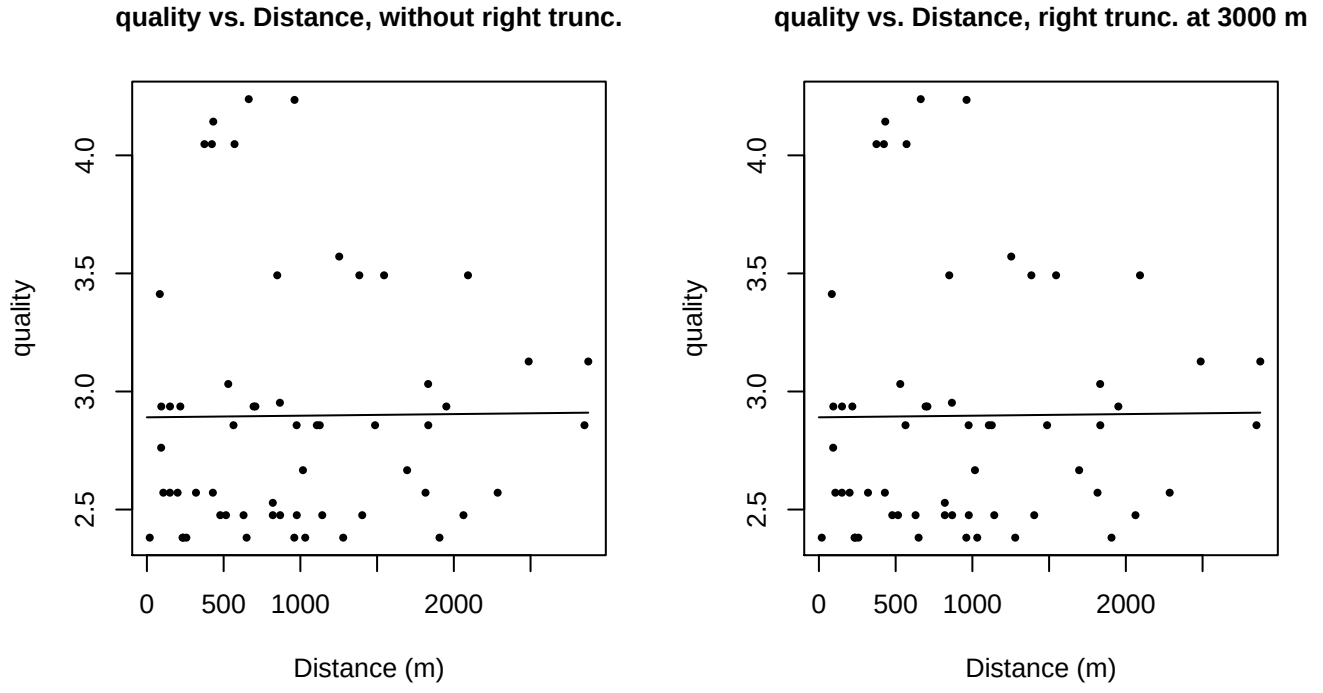

Figure 14: Scatterplots showing the relationship between the survey-specific index of the quality of observation conditions and perpendicular sighting distance, for all sightings (left) and only those not right truncated (right). Low values of the quality index correspond to better observation conditions. The line is a simple linear regression.

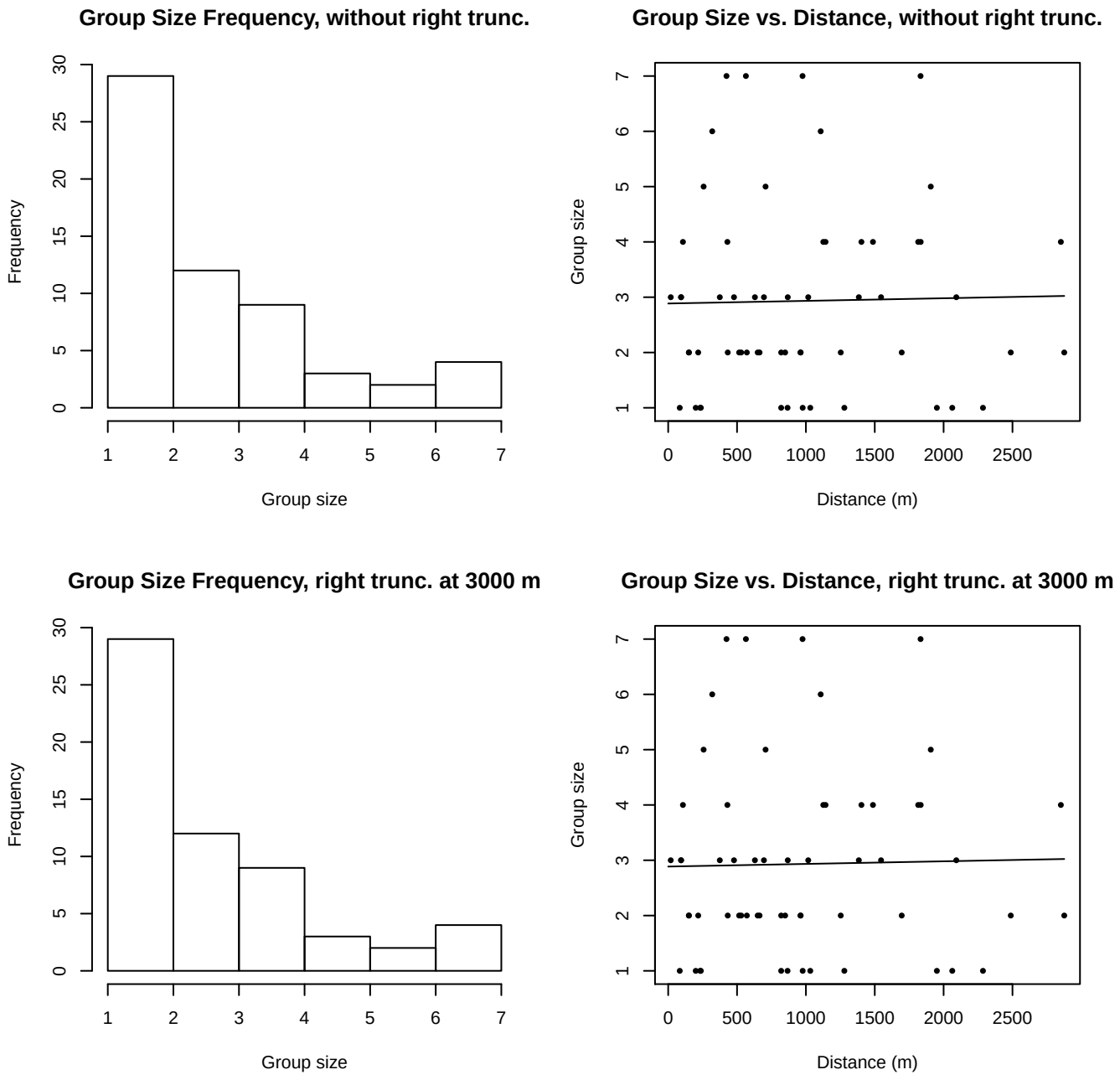

Figure 15: Histograms showing group size frequency and scatterplots showing the relationship between group size and perpendicular sighting distance, for all sightings (top row) and only those not right truncated (bottom row). In the scatterplot, the line is a simple linear regression.

SEFSC Oregon II

The sightings were right truncated at 3000m.

Covariate	Description
beaufort	Beaufort sea state.
quality	Survey-specific index of the quality of observation conditions, utilizing relevant factors other than Beaufort sea state (see methods).
size	Estimated size (number of individuals) of the sighted group.

Table 8: Covariates tested in candidate "multi-covariate distance sampling" (MCDS) detection functions.

Key	Adjustment	Order	Covariates	Succeeded	Δ AIC	Mean ESHW (m)
hn			size	Yes	0.00	1462
hn			quality, size	Yes	1.87	1464
hn			beaufort, size	Yes	1.94	1439
hn			beaufort, quality, size	Yes	3.81	1443
hr			size	Yes	4.42	1834
hr			beaufort, size	Yes	6.07	1870
hr			quality, size	Yes	6.30	1855
hr			beaufort, quality, size	Yes	7.97	1879
hn			beaufort	Yes	12.65	1399
hn			beaufort, quality	Yes	12.80	1386
hn	cos	2		Yes	13.73	1009
hr				Yes	13.84	838
hr			quality	Yes	14.86	818
hr			beaufort	Yes	14.96	1086
hr	poly	4		Yes	15.59	804
hr	poly	2		Yes	15.84	838
hr			beaufort, quality	Yes	16.30	895
hn	cos	3		Yes	16.79	1027
hn			quality	Yes	17.29	1424
hn				Yes	19.39	1390
hn	herm	4		Yes	21.25	1386

Table 9: Candidate detection functions for SEFSC Oregon II. The first one listed was selected for the density model.

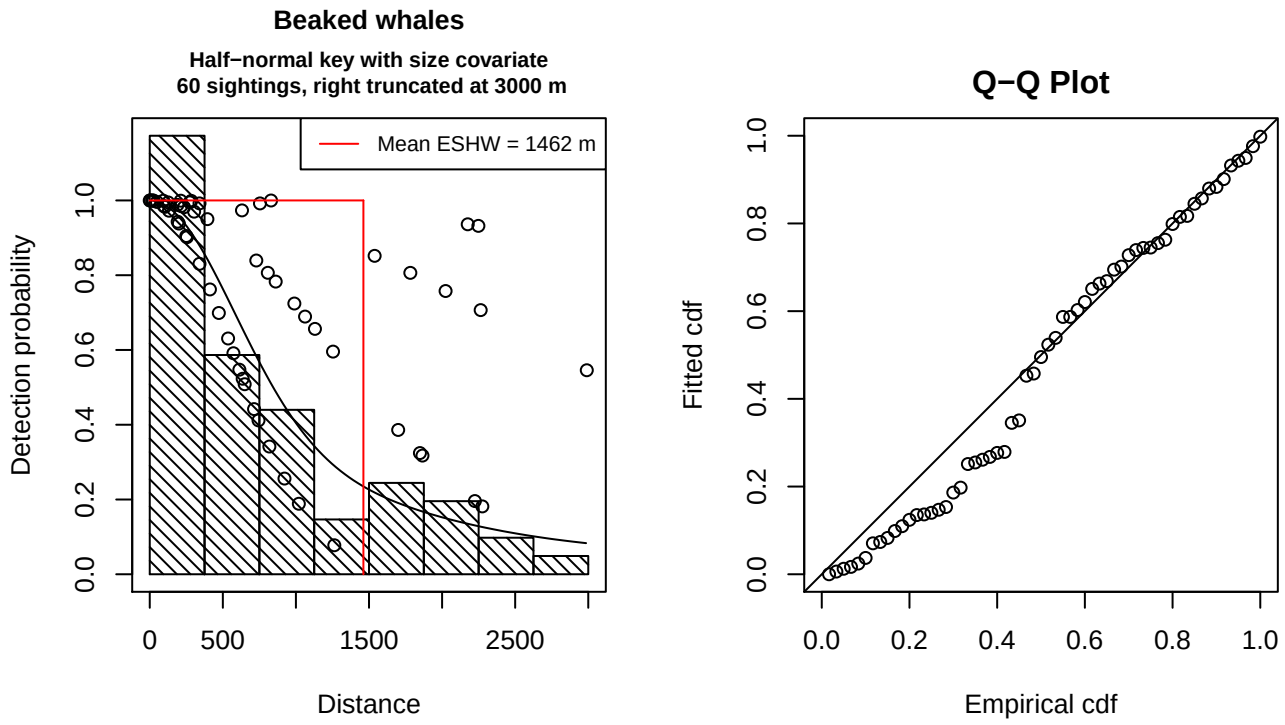

Figure 16: Detection function for SEFSC Oregon II that was selected for the density model

Statistical output for this detection function:

```
Summary for ds object
Number of observations :  60
Distance range         :  0  -  3000
AIC                    :  907.5095

Detection function:
 Half-normal key function

Detection function parameters
Scale Coefficients:
             estimate        se
(Intercept) 5.5341163 0.3555944
size        0.7910727 0.2350197

                       Estimate          SE        CV
Average p             0.3665947  0.04554777 0.1242456
N in covered region 163.6684827 27.38895820 0.1673441
```

Additional diagnostic plots:

Figure 17: Scatterplots showing the relationship between Beaufort sea state and perpendicular sighting distance, for all sightings (left) and only those not right truncated (right). The line is a simple linear regression.

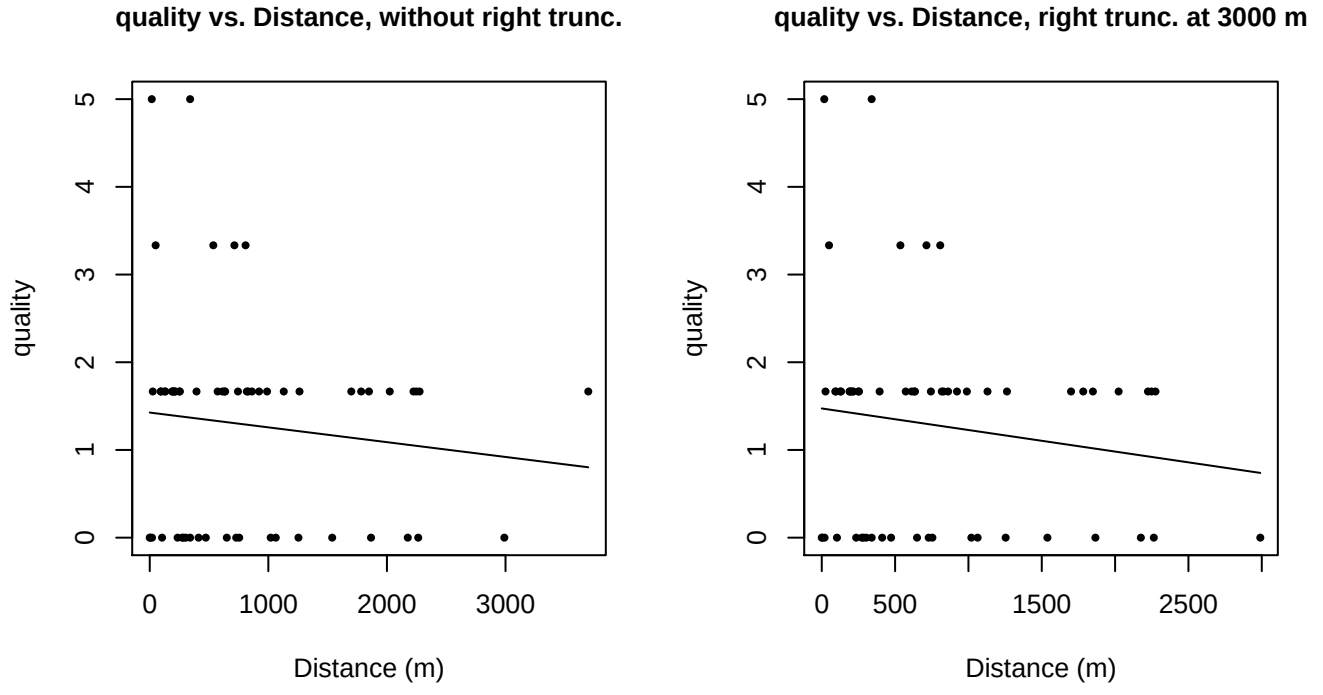

Figure 18: Scatterplots showing the relationship between the survey-specific index of the quality of observation conditions and perpendicular sighting distance, for all sightings (left) and only those not right truncated (right). Low values of the quality index correspond to better observation conditions. The line is a simple linear regression.

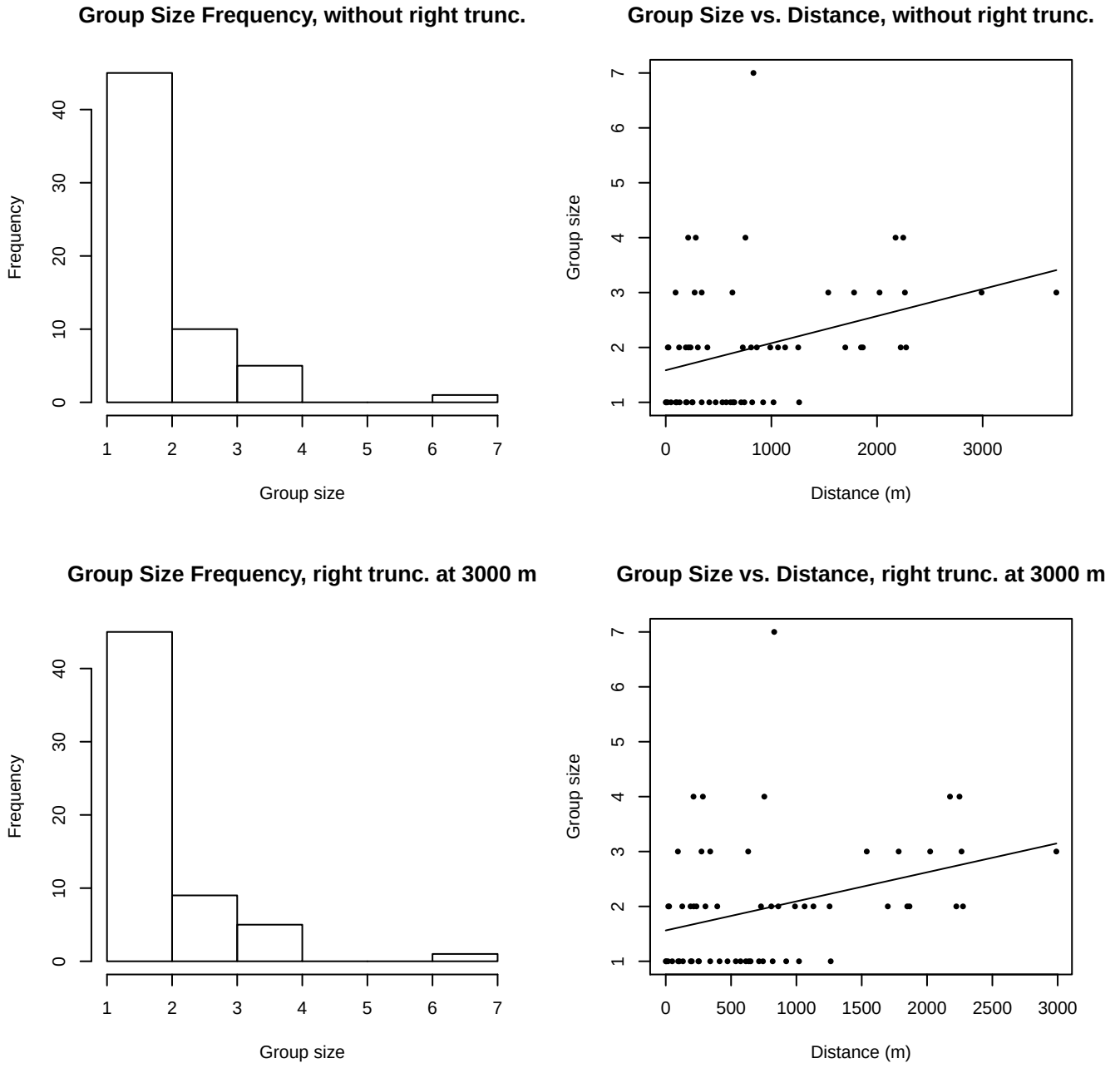

Figure 19: Histograms showing group size frequency and scatterplots showing the relationship between group size and perpendicular sighting distance, for all sightings (top row) and only those not right truncated (bottom row). In the scatterplot, the line is a simple linear regression.

High Platforms

The sightings were right truncated at 6000m.

Covariate	Description
beaufort	Beaufort sea state.
size	Estimated size (number of individuals) of the sighted group.

Table 10: Covariates tested in candidate "multi-covariate distance sampling" (MCDS) detection functions.

Key	Adjustment	Order	Covariates	Succeeded	Δ AIC	Mean ESHW (m)
hr			beaufort	Yes	0.00	2258
hr			beaufort, size	Yes	1.17	2284
hn			beaufort	Yes	1.66	2657
hr				Yes	2.76	2377
hn	cos	2		Yes	3.22	2063
hn			beaufort, size	Yes	3.45	2657
hr			size	Yes	4.10	2361
hr	poly	2		Yes	4.76	2377
hn				Yes	4.87	2512
hr	poly	4		Yes	4.90	2453
hn			size	Yes	6.25	2507
hn	herm	4		Yes	6.71	2506
hn	cos	3		Yes	6.71	2367

Table 11: Candidate detection functions for High Platforms. The first one listed was selected for the density model.

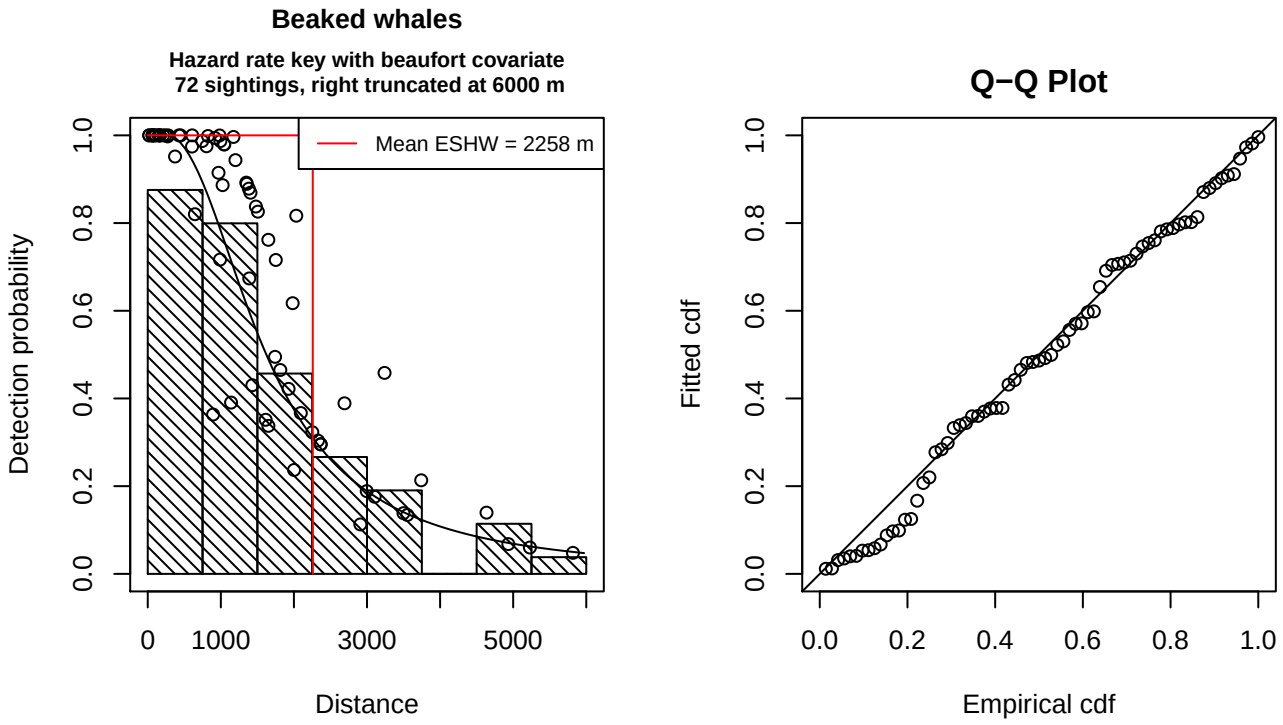

Figure 20: Detection function for High Platforms that was selected for the density model

Statistical output for this detection function:

```
Summary for ds object
```

```
Number of observations :  72
Distance range         :  0  -  6000
AIC                    :  1194.489

Detection function:
 Hazard-rate key function

Detection function parameters
Scale Coefficients:
             estimate        se
(Intercept)  7.8592898 0.3568977
beaufort    -0.2855211 0.1289825

Shape parameters:
             estimate        se
(Intercept) 0.7805475 0.2484692

                        Estimate         SE        CV
Average p              0.3425973  0.0516629 0.1507977
N in covered region 210.1592533 37.7928095 0.1798294
```

Additional diagnostic plots:

Figure 21: Scatterplots showing the relationship between Beaufort sea state and perpendicular sighting distance, for all sightings (left) and only those not right truncated (right). The line is a simple linear regression.

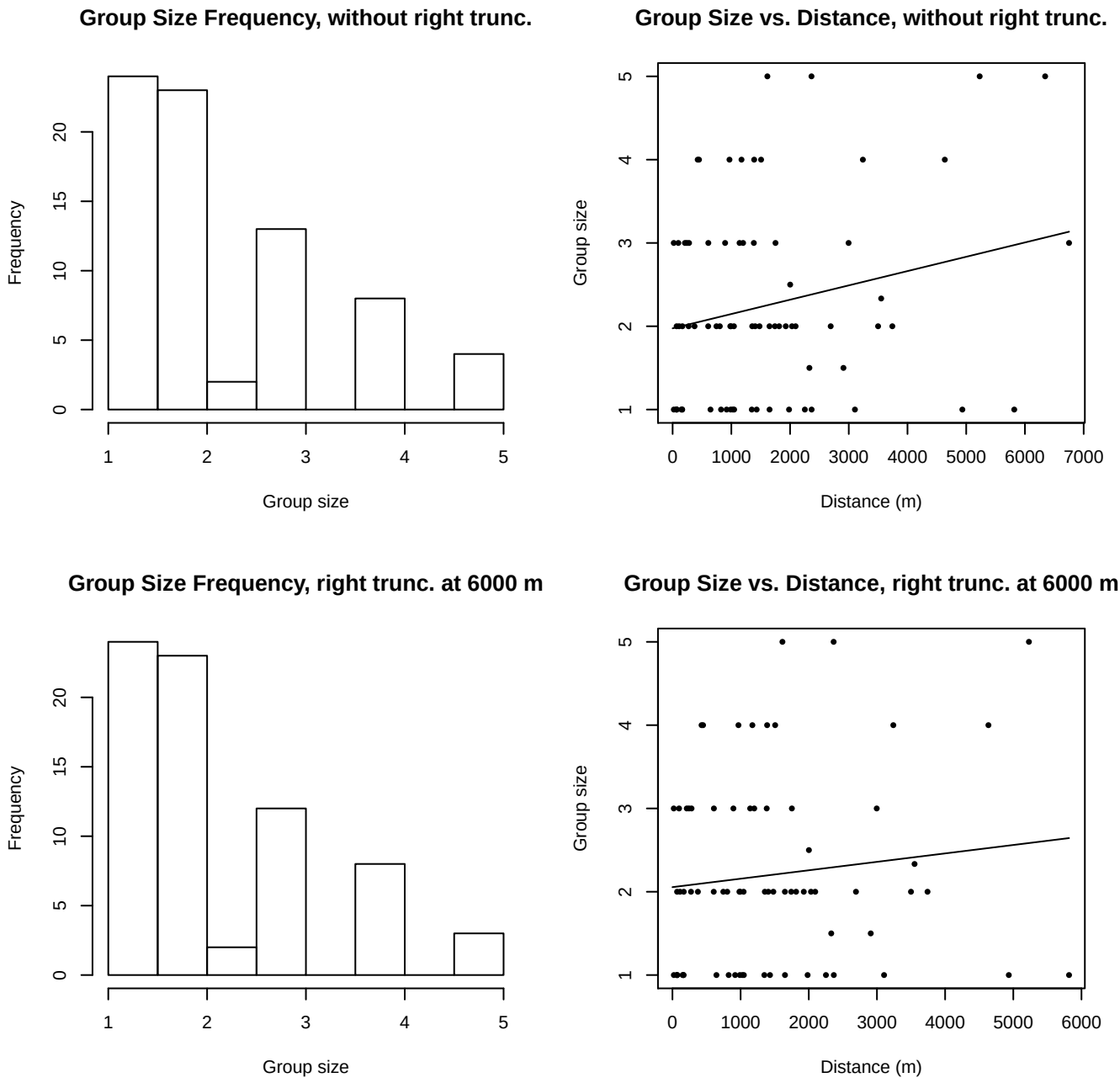

Figure 22: Histograms showing group size frequency and scatterplots showing the relationship between group size and perpendicular sighting distance, for all sightings (top row) and only those not right truncated (bottom row). In the scatterplot, the line is a simple linear regression.

Naked Eye Surveys

The sightings were right truncated at 1500m.

Key	Adjustment	Order	Covariates	Succeeded	Δ AIC	Mean ESHW (m)
hr				Yes	0.00	439
hn	cos	2		Yes	0.56	445
hr	poly	4		Yes	2.00	439

hr	poly	2	Yes	2.00	439
hn			Yes	2.39	551
hn	cos	3	Yes	2.44	424
hn	herm	4	Yes	4.31	550

Table 12: Candidate detection functions for Naked Eye Surveys. The first one listed was selected for the density model.

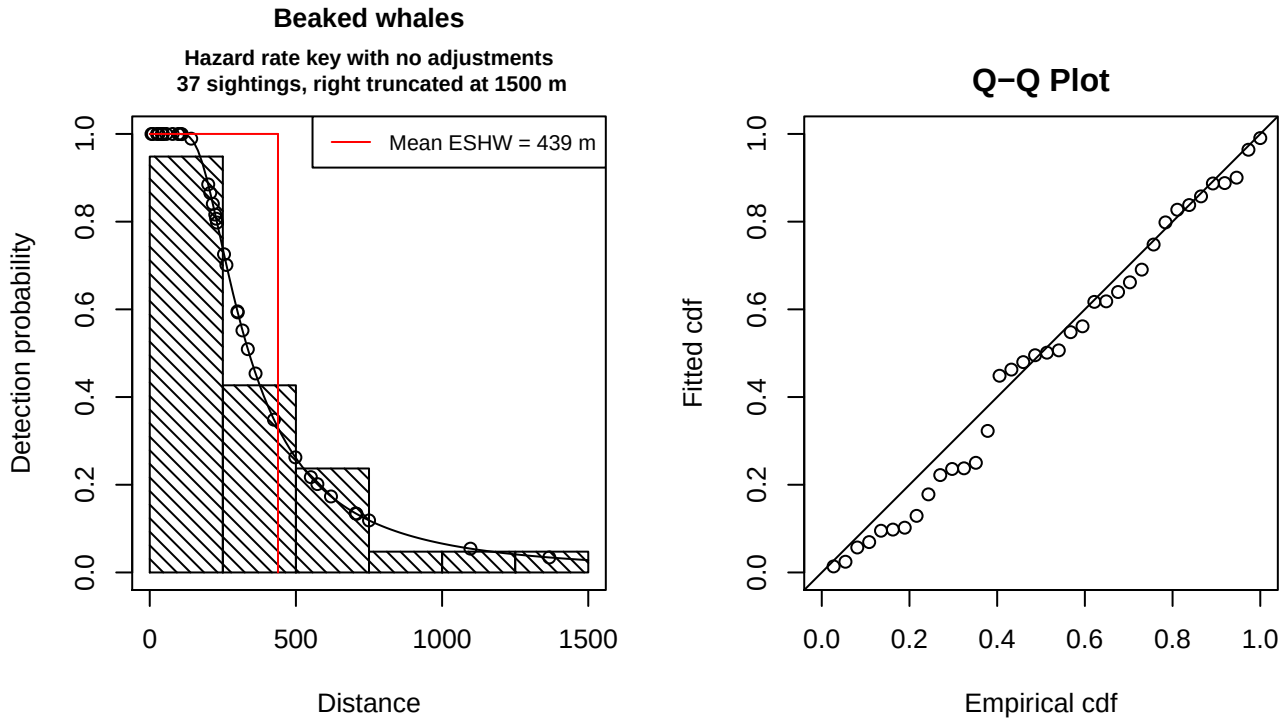

Figure 23: Detection function for Naked Eye Surveys that was selected for the density model

Statistical output for this detection function:

```
Summary for ds object
Number of observations :  37
Distance range         :  0  -  1500
AIC                    :  503.3464

Detection function:
 Hazard-rate key function

Detection function parameters
Scale Coefficients:
            estimate        se
(Intercept) 5.657308 0.3088619

Shape parameters:
             estimate        se
(Intercept) 0.7645473 0.2807783
```

```
                        Estimate          SE        CV
Average p              0.2924249  0.05911656 0.2021598
N in covered region 126.5282115 30.99094898 0.2449331
```

Aerial Surveys

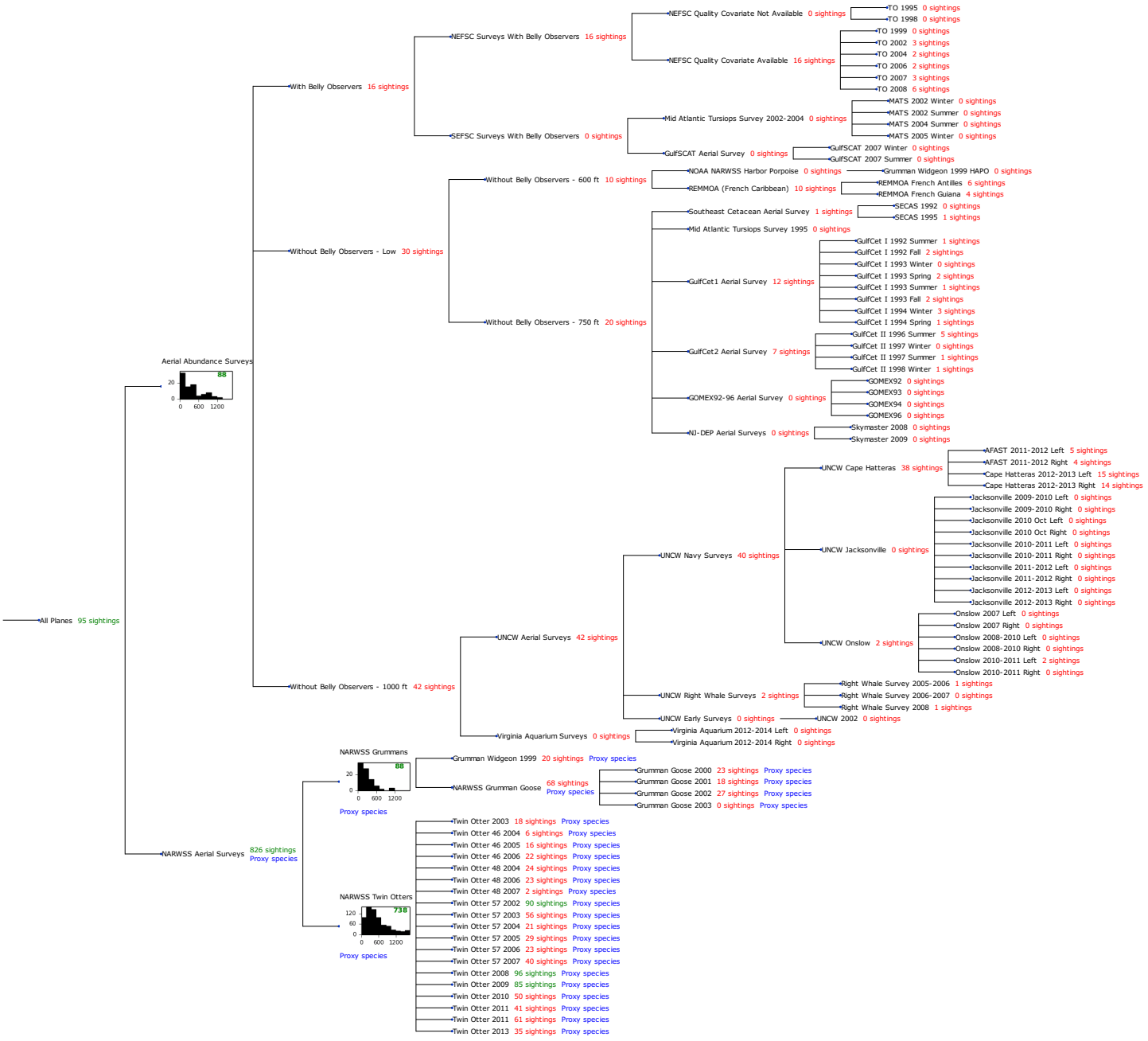

Figure 24: Detection hierarchy for aerial surveys

Aerial Abundance Surveys

The sightings were right truncated at 1500m.

Covariate	Description

beaufort	Beaufort sea state.
size	Estimated size (number of individuals) of the sighted group.

Table 13: Covariates tested in candidate "multi-covariate distance sampling" (MCDS) detection functions.

Key	Adjustment	Order	Covariates	Succeeded	Δ AIC	Mean ESHW (m)
hn	cos	3		Yes	0.00	478
hr	poly	4		Yes	2.16	479
hr	poly	2		Yes	2.50	472
hn	cos	2		Yes	3.05	544
hr				Yes	3.73	492
hn				Yes	4.42	647
hr			size	Yes	5.70	495
hn			beaufort	Yes	6.21	647
hn	herm	4		No		
hr			beaufort	No		
hn			size	No		
hn			beaufort, size	No		
hr			beaufort, size	No		

Table 14: Candidate detection functions for Aerial Abundance Surveys. The first one listed was selected for the density model.

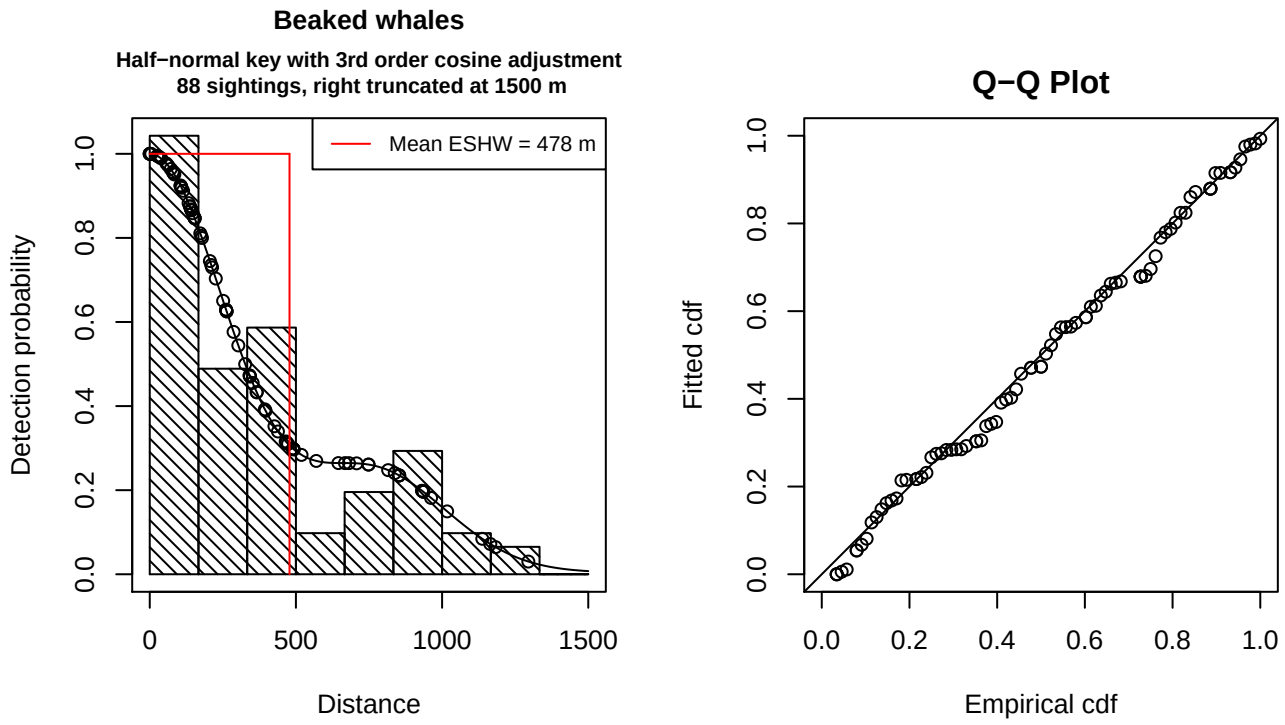

Figure 25: Detection function for Aerial Abundance Surveys that was selected for the density model

Statistical output for this detection function:

```
Summary for ds object
Number of observations :  88
Distance range         :  0  -  1500
AIC                    :  1221.593

Detection function:
 Half-normal key function with cosine adjustment term of order 3

Detection function parameters
Scale Coefficients:
            estimate         se
(Intercept) 6.257817 0.07793329

Adjustment term parameter(s):
              estimate        se
cos, order 3 0.3665265 0.1373015


Monotonicity constraints were enforced.
                       Estimate          SE        CV
Average p             0.3186994  0.03987822 0.1251280
N in covered region 276.1222435 42.23773914 0.1529675

Monotonicity constraints were enforced.
```

Additional diagnostic plots:

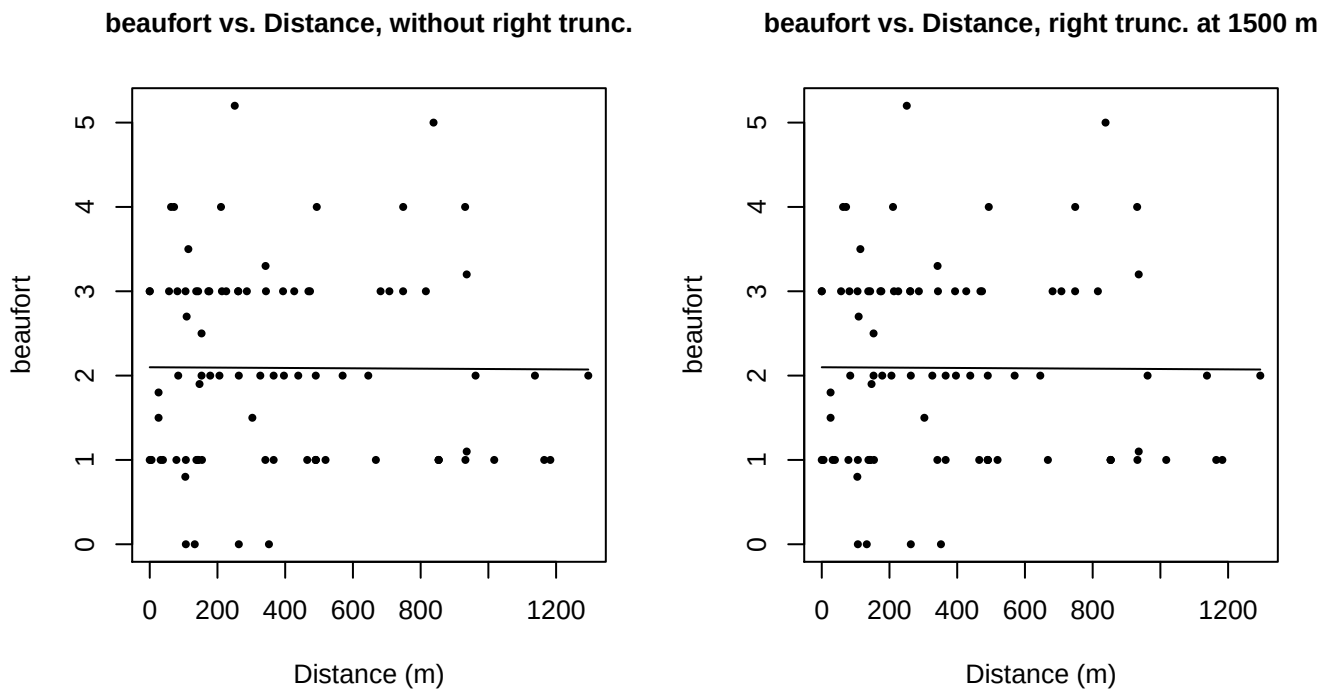

Figure 26: Scatterplots showing the relationship between Beaufort sea state and perpendicular sighting distance, for all sightings (left) and only those not right truncated (right). The line is a simple linear regression.

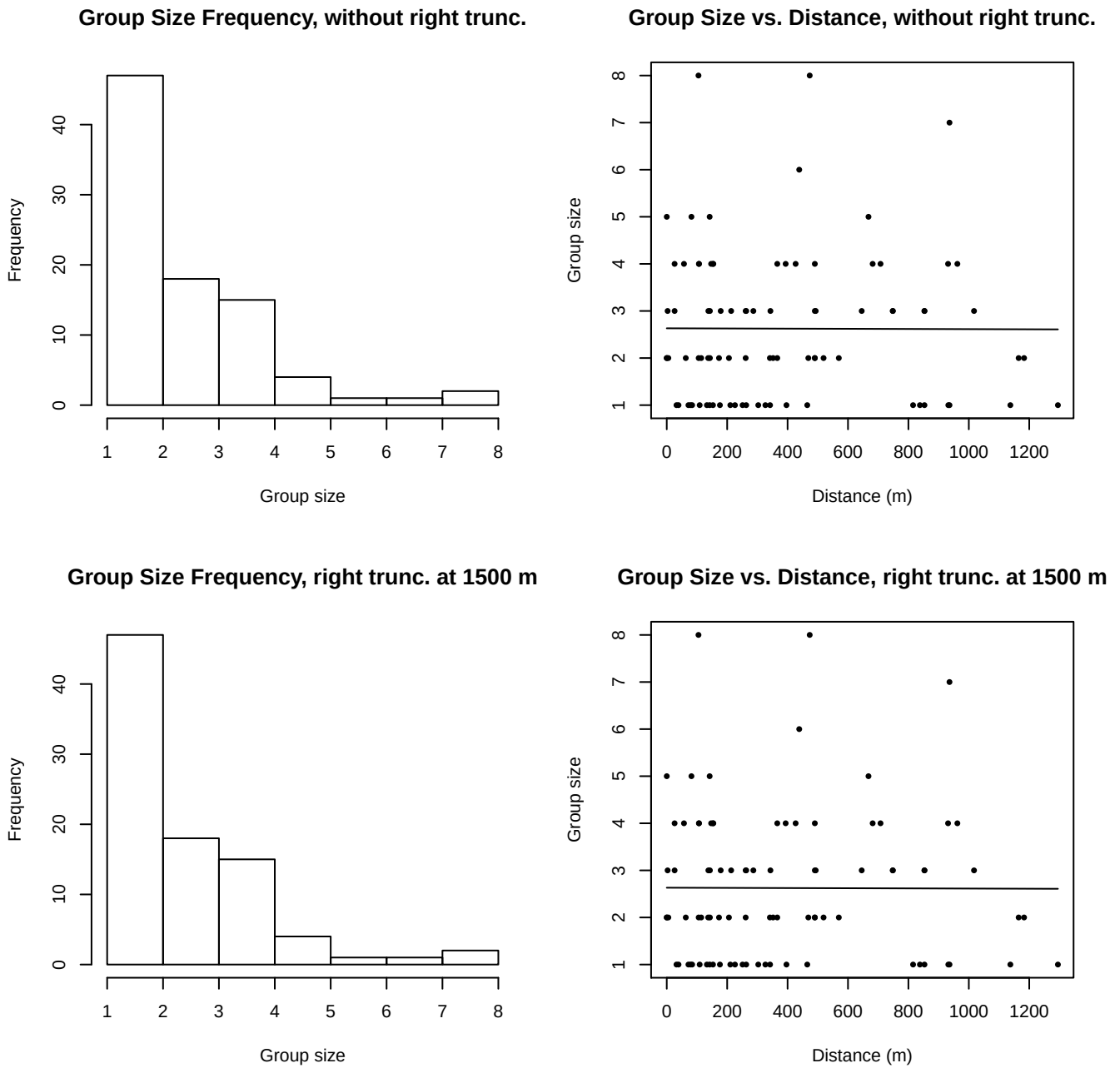

Figure 27: Histograms showing group size frequency and scatterplots showing the relationship between group size and perpendicular sighting distance, for all sightings (top row) and only those not right truncated (bottom row). In the scatterplot, the line is a simple linear regression.

NARWSS Grummans

Because this taxon was sighted too infrequently to fit a detection function to its sightings alone, we fit a detection function to the pooled sightings of several other species that we believed would exhibit similar detectability. These "proxy species" are listed below.

Reported By Observer	Common Name	n
Balaenoptera acutorostrata	Minke whale	88
Kogia	Pygmy or dwarf sperm whale	0

Kogia breviceps	Pygmy sperm whale	0
Kogia sima	Dwarf sperm whale	0
Mesoplodon	Beaked whale	0
Mesoplodon bidens	Sowerby's beaked whale	0
Mesoplodon densirostris	Blainville's beaked whale	0
Mesoplodon europaeus	Gervais' beaked whale	0
Mesoplodon mirus	True's beaked whale	0
Ziphiidae	Unidentified beaked whale	0
Ziphius cavirostris	Cuvier's beaked whale	0
Total		88

Table 15: Proxy species used to fit detection functions for NARWSS Grummans. The number of sightings, n, is before truncation.

The sightings were right truncated at 1500m.

Covariate	Description
beaufort	Beaufort sea state.
quality	Survey-specific index of the quality of observation conditions, utilizing relevant factors other than Beaufort sea state (see methods).
size	Estimated size (number of individuals) of the sighted group.

Table 16: Covariates tested in candidate "multi-covariate distance sampling" (MCDS) detection functions.

Key	Adjustment	Order	Covariates	Succeeded	Δ AIC	Mean ESHW (m)
hr			quality	Yes	0.00	453
hr			beaufort, quality	Yes	0.77	450
hr				Yes	9.44	392
hr			beaufort	Yes	9.85	400
hn	cos	2		Yes	10.32	385
hr	poly	4		Yes	10.67	391
hr	poly	2		Yes	10.94	389
hn			quality	Yes	11.22	444
hn	cos	3		Yes	14.03	371
hn				Yes	15.50	454
hn	herm	4		No		
hn			beaufort	No		
hn			size	No		
hr			size	No		
hn			beaufort, quality	No		

hn	beaufort, size	No
hr	beaufort, size	No
hn	quality, size	No
hr	quality, size	No
hn	beaufort, quality, size	No
hr	beaufort, quality, size	No

Table 17: Candidate detection functions for NARWSS Grummans. The first one listed was selected for the density model.

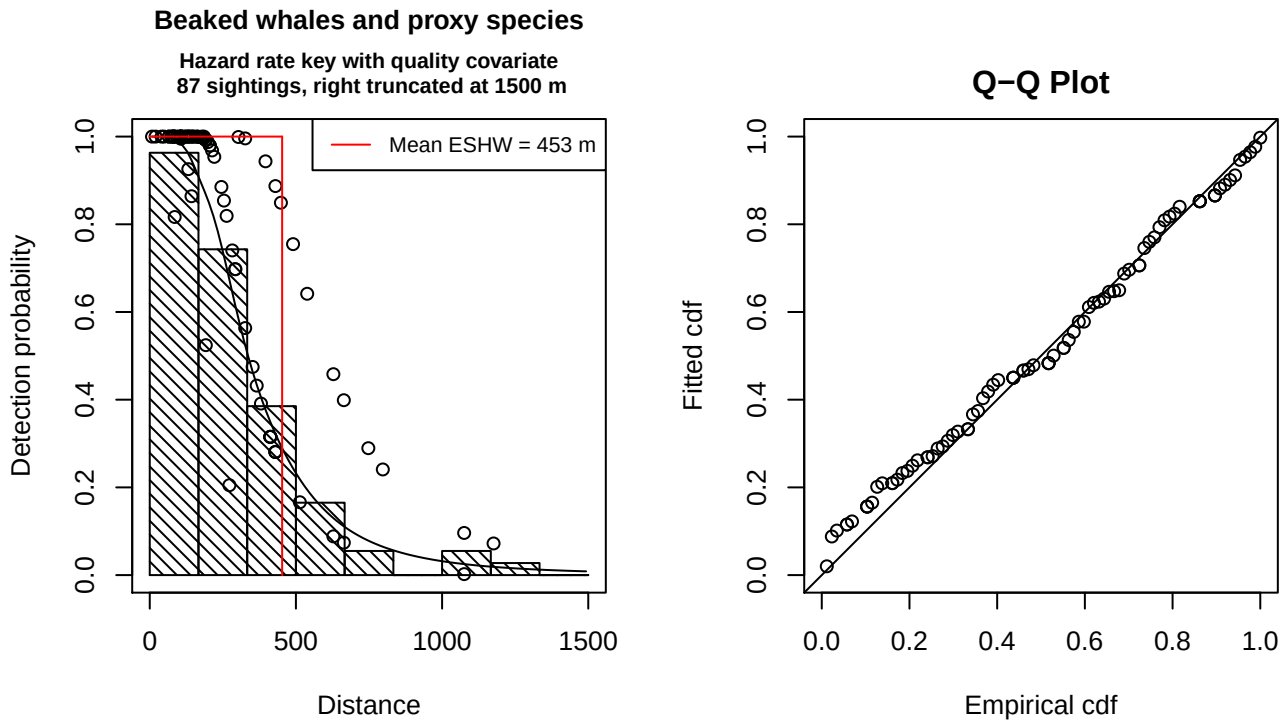

Figure 28: Detection function for NARWSS Grummans that was selected for the density model

Statistical output for this detection function:

```
Summary for ds object
Number of observations :  87
Distance range         :  0  -  1500
AIC                    :  1138.005

Detection function:
 Hazard-rate key function

Detection function parameters
Scale Coefficients:
             estimate        se
(Intercept)  6.2965502 0.1595186
quality     -0.4514297 0.1184985
```

```
Shape parameters:
            estimate        se
(Intercept) 1.209062 0.1735281

                        Estimate          SE        CV
Average p               0.2659991  0.02922489 0.1098684
N in covered region 327.0687298 47.30717620 0.1446399
```

Additional diagnostic plots:

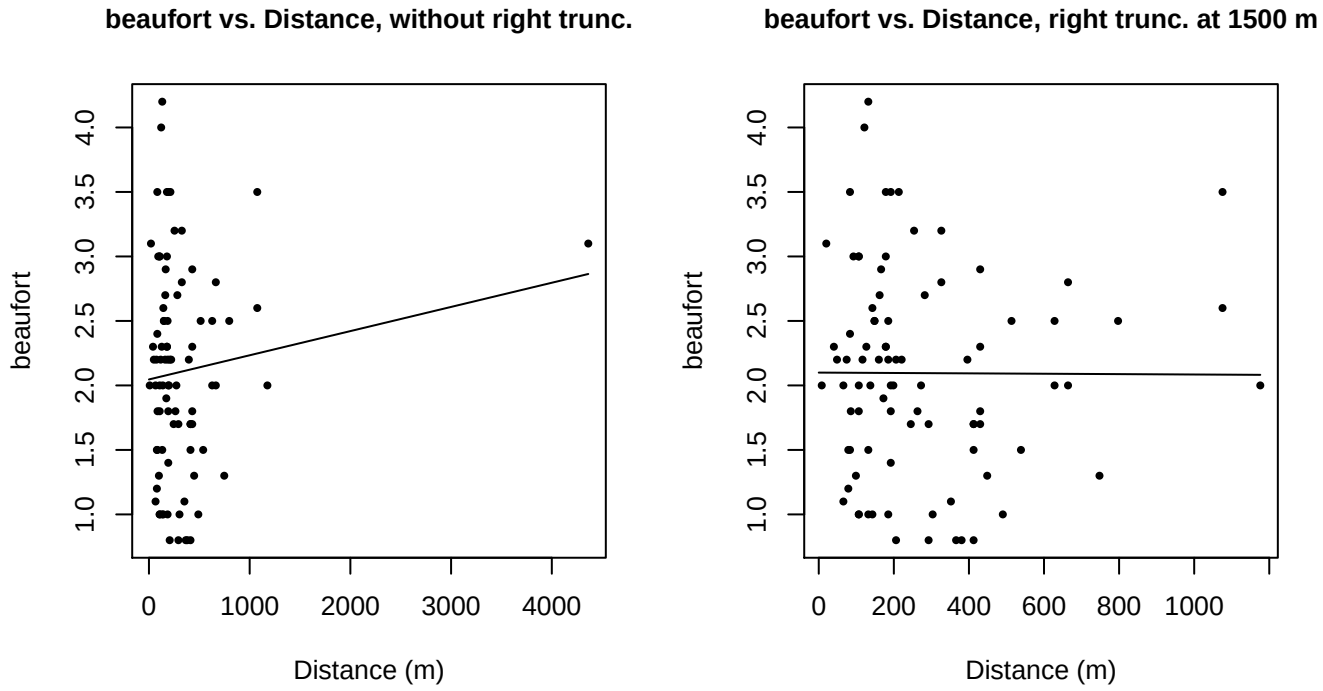

Figure 29: Scatterplots showing the relationship between Beaufort sea state and perpendicular sighting distance, for all sightings (left) and only those not right truncated (right). The line is a simple linear regression.

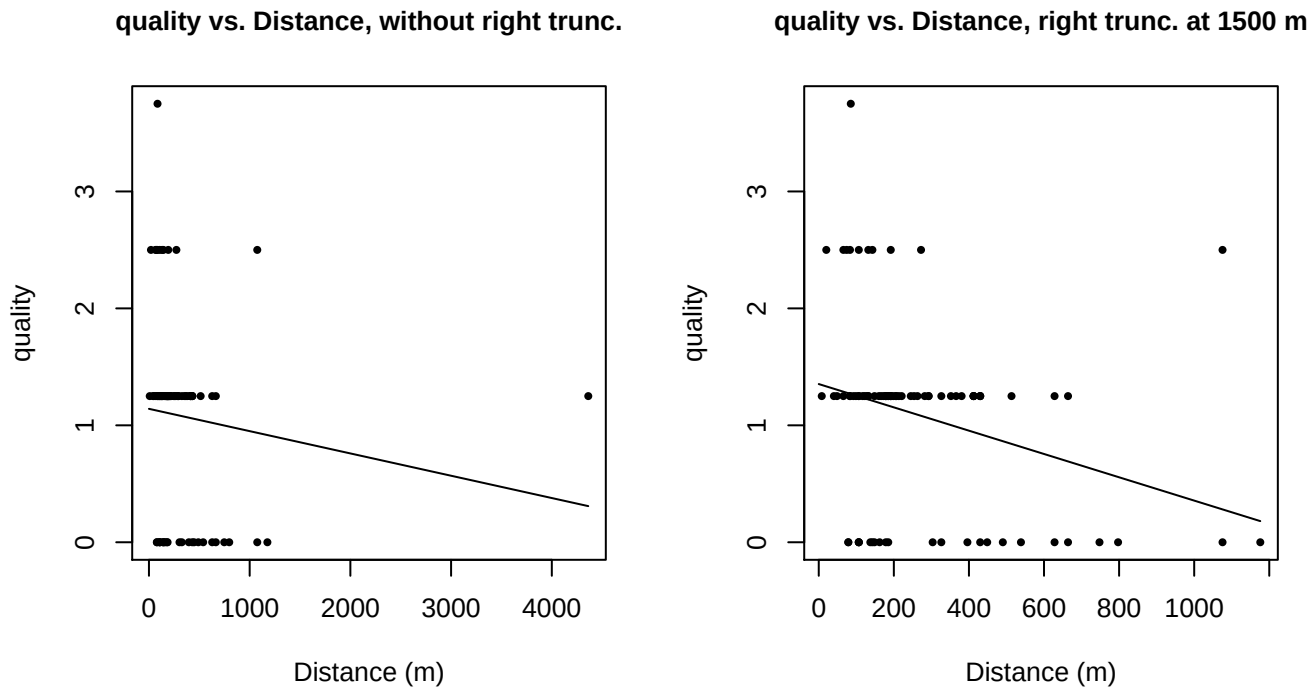

Figure 30: Scatterplots showing the relationship between the survey-specific index of the quality of observation conditions and perpendicular sighting distance, for all sightings (left) and only those not right truncated (right). Low values of the quality index correspond to better observation conditions. The line is a simple linear regression.

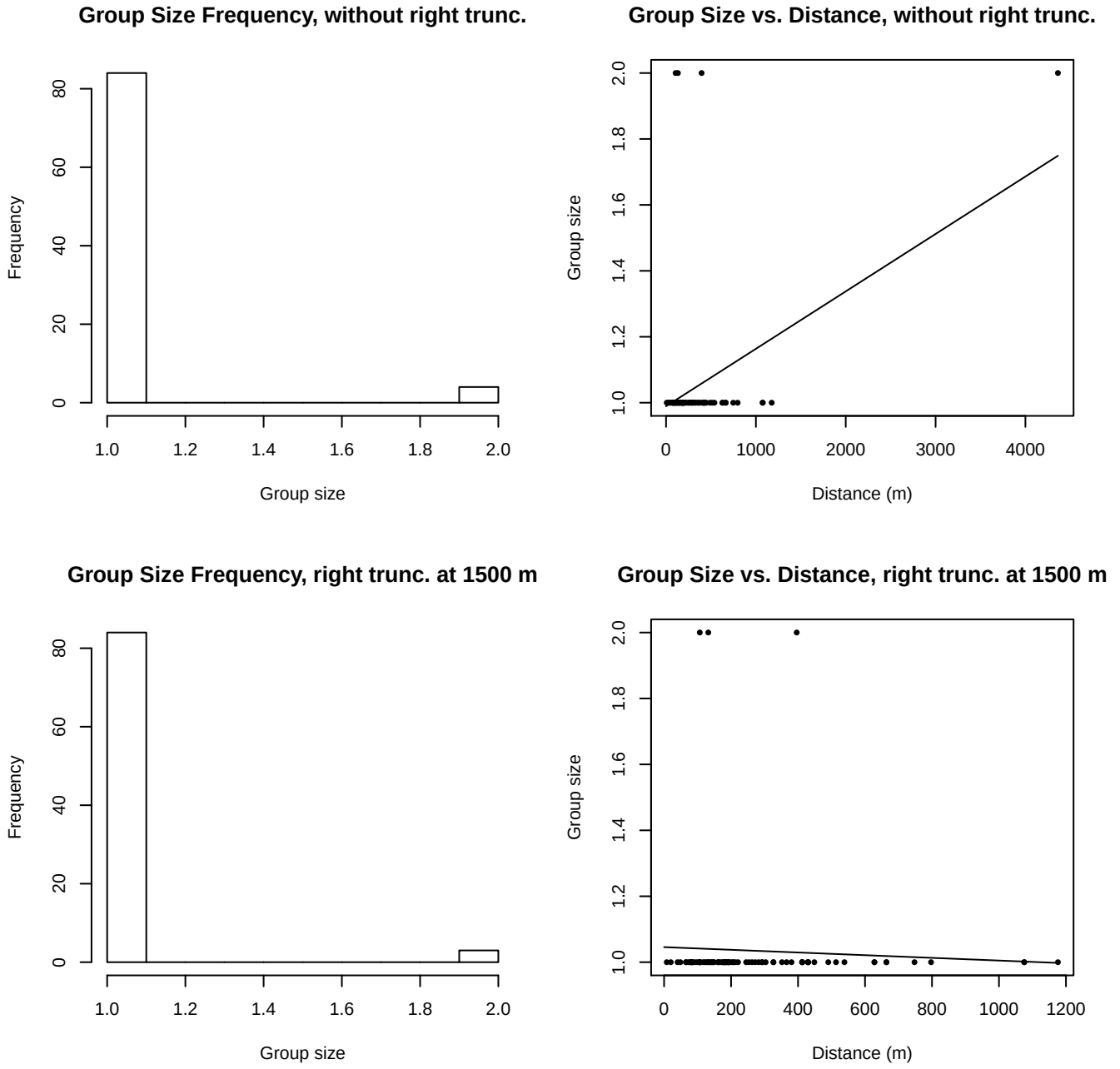

Figure 31: Histograms showing group size frequency and scatterplots showing the relationship between group size and perpendicular sighting distance, for all sightings (top row) and only those not right truncated (bottom row). In the scatterplot, the line is a simple linear regression.

NARWSS Twin Otters

Because this taxon was sighted too infrequently to fit a detection function to its sightings alone, we fit a detection function to the pooled sightings of several other species that we believed would exhibit similar detectability. These "proxy species" are listed below.

Reported By Observer	Common Name	n
Balaenoptera acutorostrata	Minke whale	731
Kogia	Pygmy or dwarf sperm whale	0

Kogia breviceps	Pygmy sperm whale	0
Kogia sima	Dwarf sperm whale	0
Mesoplodon	Beaked whale	7
Mesoplodon bidens	Sowerby's beaked whale	0
Mesoplodon densirostris	Blainville's beaked whale	0
Mesoplodon europaeus	Gervais' beaked whale	0
Mesoplodon mirus	True's beaked whale	0
Ziphiidae	Unidentified beaked whale	0
Ziphius cavirostris	Cuvier's beaked whale	0
Total		738

Table 18: Proxy species used to fit detection functions for NARWSS Twin Otters. The number of sightings, n, is before truncation.

The sightings were right truncated at 2000m. Due to a reduced frequency of sightings close to the trackline that plausibly resulted from the behavior of the observers and/or the configuration of the survey platform, the sightings were left truncted as well. Sightings closer than 107 m to the trackline were omitted from the analysis, and it was assumed that the the area closer to the trackline than this was not surveyed. This distance was estimated by inspecting histograms of perpendicular sighting distances. The vertical sighting angles were heaped at 10 degree increments up to 80 degrees and 1 degree increments thereafter, so the candidate detection functions were fitted using linear bins scaled accordingly.

Covariate	Description
beaufort	Beaufort sea state.
quality	Survey-specific index of the quality of observation conditions, utilizing relevant factors other than Beaufort sea state (see methods).
size	Estimated size (number of individuals) of the sighted group.

Table 19: Covariates tested in candidate "multi-covariate distance sampling" (MCDS) detection functions.

Key	Adjustment	Order	Covariates	Succeeded	Δ AIC	Mean ESHW (m)
hn	cos	2		Yes	0.00	599
hr				Yes	2.34	683
hr			beaufort	Yes	3.88	687
hr			quality	Yes	3.94	677
hr	poly	4		Yes	3.96	667
hr	poly	2		Yes	3.97	660
hr			size	Yes	4.06	684
hr			beaufort, quality	Yes	5.56	681
hr			beaufort, size	Yes	5.56	687
hr			quality, size	Yes	5.68	678
hr			beaufort, quality, size	Yes	7.26	682
hn	cos	3		Yes	27.27	670

hn				Yes	29.24	772
hn	herm	4		Yes	30.17	770
hn			beaufort	Yes	30.57	772
hn			size	Yes	31.02	772
hn			quality	Yes	31.22	772
hn			beaufort, size	Yes	32.38	772
hn			quality, size	Yes	33.01	772
hn			beaufort, quality	No		
hn			beaufort, quality, size	No		

Table 20: Candidate detection functions for NARWSS Twin Otters. The first one listed was selected for the density model.

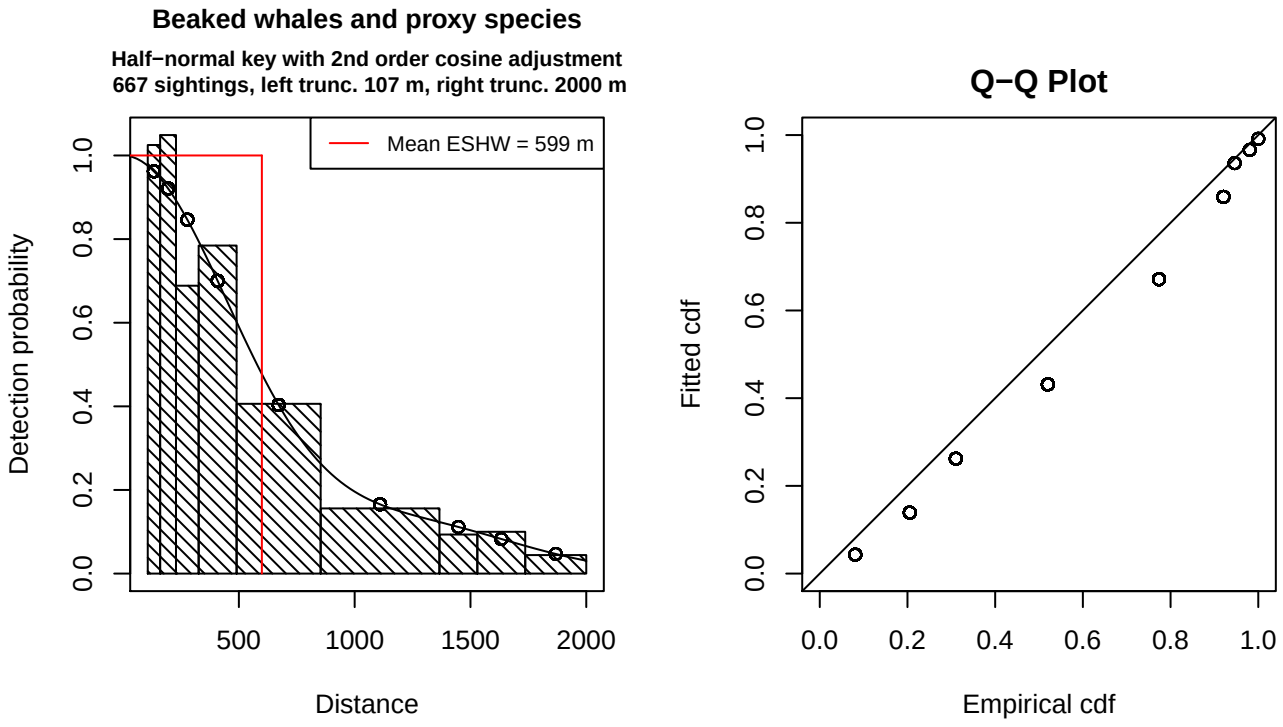

Figure 32: Detection function for NARWSS Twin Otters that was selected for the density model

Statistical output for this detection function:

```
Summary for ds object
Number of observations :  667
Distance range         :  106.5979  -  2000
AIC                    :  2606.934

Detection function:
 Half-normal key function with cosine adjustment term of order 2

Detection function parameters
Scale Coefficients:
```

```
            estimate         se
(Intercept) 6.630948 0.03193456

Adjustment term parameter(s):
              estimate        se
cos, order 2 0.3626815 0.0605525


Monotonicity constraints were enforced.
                        Estimate           SE         CV
Average p              0.2996382   0.01430097 0.04772748
N in covered region 2226.0182751 128.41501679 0.05768821

Monotonicity constraints were enforced.
```

Additional diagnostic plots:

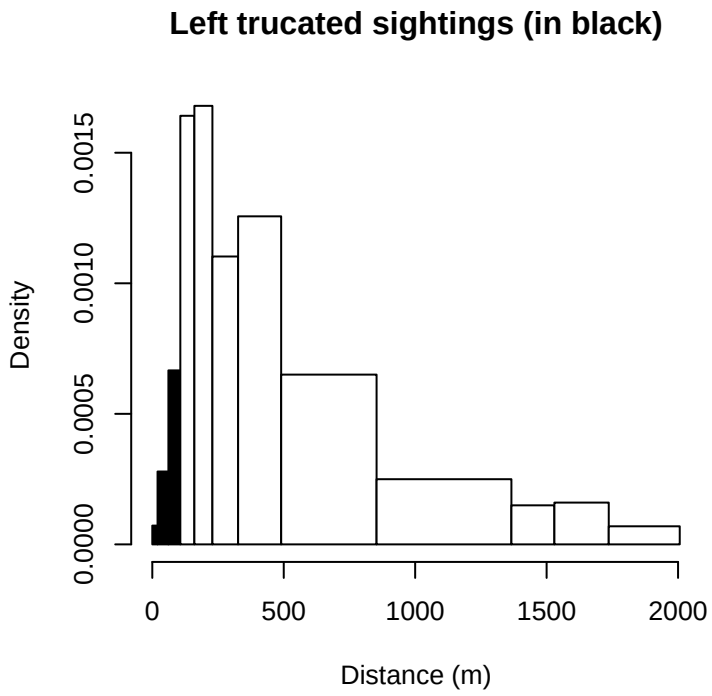

Figure 33: Density of sightings by perpendicular distance for NARWSS Twin Otters. Black bars on the left show sightings that were left truncated.

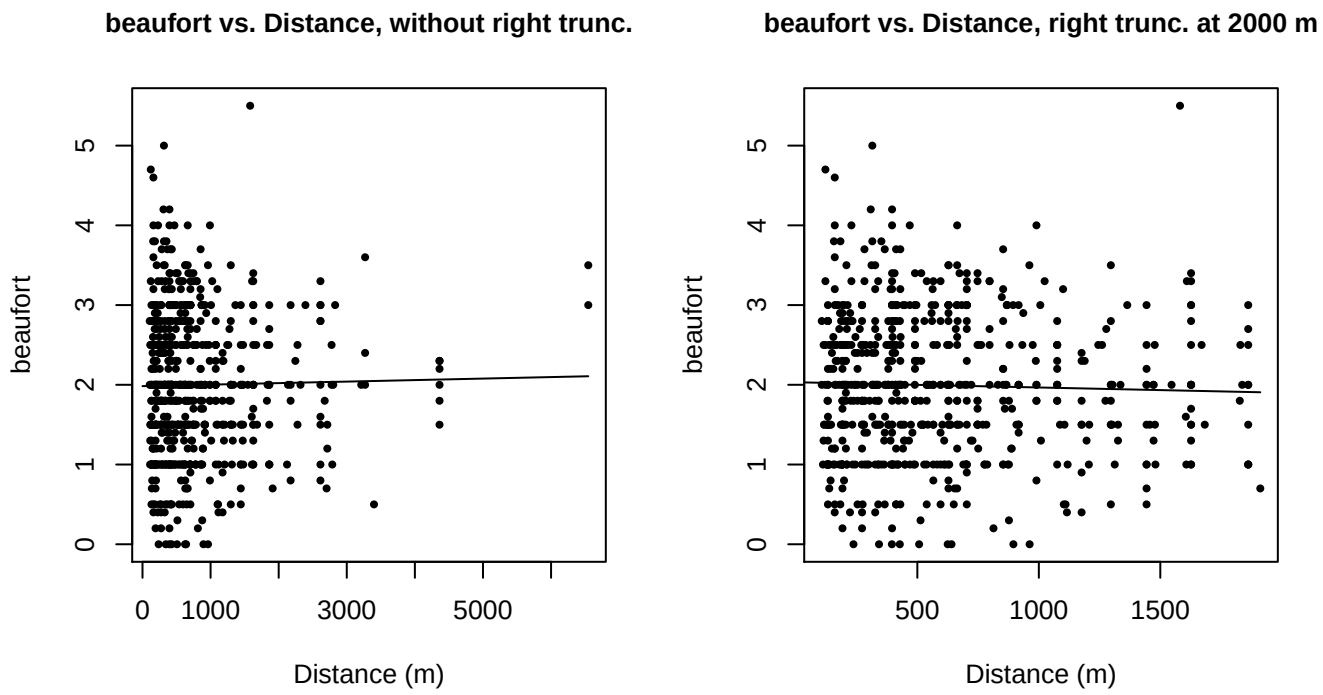

Figure 34: Scatterplots showing the relationship between Beaufort sea state and perpendicular sighting distance, for all sightings (left) and only those not right truncated (right). The line is a simple linear regression.

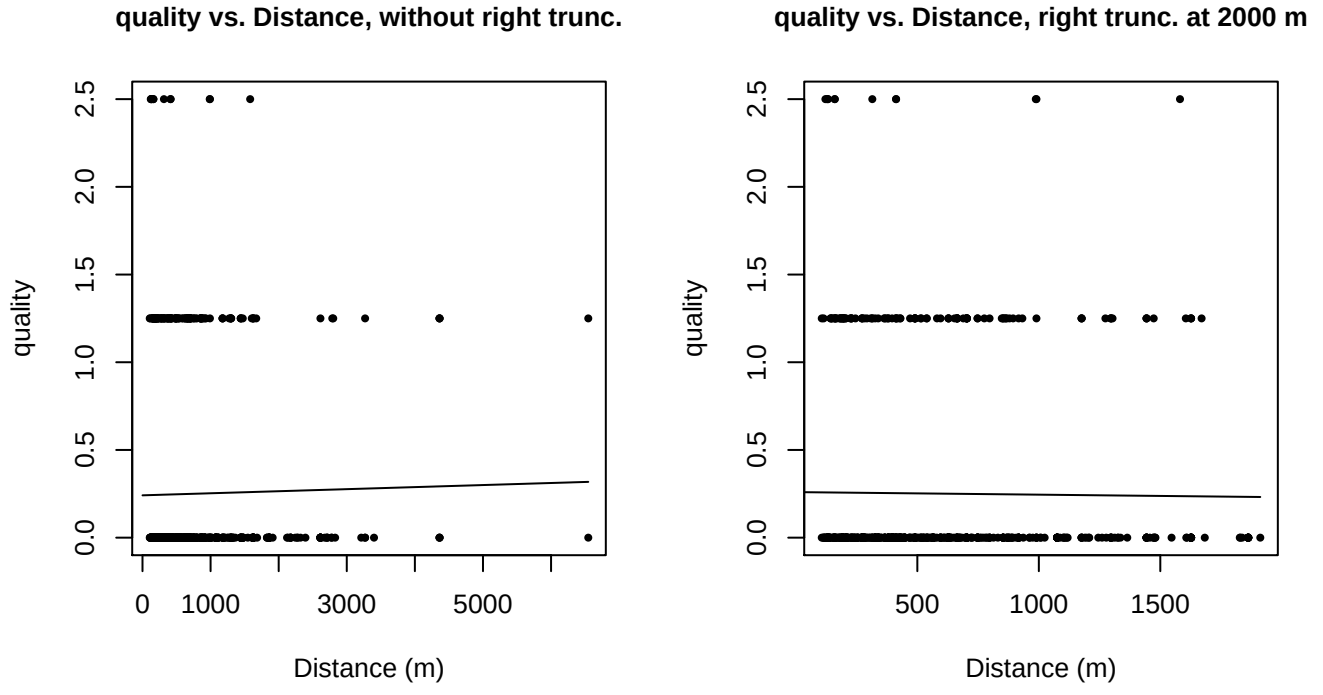

Figure 35: Scatterplots showing the relationship between the survey-specific index of the quality of observation conditions and perpendicular sighting distance, for all sightings (left) and only those not right truncated (right). Low values of the quality index correspond to better observation conditions. The line is a simple linear regression.

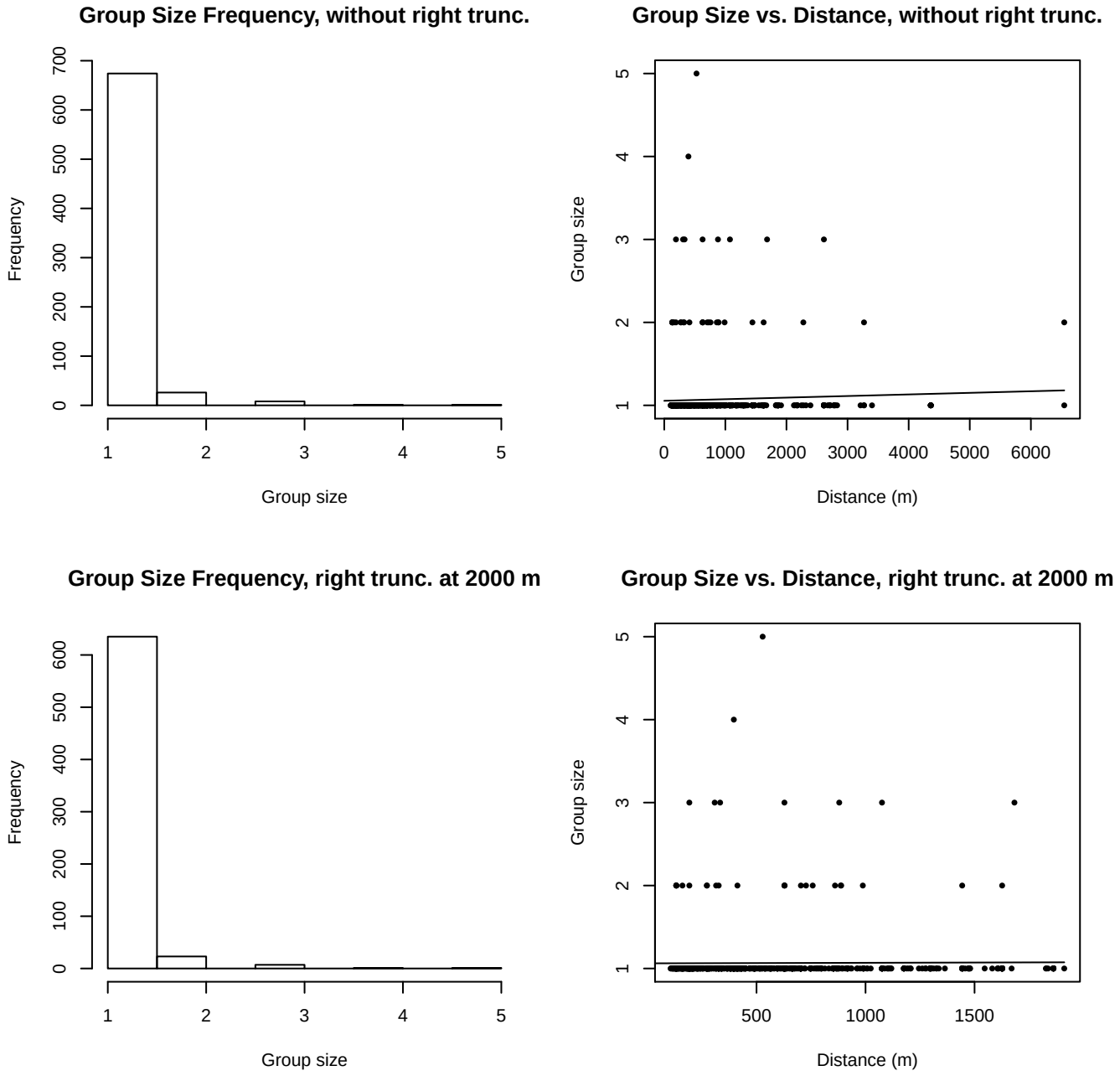

Figure 36: Histograms showing group size frequency and scatterplots showing the relationship between group size and perpendicular sighting distance, for all sightings (top row) and only those not right truncated (bottom row). In the scatterplot, the line is a simple linear regression.

g(0) Estimates

Platform	Surveys	Group Size	*g(0)*	Biases Addressed	Source
Shipboard	All	Any	0.23	Both	Barlow (1999)
Shipboard	NEFSC Abel-J Binocular Surveys	Any	0.46	Perception	Palka (2006)
Shipboard	NEFSC Endeavor	Any	0.31	Perception	Palka (2006)
Aerial	All	Any	0.074	Availability	Barlow (1999)

Table 21: Estimates of *g(0)* used in this density model.

Palka (2006) provided survey-specific g(0) estimates for two NOAA NEFSC shipboard surveys that used bigeye binoculars: the Abel-J 1998 survey (0.46) and the Endeavor 2004 survey (0.31). We used the estimates for the lower team, which was the primary team and the one for which we have sightings. These estimates used a dual-team methodology that accounted for perception bias but not availability bias. Because beaked whales are long-diving animals, these g(0) estimates may be biased high, possibly resulting in an underestimation of abundance.

No survey-specific g(0) estimates were available for our other shipboard surveys. For these, we relied on results from Barlow's (1999) simulation model, who modeled g(0) for Ziphius cavirostris (Cuvier's beaked whale) and the Mesoplodon genus (several species) from shipboard surveys that utilized 25x binoculars, reporting g(0) estimates of 0.23 and 0.45, respectively, accounting for both availability and perception bias. But because roughly 75% of our beaked whale sightings had ambiguous species identifications, we were unable to build species-specific models, making the use of Barlow's estimates problematic: which should we use? We selected the Ziphius cavirostris estimate, the lower of the two, as over 80% of our definitive beaked whale sightings were for Ziphius cavirostris. Also, Barlow's simulation assumed a dive model in which the mean dive duration of Mesoplodon spp. was 20.4 min and Ziphius cavirostris was 28.6 min. These durations were based on shipboard observations of 27 and 43 dive cycles, respectively. Research since that time has shown that foraging beaked whales exhibit a complex dive pattern in which a deep dive of 45-60 min to followed by several shallower dives of roughly 20 min (Baird et al. 2006, Tyack et al. 2006, Schorr et al. 2014). If this pattern were accounted for in Barlow's simulation, the g(0) estimates would decrease; our choice of the lower g(0) value was precautionary against that eventuality.

Finally, although Barlow cautioned that his results cannot be extrapolated to other survey methods, we utilized his g(0) estimate for naked eye shipboard surveys as well, as no alternative estimate was available in the literature. But this decision turned out to be relatively unimportant because no beaked whales were sighted on the only naked eye cruise we had that occurred within the U.S. EEZ.

No estimate of g(0) was available in the literature for beaked whales sighted on aerial surveys. Beaked whales are long-diving animals, thus availability bias is likely to be substantial. Utilizing equation (3) of Carretta et al. (2000) (which follows Barlow et al. 1988), we computed the availability bias component of g(0) from the mean surface and dive intervals (126 s and 28.6 min) for Ziphius cavirostris reported by Barlow (1999). (Our choice of Ziphius cavirostris was consistent with the shipboard g(0) we used). We did not incorporate an estimate of perception bias or account for the periodic deep dives that last 45-60 min, thus our g(0) estimate is likely to be biased high. We note, however that our estimate (0.074) is similar to the mean daytime % time in surface bouts (7.0%) reported by Schorr et al. (2014) for 3732 hr of dive data collected from 8 Ziphius cavirostris, the largest database of beaked whale dive records yet published.

Density Models

Beaked whales are difficult for observers to identify at sea (Waring et al. 2014). Although some of the more recent surveys in our database provided full species identifications for some sightings, or at least determined the identification to the genus level, the large majority of sightings available over the study period reported "unidentified beaked whale" as the taxonomic identification. At a review meeting, NOAA coauthors confirmed that these sightings corresponded to beaked whales of either the Mesoplodon or Ziphius genera, but not Hyperoodon. This model, therefore, is of the guild comprising the four Mesoplodon species and the one Ziphius species that inhabit the North Atlantic: Sowerby's beaked whale (M. bidens), Blainville's beaked whale (M. densirostris), Gervais' beaked whale (M. europaeus), True's beaked whale (M. mirus), and Cuvier's beaked whale (Z. cavirostris). We modeled the extant Hyperoodon, northern bottlenose whale (H. ampullatus), separately.

Although there appear to be broad-scale differences in these species' habitats, all five occupy our East Coast study area (MacLeod 2000, Waring et al. 2014). Beaked whales are generally believed to occupy similar foraging niches, undertaking long, deep dives to hunt for mesopelagic squid and fish (Madsen et al. 2014). Beaked whales are often found in deep water near high-relief bathymetric features, such as slopes, canyons, and escarpments (MacLeod and D'Amico 2006), where preferred prey are believed to aggregate (Moors-Murphy 2014).

Almost all of the sightings reported by our surveys occurred over the continental slope or the abyss; only a few were reported over the continental shelf. Given that the shelf was not reported to be preferred beaked whale habitat, we split the study area into two regions–the Shelf and the Slope and Abyss–and modeled them separately. Only a few sightings were reported for the Shelf; here, we fitted a uniform density model. For the Slope and Abyss region, we fitted a full habitat-based model. Compared to other cetacean species, little is known about beaked whales and our literature review did not yield any descriptions of seasonal movements for these species, so we fitted year-round models.

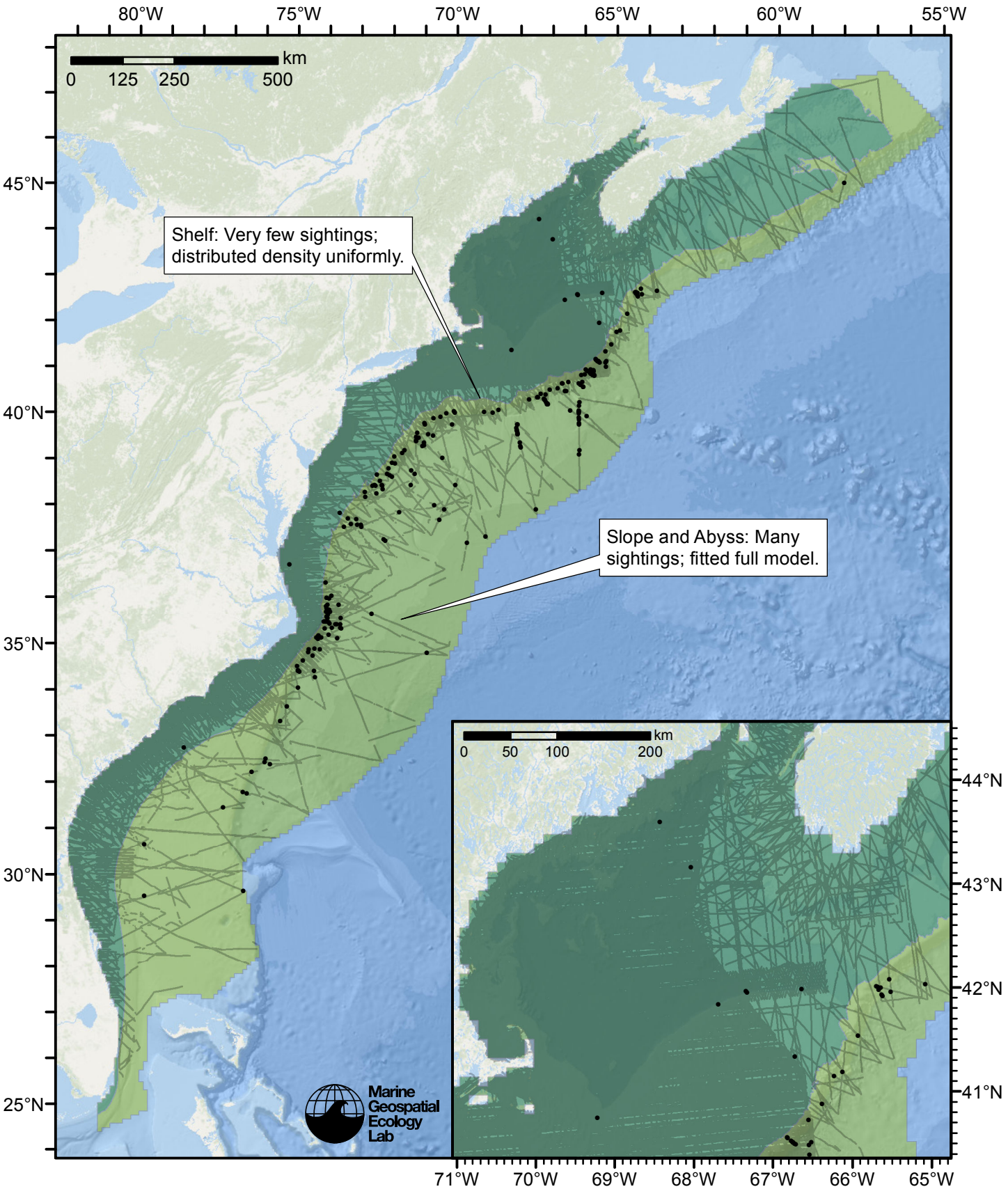

Figure 37: Beaked whales density model schematic. All on-effort sightings are shown, including those that were truncated when detection functions were fitted.

Climatological Model

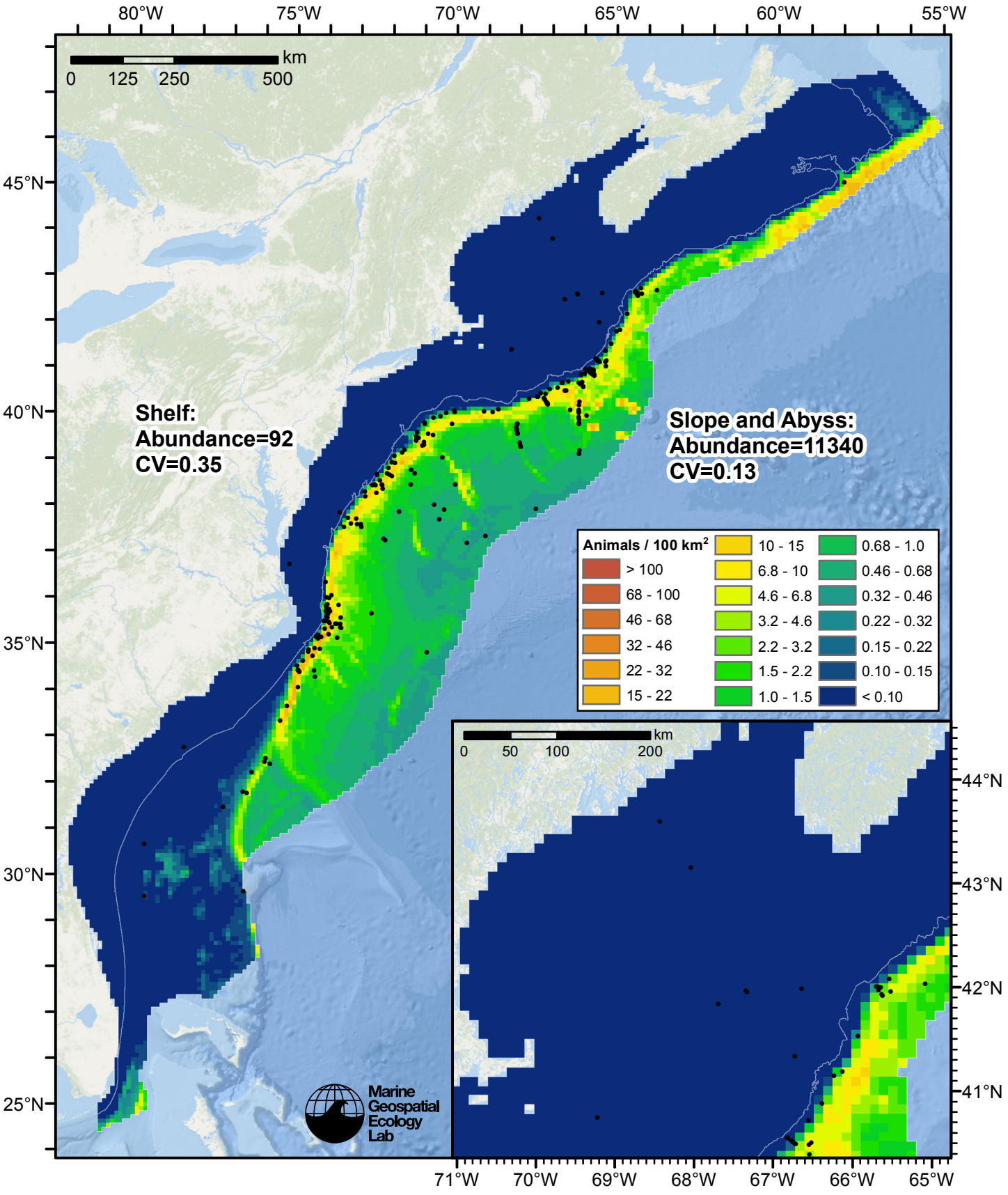

Figure 38: Beaked whales density predicted by the climatological model that explained the most deviance. Pixels are 10x10 km. The legend gives the estimated individuals per pixel; breaks are logarithmic. Abundance for each region was computed by summing the density cells occuring in that region.

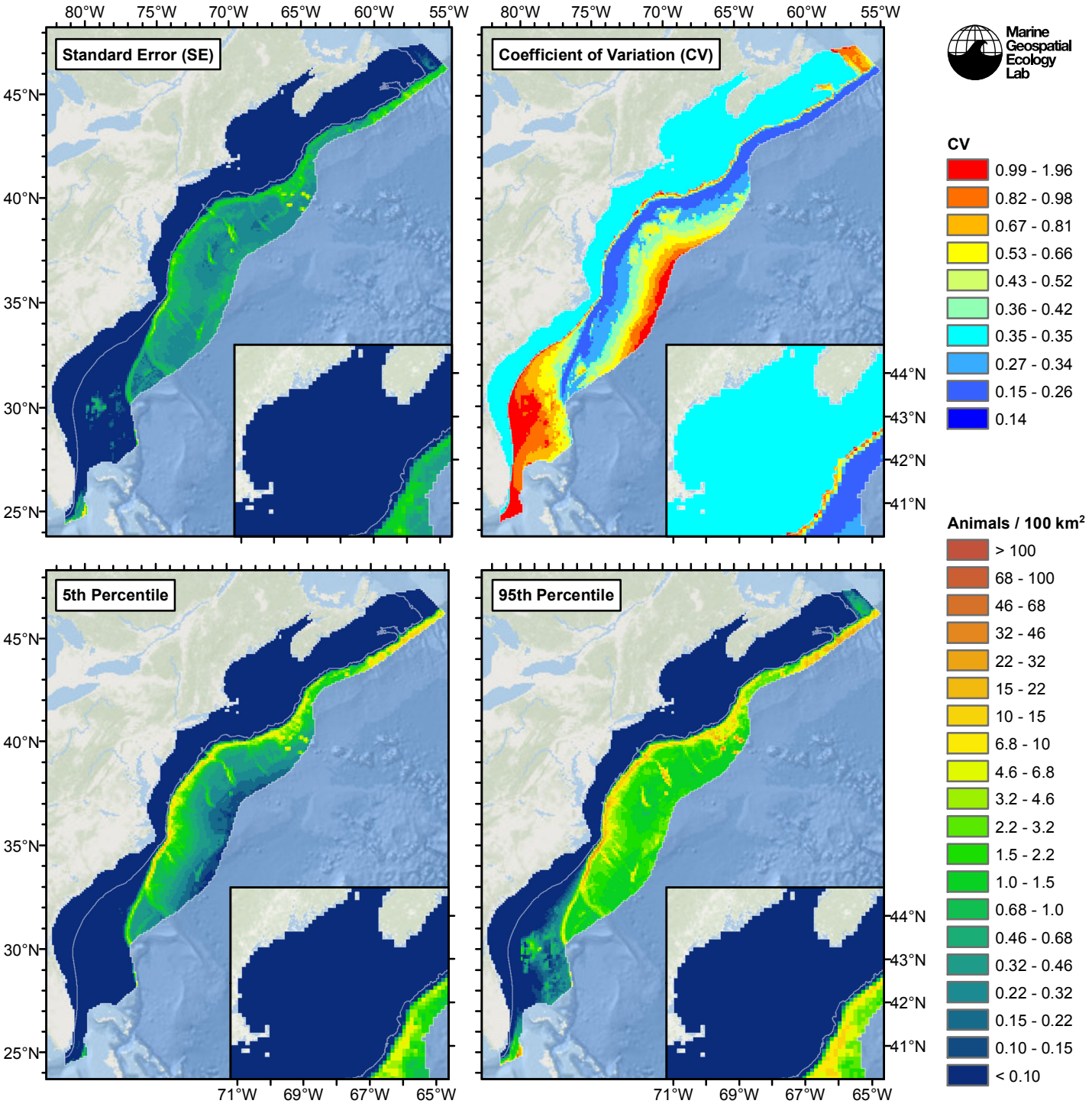

Figure 39: Estimated uncertainty for the climatological model that explained the most deviance. These estimates only incorporate the statistical uncertainty estimated for the spatial model (by the R mgcv package). They do not incorporate uncertainty in the detection functions, g(0) estimates, predictor variables, and so on.

Slope and Abyss

Statistical output

```
Rscript.exe: This is mgcv 1.8-3. For overview type 'help("mgcv-package")'.


Family: Tweedie(p=1.443)
```

```
Link function: log

Formula:
abundance ~ offset(log(area_km2)) + s(log10(Depth), bs = "ts",
    k = 5) + s(log10(Slope), bs = "ts", k = 5) + s(I(DistTo1500m/1000),
    bs = "ts", k = 5) + s(I(ClimDistToAEddy/1000), bs = "ts",
    k = 5)

Parametric coefficients:
            Estimate Std. Error t value Pr(>|t|)
(Intercept)  -7.5238     0.4213  -17.86   <2e-16 ***
---
Signif. codes:  0 '***' 0.001 '**' 0.01 '*' 0.05 '.' 0.1 ' ' 1

Approximate significance of smooth terms:
                             edf Ref.df      F  p-value
s(log10(Depth))            1.380      4 11.988 2.23e-14 ***
s(log10(Slope))            3.105      4 18.269  < 2e-16 ***
s(I(DistTo1500m/1000))     2.522      4  5.037 1.37e-05 ***
s(I(ClimDistToAEddy/1000)) 1.022      4  5.241 2.68e-06 ***
---
Signif. codes:  0 '***' 0.001 '**' 0.01 '*' 0.05 '.' 0.1 ' ' 1

R-sq.(adj) =  -0.00933   Deviance explained = 42.2%
-REML = 1680.5  Scale est. = 82.239    n = 17198

All predictors were significant. This is the final model.
Creating term plots.
Diagnostic output from gam.check():

Method: REML   Optimizer: outer newton
full convergence after 11 iterations.
Gradient range [-4.576546e-05,3.314431e-05]
(score 1680.544 & scale 82.23889).
Hessian positive definite, eigenvalue range [0.1460534,454.462].
Model rank =  17 / 17

Basis dimension (k) checking results. Low p-value (k-index<1) may
indicate that k is too low, especially if edf is close to k'.

                              k'   edf k-index p-value
s(log10(Depth))            4.000 1.380   0.733    0.00
s(log10(Slope))            4.000 3.105   0.741    0.00
s(I(DistTo1500m/1000))     4.000 2.522   0.707    0.00
s(I(ClimDistToAEddy/1000)) 4.000 1.022   0.810    0.06

Predictors retained during the model selection procedure: Depth, Slope, DistTo1500m, ClimDistToAEddy

Predictors dropped during the model selection procedure: DistToCanyonOrSeamount, ClimSST,
ClimDistToFront1, ClimTKE, ClimDistToCEddy, ClimCumVGPM45
```

Model term plots

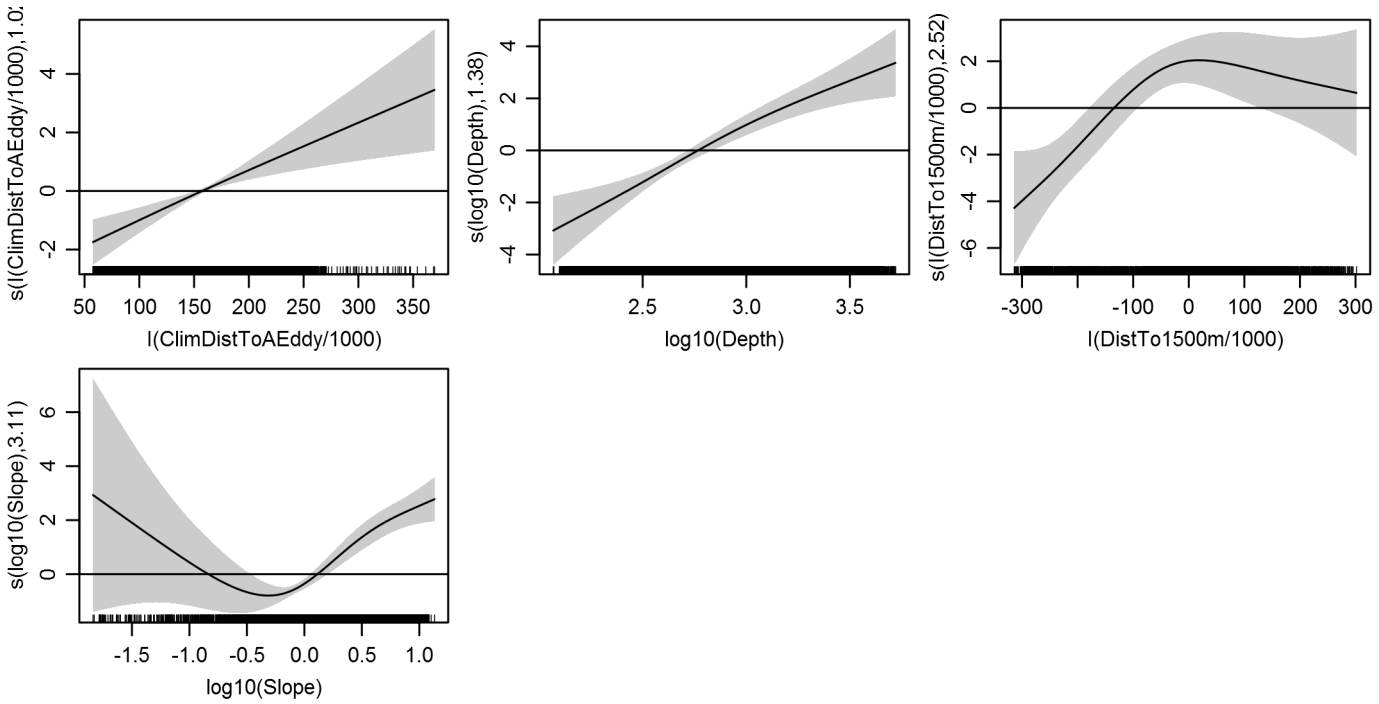

Diagnostic plots

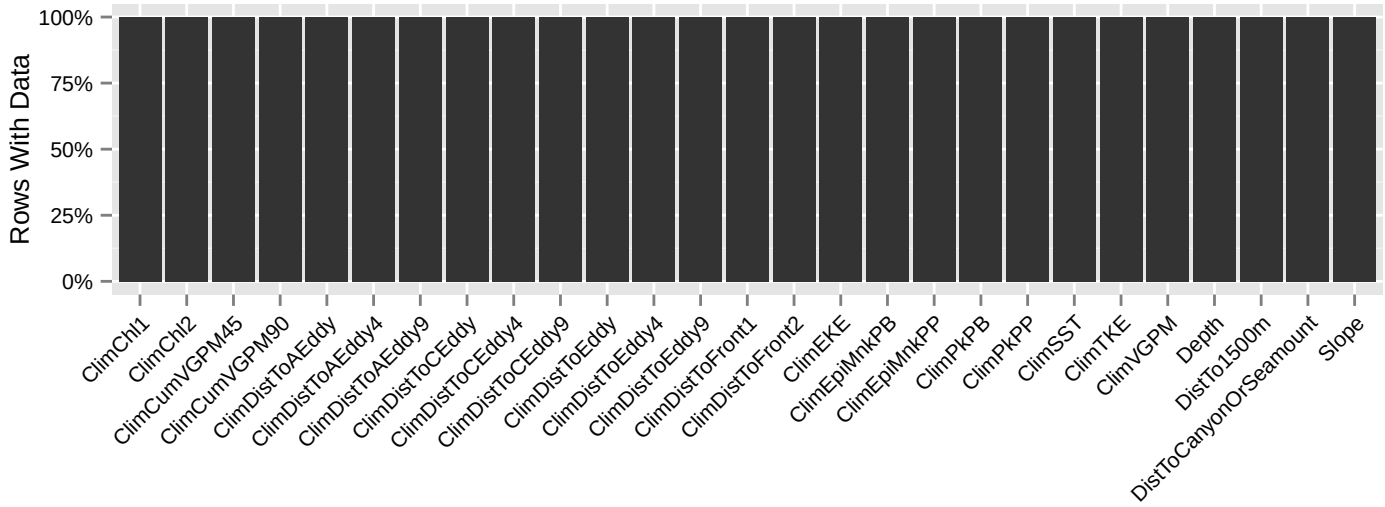

Figure 40: Segments with predictor values for the Beaked whales Climatological model, Slope and Abyss. This plot is used to assess how many segments would be lost by including a given predictor in a model.

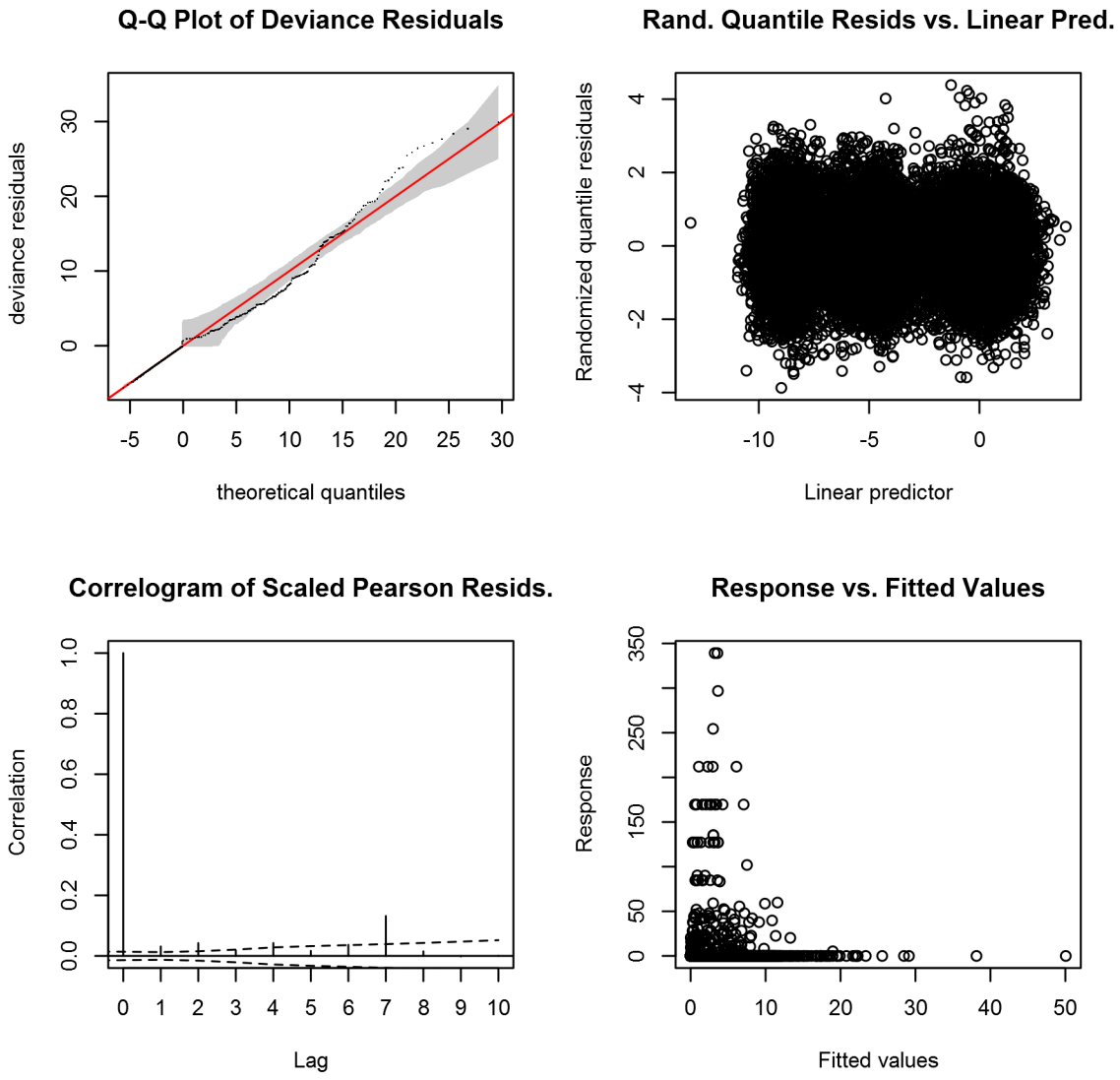

Figure 41: Statistical diagnostic plots for the Beaked whales Climatological model, Slope and Abyss.

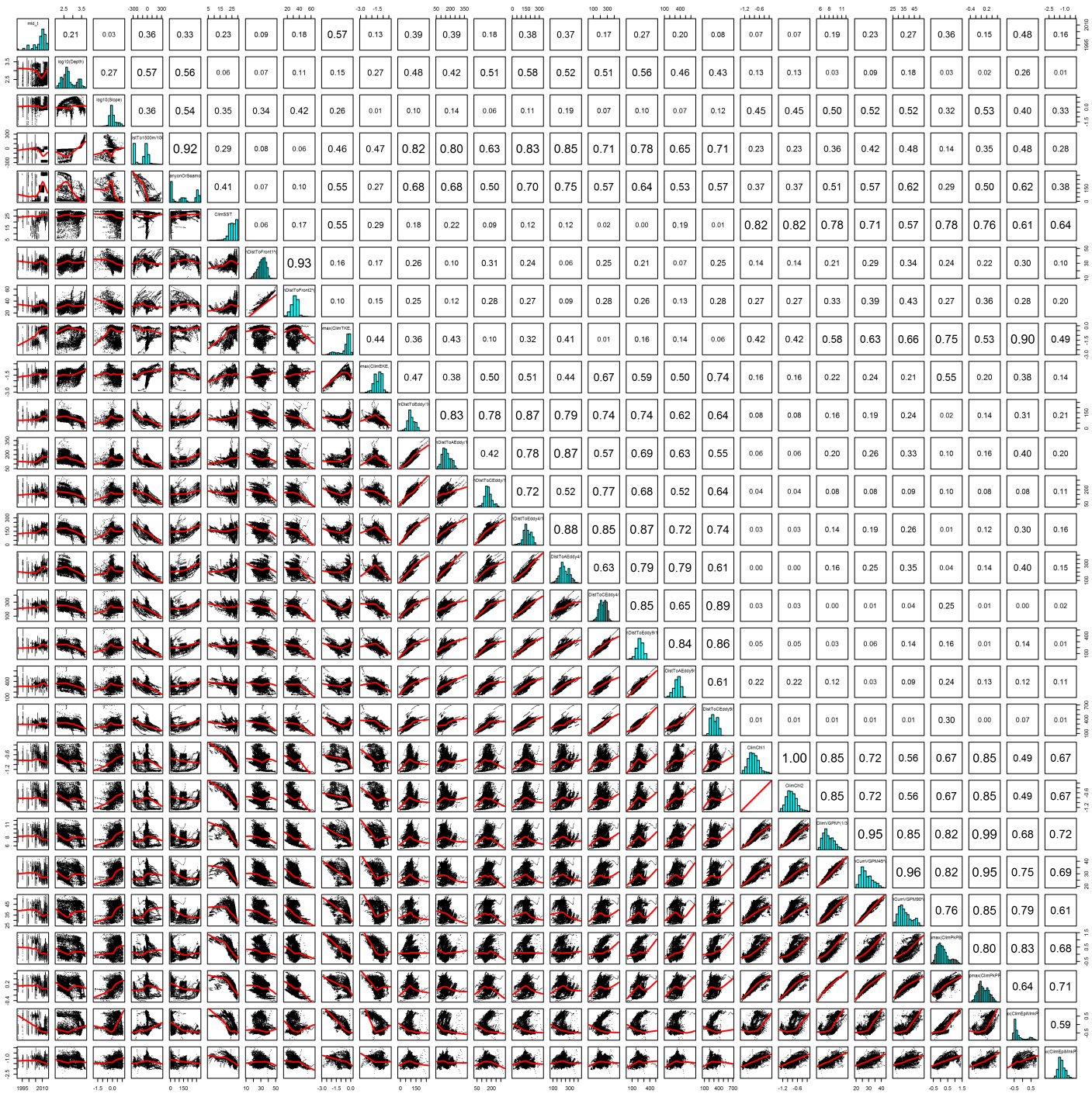

Figure 42: Scatterplot matrix for the Beaked whales Climatological model, Slope and Abyss. This plot is used to inspect the distribution of predictors (via histograms along the diagonal), simple correlation between predictors (via pairwise Pearson coefficients above the diagonal), and linearity of predictor correlations (via scatterplots below the diagonal). This plot is best viewed at high magnification.

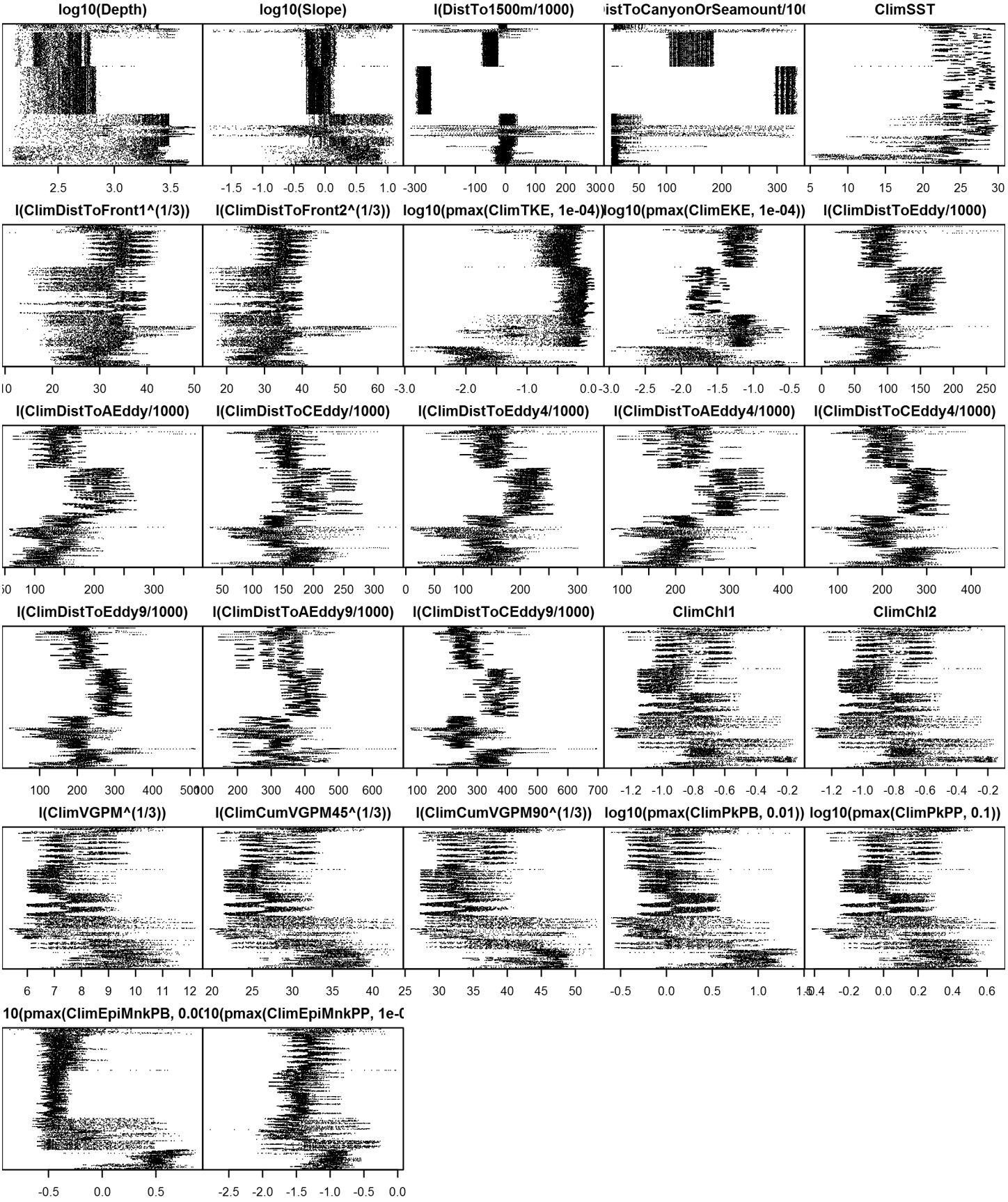

Figure 43: Dotplot for the Beaked whales Climatological model, Slope and Abyss. This plot is used to check for suspicious patterns and outliers in the data. Points are ordered vertically by transect ID, sequentially in time.

Shelf

A mean density estimate was made for this region. First, density (individuals per square kilometer) was calculated as the number of animals encountered divided by the area effectively surveyed, corrected by the detection functions and g(0) estimates. Then, density was multiplied by the size of each grid cell, in square kilometers, to obtain abundance (number of individuals) per grid cell. Finally, all grid cells in the region were assigned this abundance value.

Contemporaneous Model

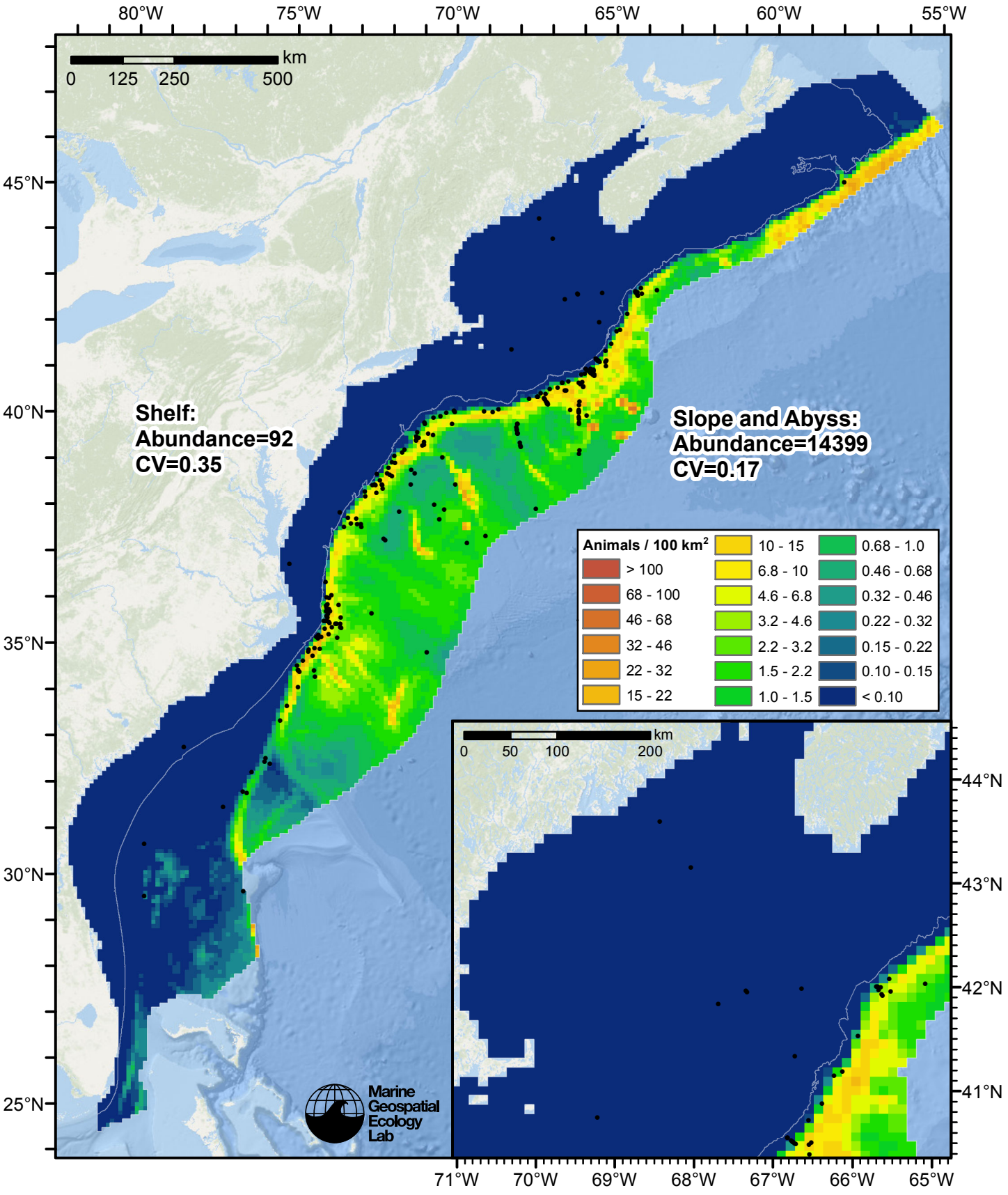

Figure 44: Beaked whales density predicted by the contemporaneous model that explained the most deviance. Pixels are 10x10 km. The legend gives the estimated individuals per pixel; breaks are logarithmic. Abundance for each region was computed by summing the density cells occuring in that region.

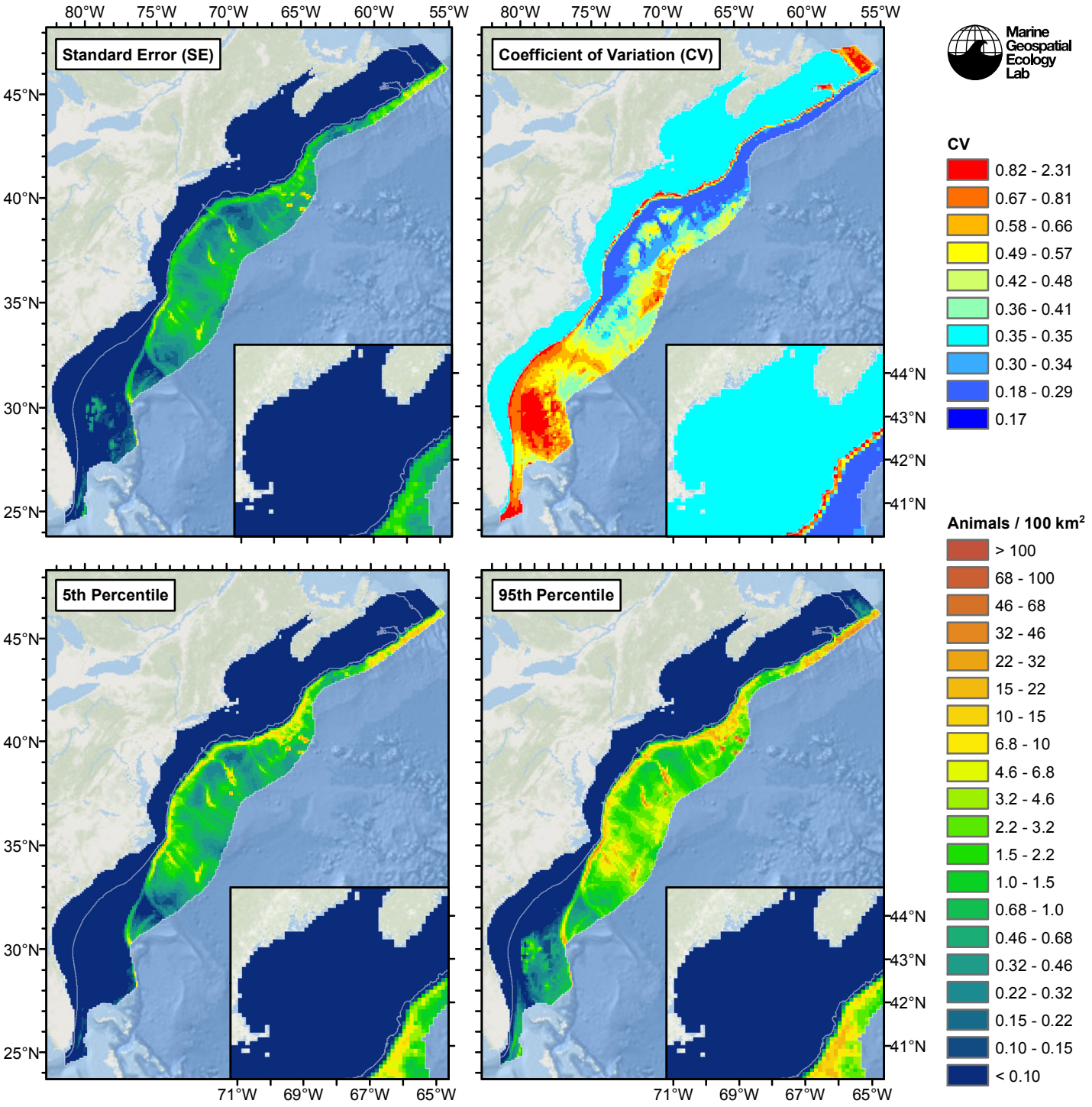

Figure 45: Estimated uncertainty for the contemporaneous model that explained the most deviance. These estimates only incorporate the statistical uncertainty estimated for the spatial model (by the R mgcv package). They do not incorporate uncertainty in the detection functions, g(0) estimates, predictor variables, and so on.

Slope and Abyss

Statistical output

```
Rscript.exe: This is mgcv 1.8-3. For overview type 'help("mgcv-package")'.


Family: Tweedie(p=1.466)
```

```
Link function: log

Formula:
abundance ~ offset(log(area_km2)) + s(log10(Depth), bs = "ts",
    k = 5) + s(log10(Slope), bs = "ts", k = 5) + s(I(DistToCanyonOrSeamount/1000),
    bs = "ts", k = 5) + s(I(DistToFront2^(1/3)), bs = "ts", k = 5) +
    s(I(DistToAEddy/1000), bs = "ts", k = 5) + s(I(CumVGPM90^(1/3)),
    bs = "ts", k = 5)

Parametric coefficients:
            Estimate Std. Error t value Pr(>|t|)
(Intercept)  -7.7714     0.3716  -20.91   <2e-16 ***
---
Signif. codes:  0 '***' 0.001 '**' 0.01 '*' 0.05 '.' 0.1 ' ' 1

Approximate significance of smooth terms:
                                    edf Ref.df      F  p-value
s(log10(Depth))                  1.2775      4 11.513 3.06e-12 ***
s(log10(Slope))                  2.9892      4 17.013  < 2e-16 ***
s(I(DistToCanyonOrSeamount/1000)) 1.0002      4  3.660 6.76e-05 ***
s(I(DistToFront2^(1/3)))         0.8714      4  1.165 0.018152 *
s(I(DistToAEddy/1000))           2.7835      4  4.426 0.000148 ***
s(I(CumVGPM90^(1/3)))            2.6912      4  2.882 0.003423 **
---
Signif. codes:  0 '***' 0.001 '**' 0.01 '*' 0.05 '.' 0.1 ' ' 1

R-sq.(adj) =  -0.0348   Deviance explained = 45.3%
-REML = 1430.3  Scale est. = 91.831    n = 16520

All predictors were significant. This is the final model.
Creating term plots.
Diagnostic output from gam.check():

Method: REML   Optimizer: outer newton
full convergence after 10 iterations.
Gradient range [-4.621484e-05,0.0002962233]
(score 1430.288 & scale 91.83085).
Hessian positive definite, eigenvalue range [0.05570196,368.7672].
Model rank =  25 / 25

Basis dimension (k) checking results. Low p-value (k-index<1) may
indicate that k is too low, especially if edf is close to k'.

                                   k'   edf k-index p-value
s(log10(Depth))                 4.000 1.277   0.517    0.00
s(log10(Slope))                 4.000 2.989   0.594    0.00
s(I(DistToCanyonOrSeamount/1000)) 4.000 1.000   0.578    0.00
s(I(DistToFront2^(1/3)))        4.000 0.871   0.718    0.01
s(I(DistToAEddy/1000))          4.000 2.784   0.714    0.00
s(I(CumVGPM90^(1/3)))           4.000 2.691   0.709    0.00

Predictors retained during the model selection procedure: Depth, Slope, DistToCanyonOrSeamount,
DistToFront2, DistToAEddy, CumVGPM90

Predictors dropped during the model selection procedure: DistTo1500m, SST, TKE, DistToCEddy
```

Model term plots

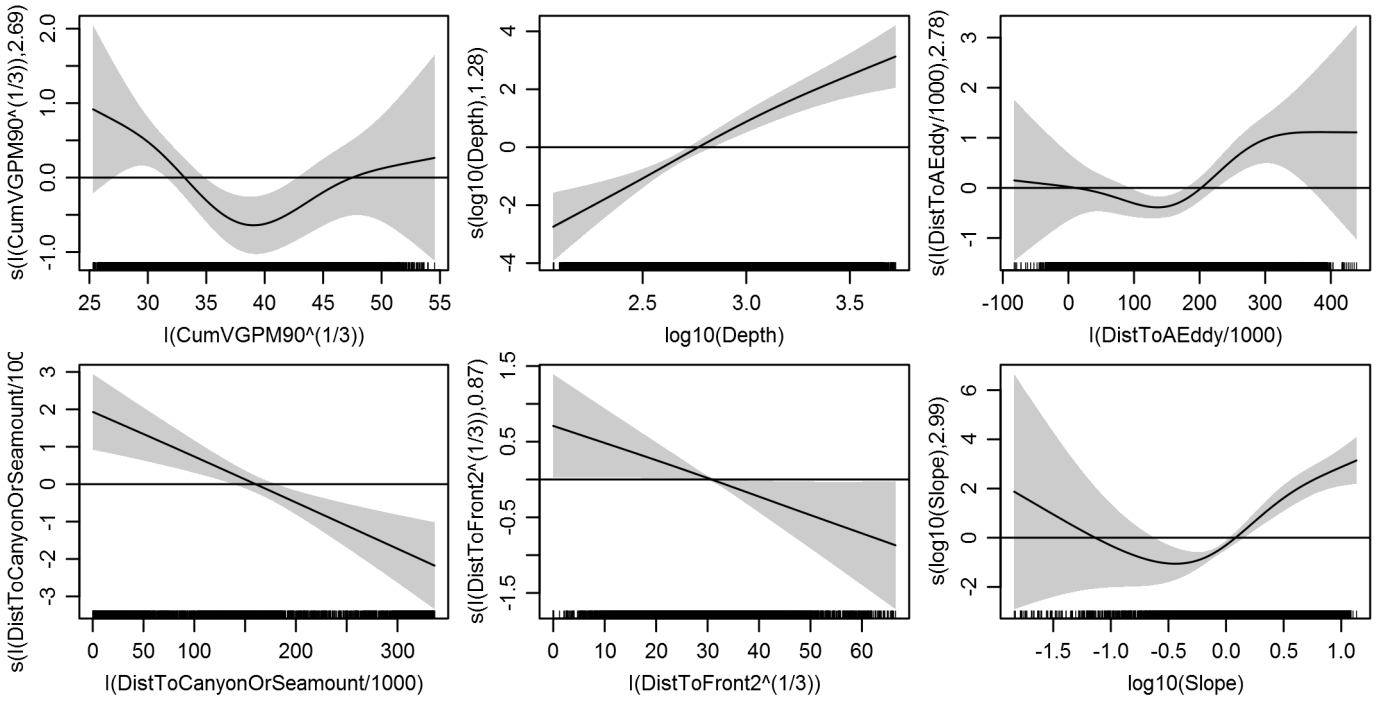

Diagnostic plots

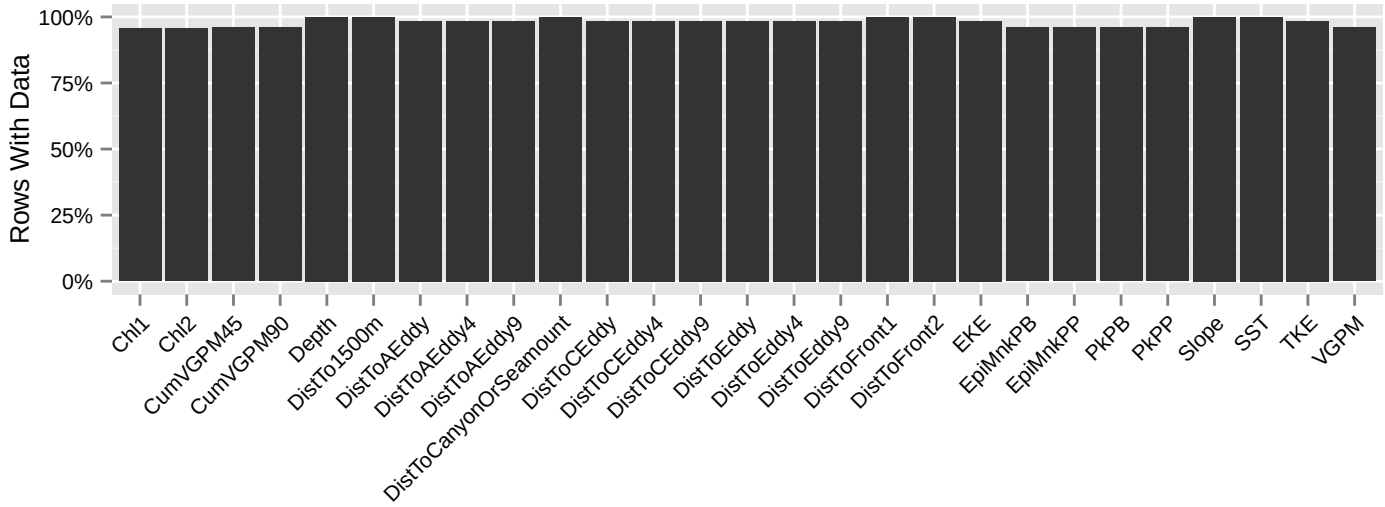

Figure 46: Segments with predictor values for the Beaked whales Contemporaneous model, Slope and Abyss. This plot is used to assess how many segments would be lost by including a given predictor in a model.

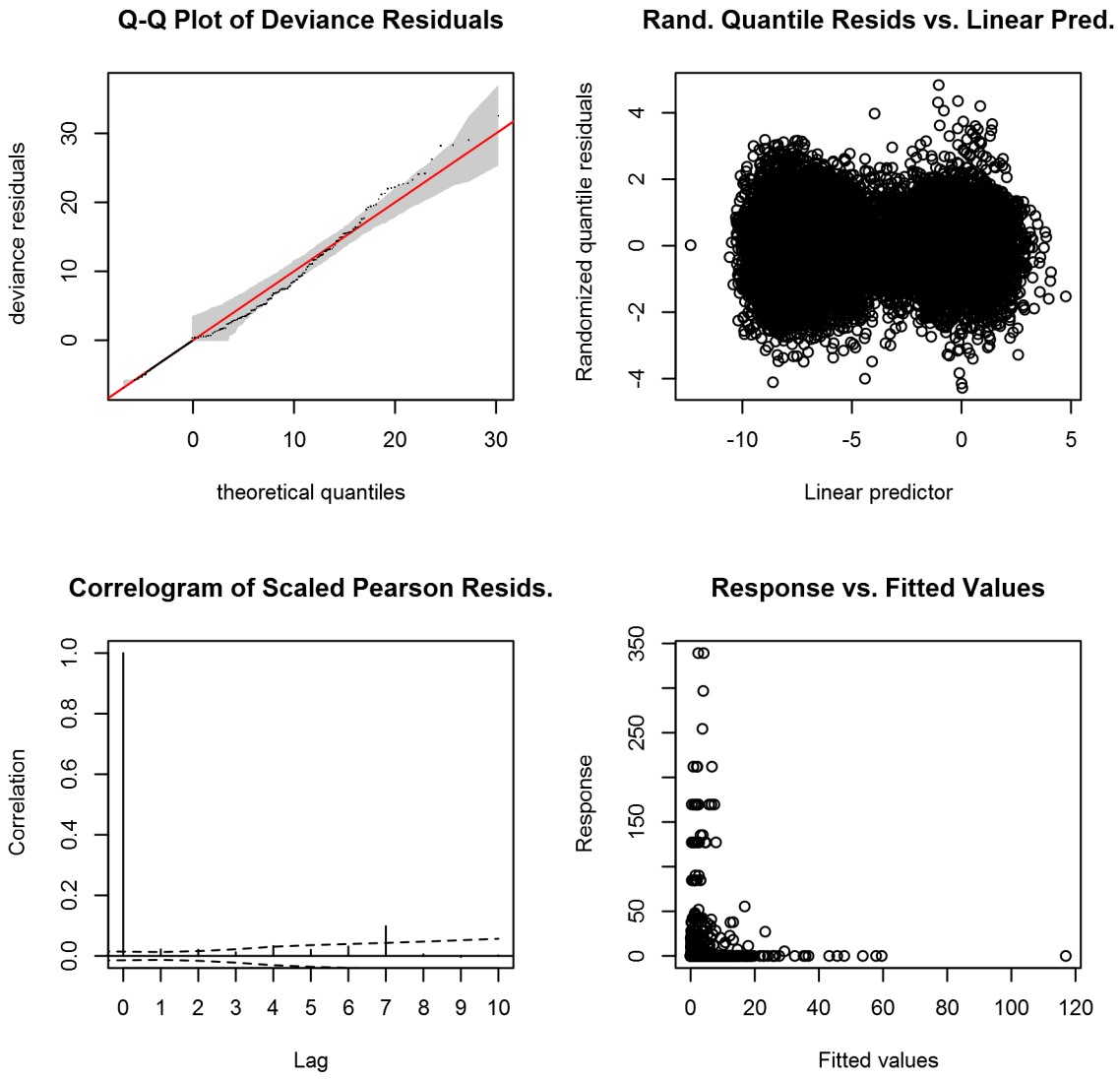

Figure 47: Statistical diagnostic plots for the Beaked whales Contemporaneous model, Slope and Abyss.

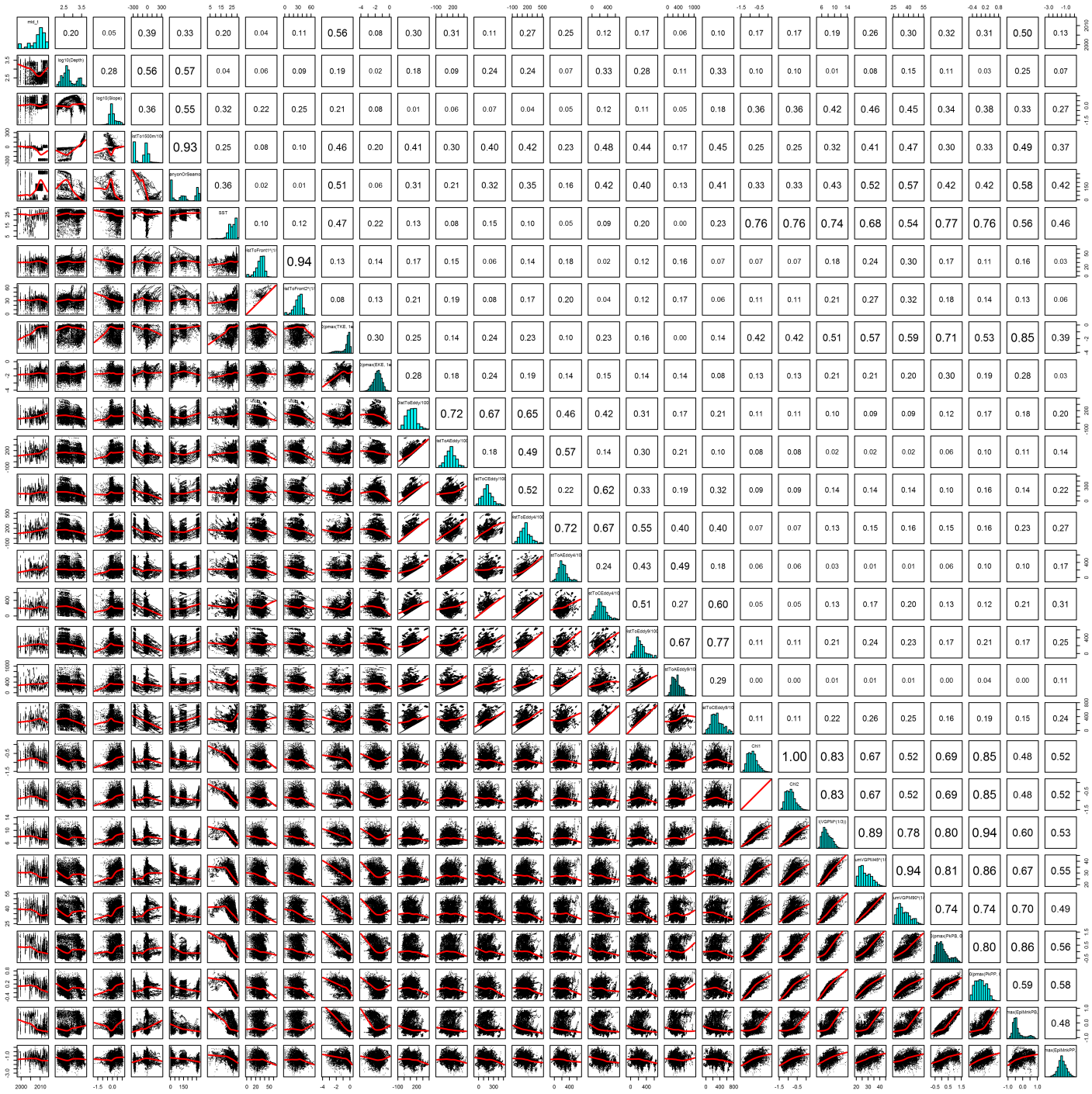

Figure 48: Scatterplot matrix for the Beaked whales Contemporaneous model, Slope and Abyss. This plot is used to inspect the distribution of predictors (via histograms along the diagonal), simple correlation between predictors (via pairwise Pearson coefficients above the diagonal), and linearity of predictor correlations (via scatterplots below the diagonal). This plot is best viewed at high magnification.

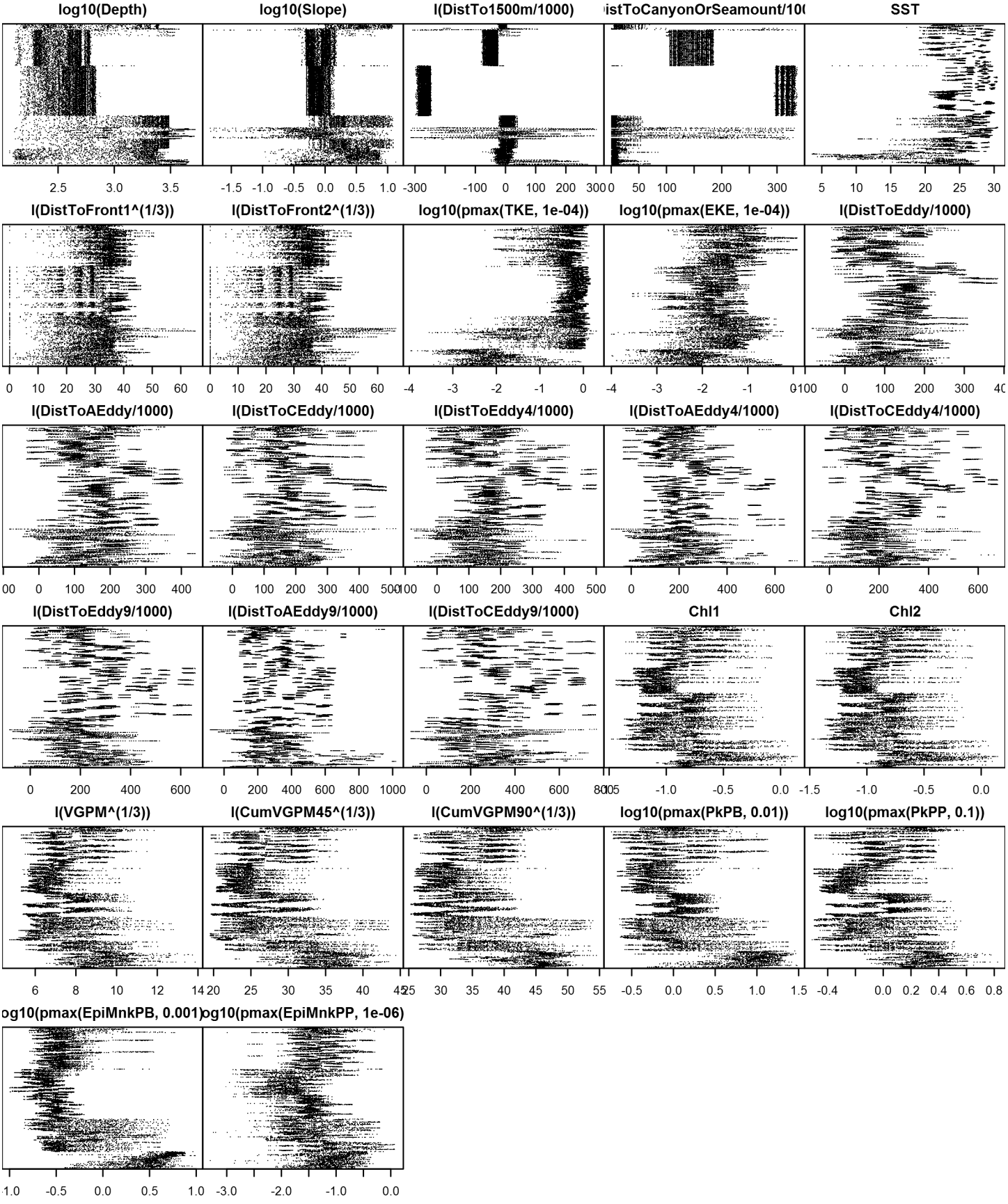

Figure 49: Dotplot for the Beaked whales Contemporaneous model, Slope and Abyss. This plot is used to check for suspicious patterns and outliers in the data. Points are ordered vertically by transect ID, sequentially in time.

Shelf

A mean density estimate was made for this region. First, density (individuals per square kilometer) was calculated as the number of animals encountered divided by the area effectively surveyed, corrected by the detection functions and g(0) estimates. Then, density was multiplied by the size of each grid cell, in square kilometers, to obtain abundance (number of individuals) per grid cell. Finally, all grid cells in the region were assigned this abundance value.

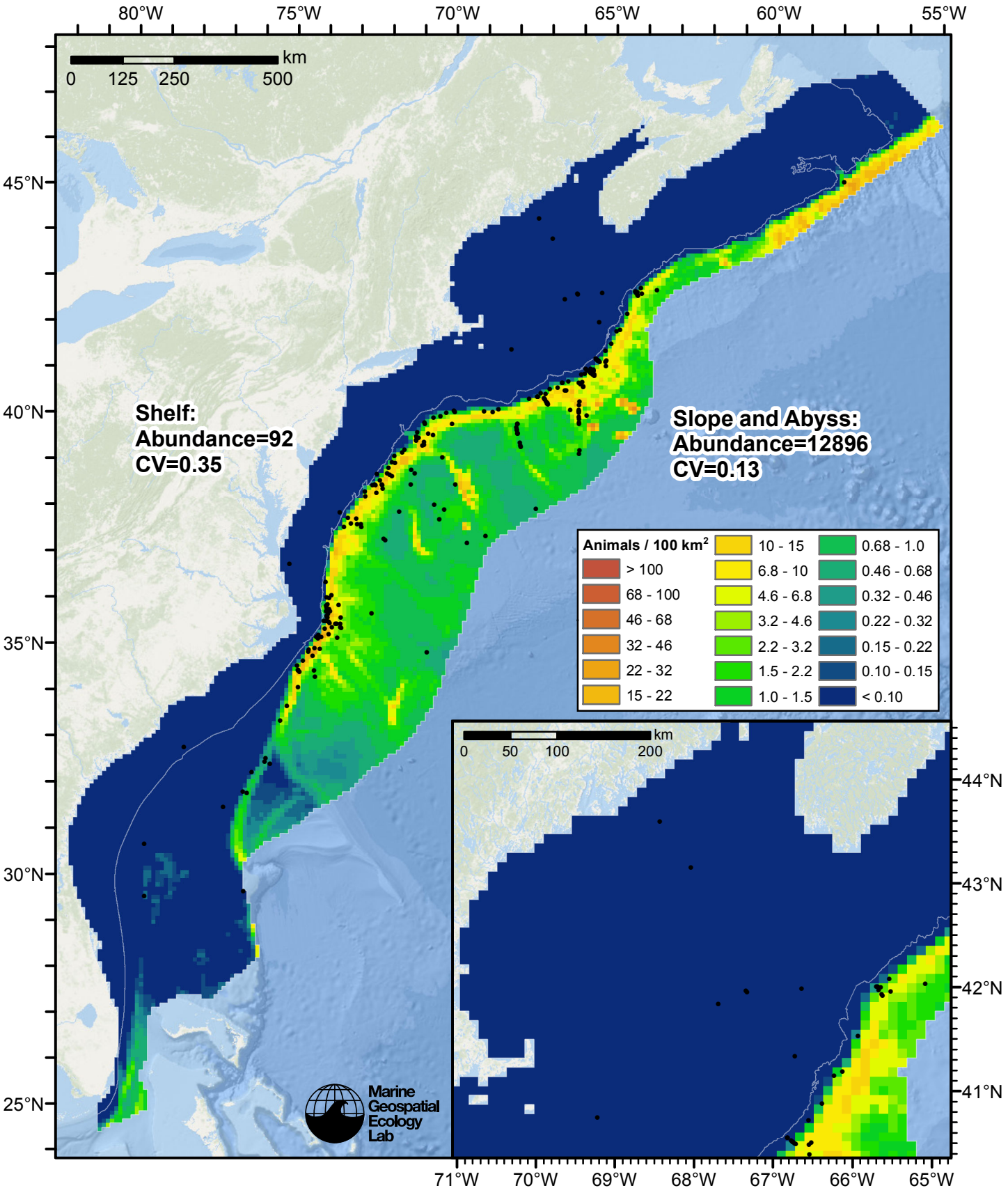

Figure 50: Beaked whales density predicted by the climatological same segments model that explained the most deviance. Pixels are 10x10 km. The legend gives the estimated individuals per pixel; breaks are logarithmic. Abundance for each region was computed by summing the density cells occuring in that region.

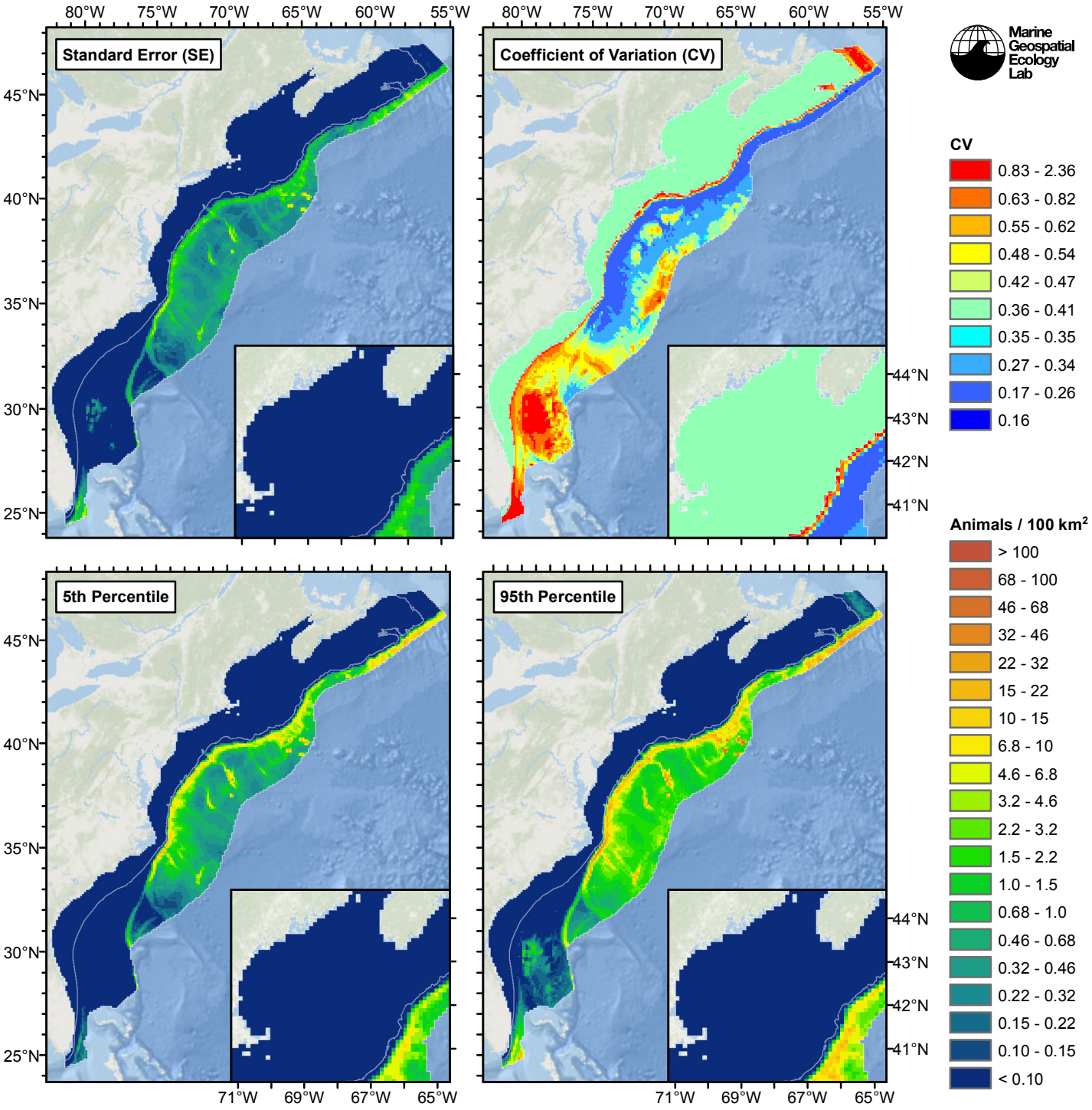

Figure 51: Estimated uncertainty for the climatological same segments model that explained the most deviance. These estimates only incorporate the statistical uncertainty estimated for the spatial model (by the R mgcv package). They do not incorporate uncertainty in the detection functions, g(0) estimates, predictor variables, and so on.

Slope and Abyss

Statistical output

```
Rscript.exe: This is mgcv 1.8-3. For overview type 'help("mgcv-package")'.


Family: Tweedie(p=1.462)
```

```
Link function: log

Formula:
abundance ~ offset(log(area_km2)) + s(log10(Depth), bs = "ts",
    k = 5) + s(log10(Slope), bs = "ts", k = 5) + s(I(DistToCanyonOrSeamount/1000),
    bs = "ts", k = 5) + s(I(ClimDistToAEddy/1000), bs = "ts",
    k = 5)

Parametric coefficients:
            Estimate Std. Error t value Pr(>|t|)
(Intercept)  -7.2068     0.3141  -22.94   <2e-16 ***
---
Signif. codes:  0 '***' 0.001 '**' 0.01 '*' 0.05 '.' 0.1 ' ' 1

Approximate significance of smooth terms:
                                    edf Ref.df      F  p-value
s(log10(Depth))                  1.3573      4 14.554 2.79e-15 ***
s(log10(Slope))                  2.9663      4 15.842  < 2e-16 ***
s(I(DistToCanyonOrSeamount/1000)) 0.9778      4  3.084 0.000235 ***
s(I(ClimDistToAEddy/1000))       1.0042      4  3.345 0.000133 ***
---
Signif. codes:  0 '***' 0.001 '**' 0.01 '*' 0.05 '.' 0.1 ' ' 1

R-sq.(adj) =  -0.0137   Deviance explained = 42.7%
-REML = 1429.3  Scale est. = 94.083    n = 16520

All predictors were significant. This is the final model.
Creating term plots.
Diagnostic output from gam.check():

Method: REML   Optimizer: outer newton
full convergence after 12 iterations.
Gradient range [-0.0001256147,0.0004366088]
(score 1429.257 & scale 94.08336).
Hessian positive definite, eigenvalue range [0.1832516,376.7227].
Model rank =  17 / 17

Basis dimension (k) checking results. Low p-value (k-index<1) may
indicate that k is too low, especially if edf is close to k'.

                                   k'   edf k-index p-value
s(log10(Depth))                 4.000 1.357   0.644    0.00
s(log10(Slope))                 4.000 2.966   0.645    0.00
s(I(DistToCanyonOrSeamount/1000)) 4.000 0.978   0.643    0.00
s(I(ClimDistToAEddy/1000))      4.000 1.004   0.759    0.08

Predictors retained during the model selection procedure: Depth, Slope, DistToCanyonOrSeamount,
ClimDistToAEddy

Predictors dropped during the model selection procedure: DistTo1500m, ClimSST, ClimDistToFront1,
ClimTKE, ClimDistToCEddy, ClimChl1
```

Model term plots

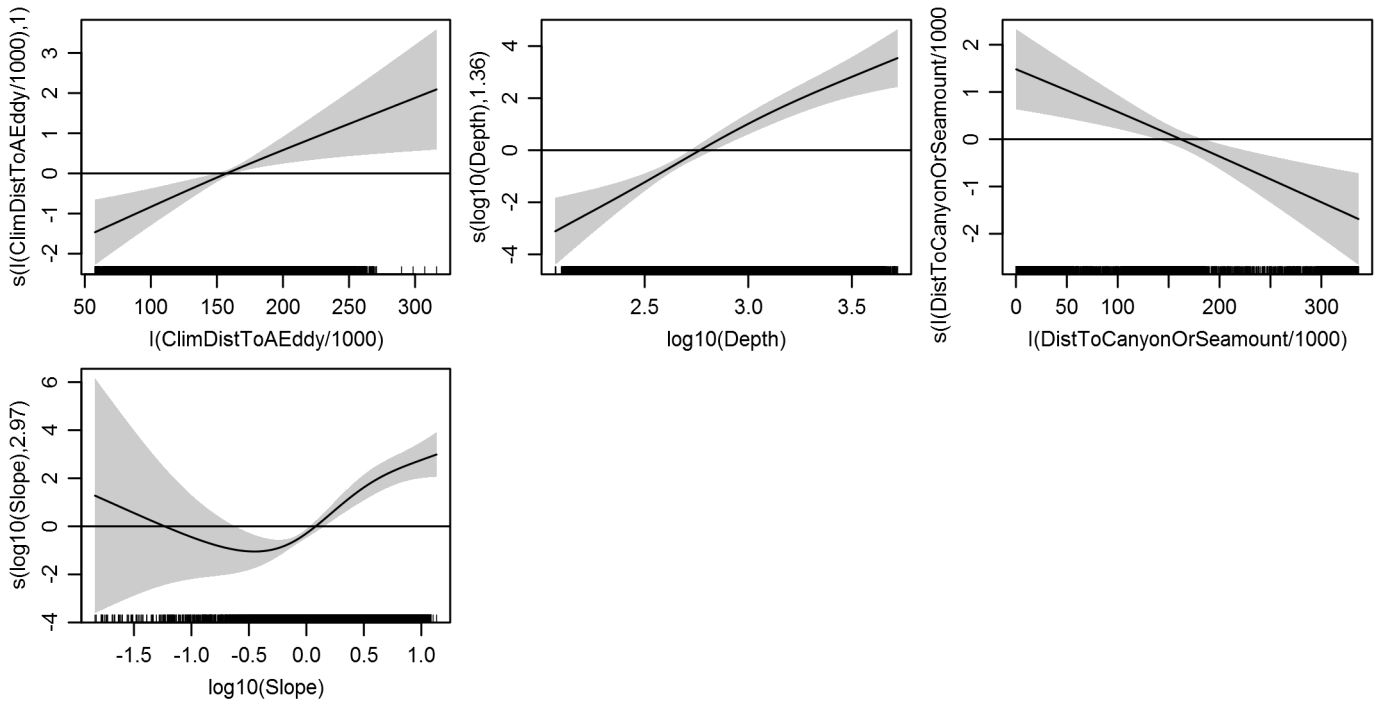

Diagnostic plots

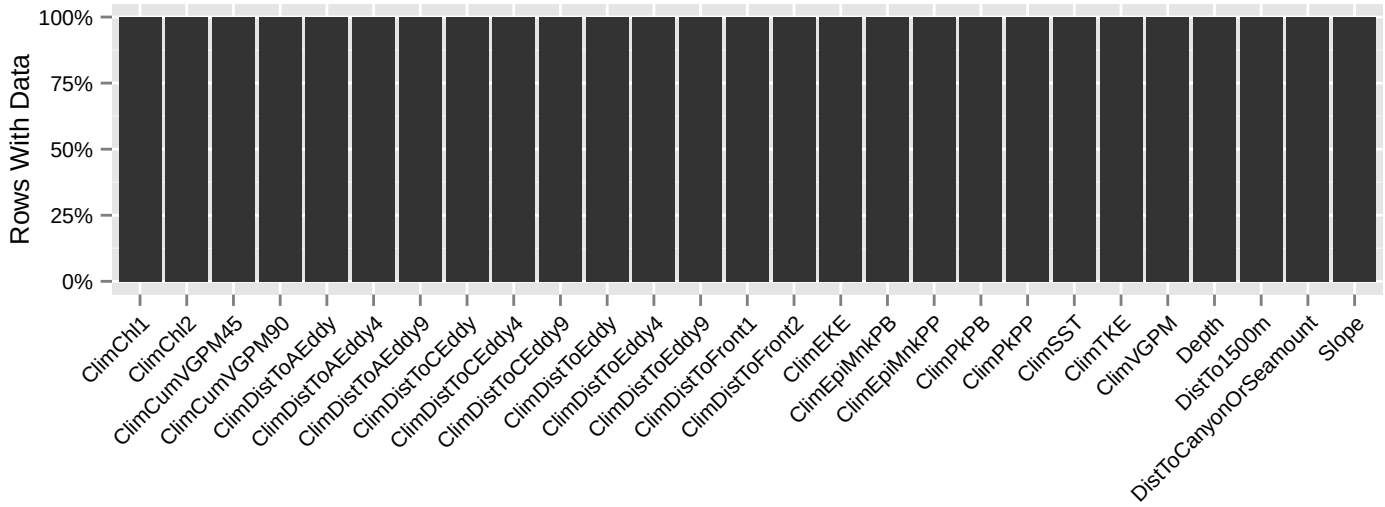

Figure 52: Segments with predictor values for the Beaked whales Climatological model, Slope and Abyss. This plot is used to assess how many segments would be lost by including a given predictor in a model.

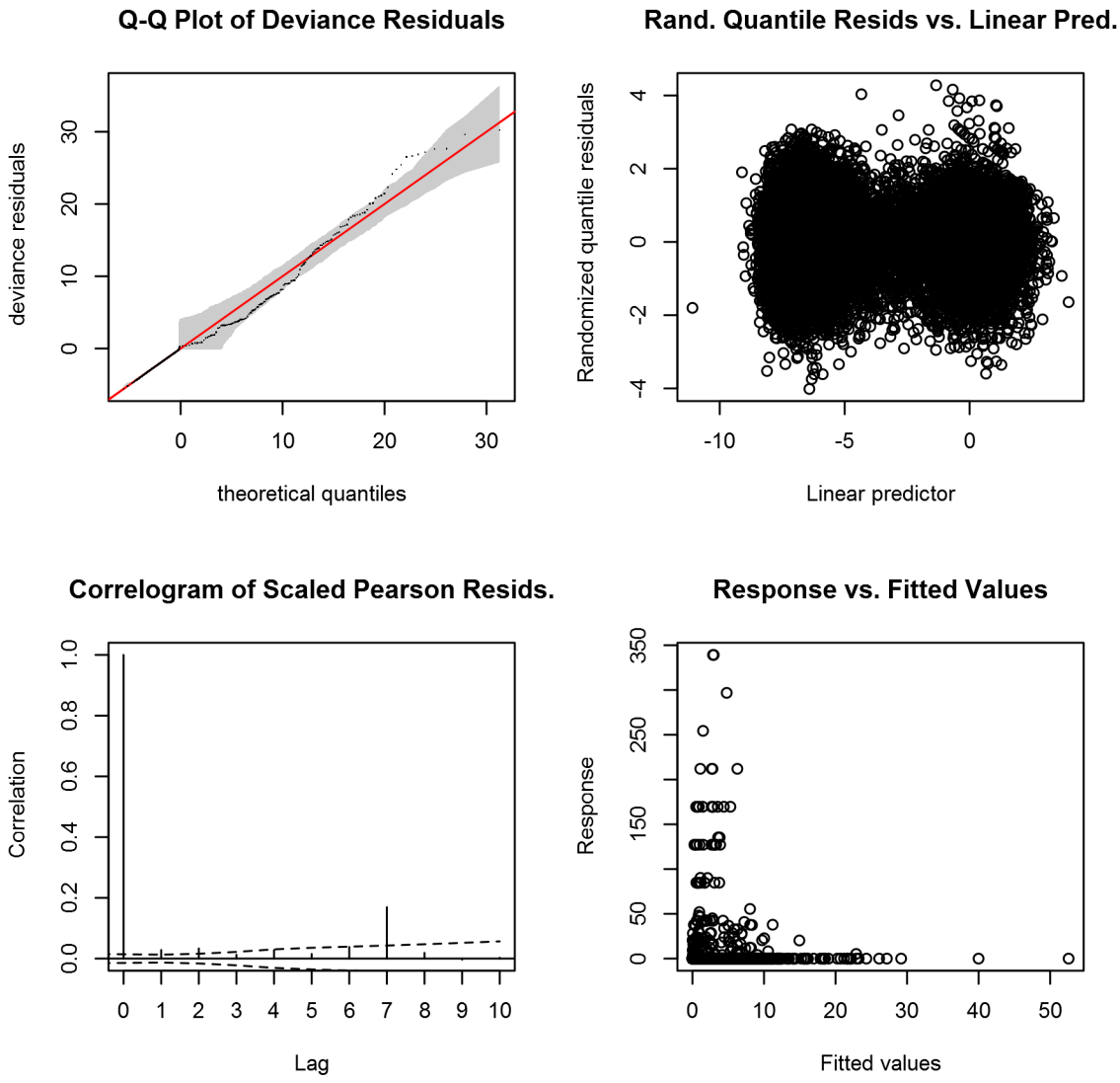

Figure 53: Statistical diagnostic plots for the Beaked whales Climatological model, Slope and Abyss.

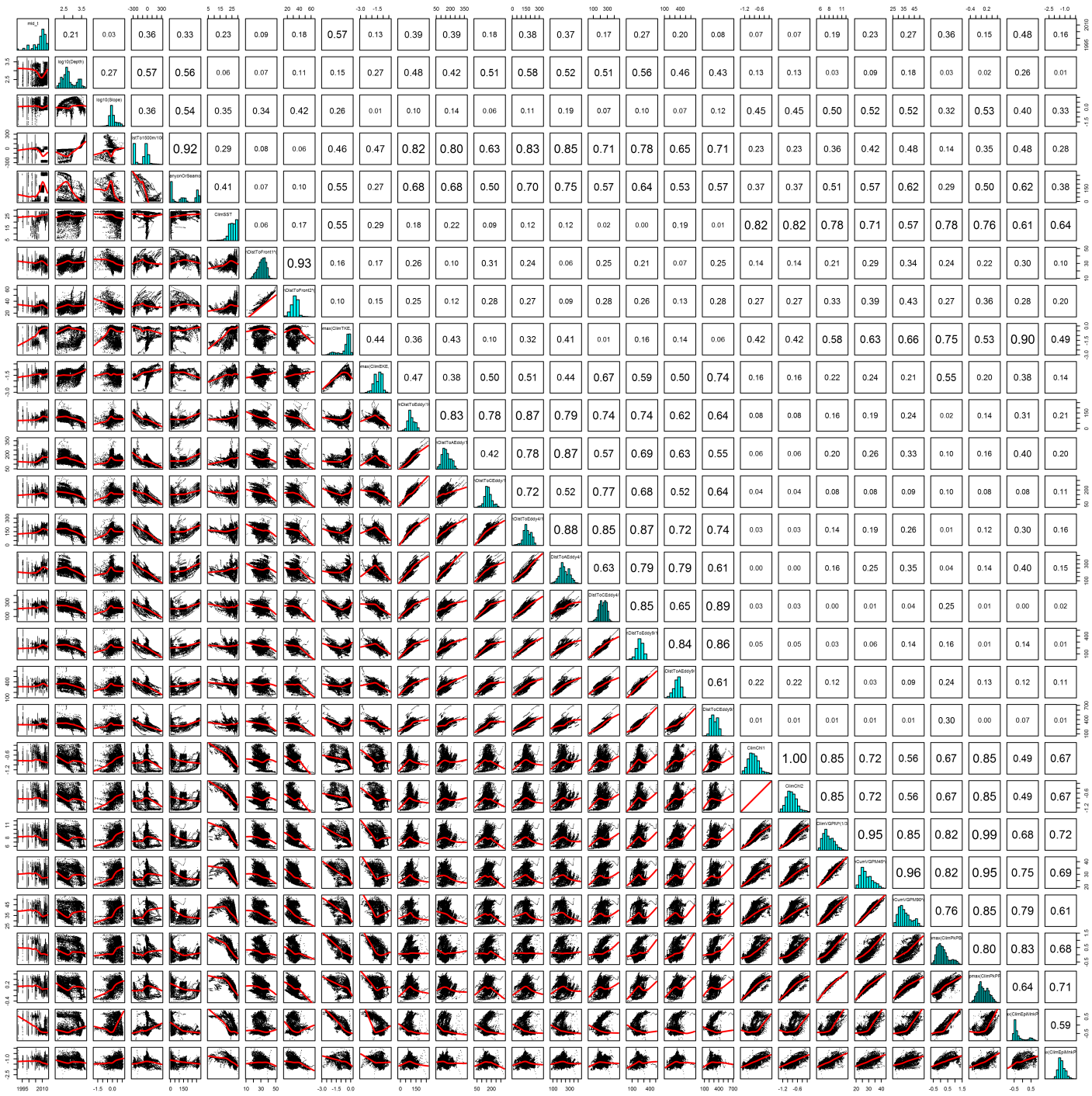

Figure 54: Scatterplot matrix for the Beaked whales Climatological model, Slope and Abyss. This plot is used to inspect the distribution of predictors (via histograms along the diagonal), simple correlation between predictors (via pairwise Pearson coefficients above the diagonal), and linearity of predictor correlations (via scatterplots below the diagonal). This plot is best viewed at high magnification.

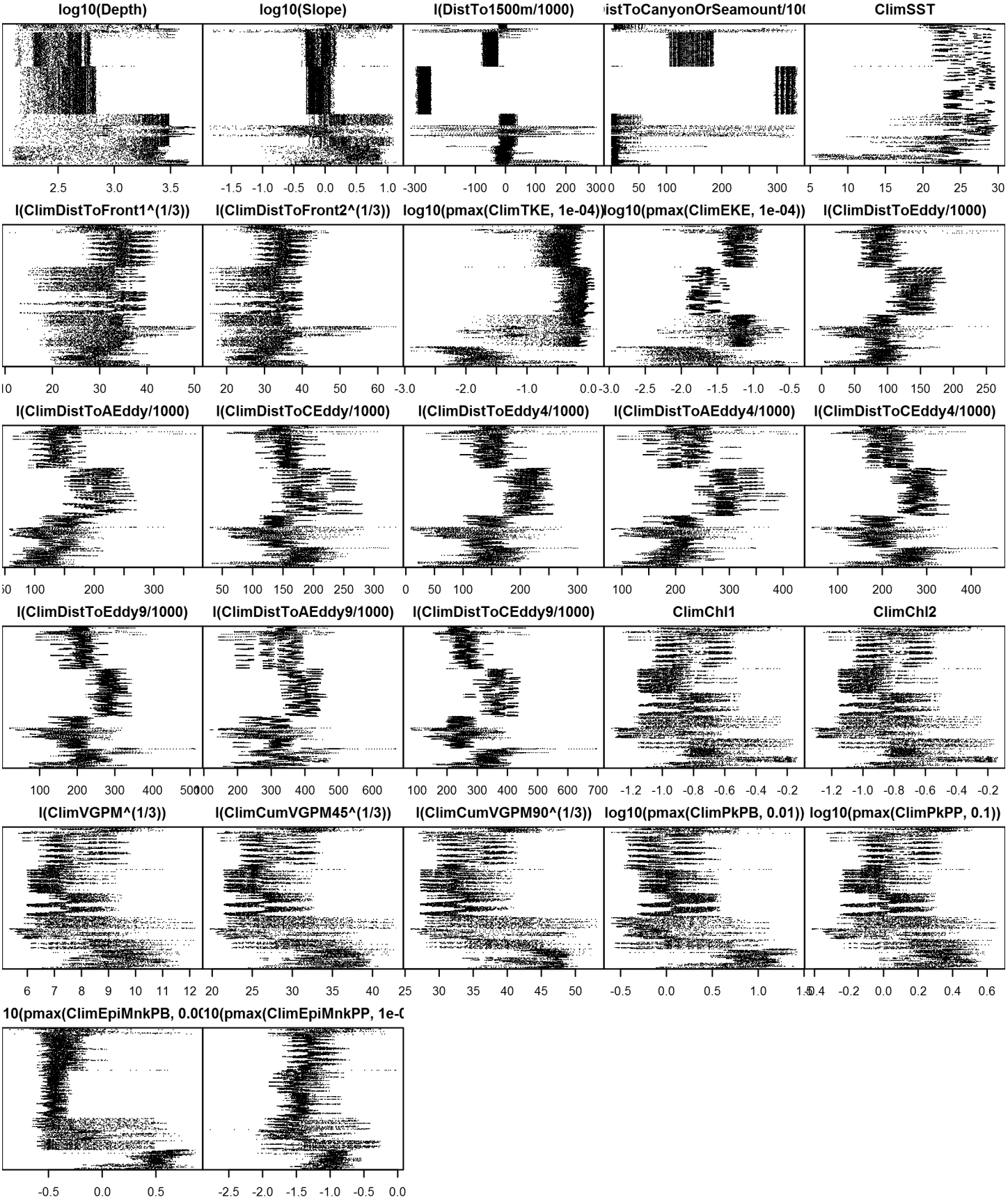

Figure 55: Dotplot for the Beaked whales Climatological model, Slope and Abyss. This plot is used to check for suspicious patterns and outliers in the data. Points are ordered vertically by transect ID, sequentially in time.

Shelf

A mean density estimate was made for this region. First, density (individuals per square kilometer) was calculated as the number of animals encountered divided by the area effectively surveyed, corrected by the detection functions and g(0) estimates. Then, density was multiplied by the size of each grid cell, in square kilometers, to obtain abundance (number of individuals) per grid cell. Finally, all grid cells in the region were assigned this abundance value.

Model Comparison

Spatial Model Performance

The table below summarizes the performance of the candidate spatial models that were tested. The first model contained only physiographic predictors. Subsequent models added additional suites of predictors of based on when they became available via remote sensing.

For each model, three versions were fitted; the % Dev Expl columns give the % deviance explained by each one. The "climatological" models were fitted to 8-day climatologies of the environmental predictors. Because the environmental predictors were always available, no segments were lost, allowing these models to consider the maximal amount of survey data. The "contemporaneous" models were fitted to day-of-sighting images of the environmental predictors; these were smoothed to reduce data loss due to clouds, but some segments still failed to retrieve environmental values and were lost. Finally, the "climatological same segments" models fitted climatological predictors to the segments retained by the contemporaneous model, so that the explantory power of the two types of predictors could be directly compared. For each of the three models, predictors were selected independently via shrinkage smoothers; thus the three models did not necessarily utilize the same predictors.

Predictors derived from ocean currents first became available in January 1993 after the launch of the TOPEX/Poseidon satellite; productivity predictors first became available in September 1997 after the launch of the SeaWiFS sensor. Contemporaneous and climatological same segments models considering these predictors usually suffered data loss. Date Range shows the years spanned by the retained segments. The Segments column gives the number of segments retained; % Lost gives the percentage lost.

Predictors	Climatol % Dev Expl	Contemp % Dev Expl	Climatol Same Segs % Dev Expl	Segments	% Lost	Date Range
Phys	40.4			17198		1992-2013
Phys+SST	41.0	41.3	41.0	17198	0.0	1992-2013
Phys+SST+Curr	41.2	43.0	42.0	16939	1.5	1995-2013
Phys+SST+Curr+Prod	42.2	45.3	42.7	16520	3.9	1998-2013

Table 22: Deviance explained by the candidate density models.

Abundance Estimates

The table below shows the estimated mean abundance (number of animals) within the study area, for the models that explained the most deviance for each model type. Mean abundance was calculated by first predicting density maps for a series of time steps, then computing the abundance for each map, and then averaging the abundances. For the climatological models, we used 8-day climatologies, resulting in 46 abundance maps. For the contemporaneous models, we used daily images, resulting in 365 predicted abundance maps per year that the prediction spanned. The Dates column gives the dates to which the estimates apply. For our models, these are the years for which both survey data and remote sensing data were available.

The Assumed g(0)=1 column specifies whether the abundance estimate assumed that detection was certain along the survey trackline. Studies that assumed this did not correct for availability or perception bias, and therefore underestimated abundance. The In our models column specifies whether the survey data from the study was also used in our models. If not, the study provides a completely independent estimate of abundance.

Dates	Model or study	Estimated abundance	CV	Assumed g(0)=1	In our models
1992-2013	Climatological model	11432	0.13	No	
1998-2013	Contemporaneous model*	14491	0.17	No	
1992-2013	Climatological same segments model	12988	0.13	No	
Jun-Aug 2011	Central Virginia to lower Bay of Fundy, Mesoplodon spp. (Waring et al. 2014)	5500	0.67	No	No
Jun-Aug 2011	Central Virginia to lower Bay of Fundy, Ziphius cavirostris (Waring et al. 2014)	4962	0.37	No	No
Jun-Aug 2011	Central Virginia to lower Bay of Fundy, all species	10462		No	No
Jun-Aug 2011	Central Florida to central Virginia, Mesoplodon spp. (Waring et al. 2014)	1592	0.67	No	No
Jun-Aug 2011	Central Florida to central Virginia, Ziphius cavirostris (Waring et al. 2014)	1570	0.65	No	No
Jun-Aug 2011	Central Florida to central Virginia, all species	1570	3162	No	No
Jun-Aug 2011	Central Florida to lower Bay of Fundy, combined, Mesoplodon spp.	7092	0.54	No	No
Jun-Aug 2011	Central Florida to lower Bay of Fundy, combined, Ziphius cavirostris	6532	0.32	No	No
Jun-Aug 2011	Central Florida to lower Bay of Fundy, combined, all species	13624		No	No
Jun-Aug 2004	Maryland to Bay of Fundy, all species (Waring et al. 2013)	2839	0.78	No	Yes
Jun-Aug 2004	Florida to Maryland, all species (Waring et al. 2013)	674	0.36	No	Yes
Jun-Aug 2004	Florida to Bay of Fundy, combined, all species	3513	0.63	No	Yes
Jul-Sep 1998	Maryland to Gulf of St. Lawrence, all species (Waring et al. 2006)	2600	0.40	No	Yes
Jul-Aug 1998	Florida to Maryland, all species (Waring et al. 2006)	541	0.55	Yes	Yes
Jul-Aug 1998	Florida to Gulf of St. Lawrence, combined, all species	3141	0.34	Yes/No	Yes

Table 23: Estimated mean abundance within the study area. We selected the model marked with * as our best estimate of the abundance and distribution of this taxon. For comparison, independent abundance estimates from NOAA technical reports and/or the scientific literature are shown. Please see the Discussion section below for our evaluation of our models compared to the other estimates. Note that our abundance estimates are averaged over the whole year, while the other studies may have estimated abundance for specific months or seasons. Our coefficients of variation (CVs) underestimate the true uncertainty in our estimates, as they only incorporated the uncertainty of the GAM stage of our models. Other sources of uncertainty include the detection functions and g(0) estimates. It was not possible to incorporate these into our CVs without undertaking a computationally-prohibitive bootstrap; we hope to attempt that in a future version of our models.

Density Maps

Climatological Model

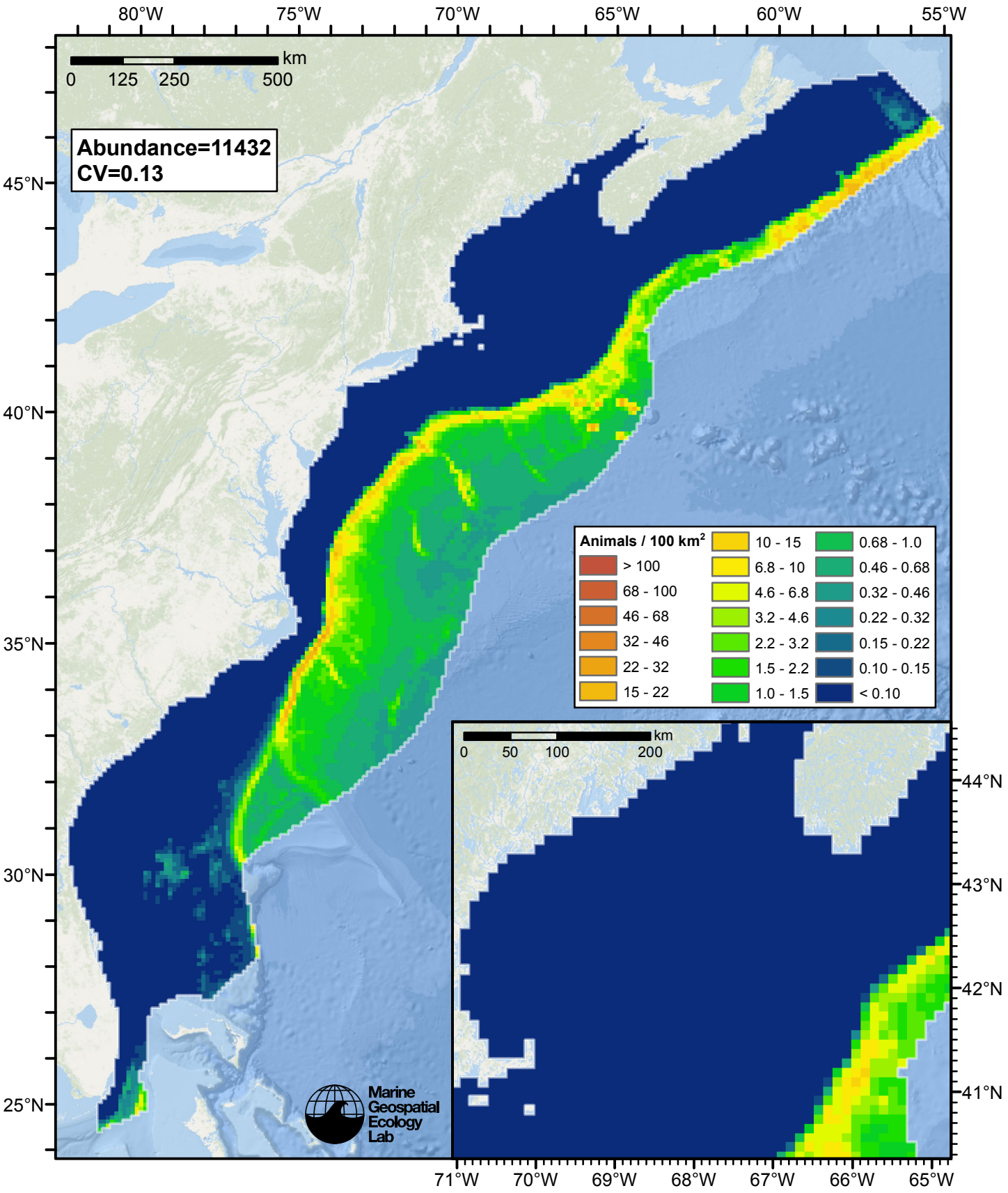

Figure 56: Beaked whales density and abundance predicted by the climatological model that explained the most deviance. Regions inside the study area (white line) where the background map is visible are areas we did not model (see text).

Contemporaneous Model

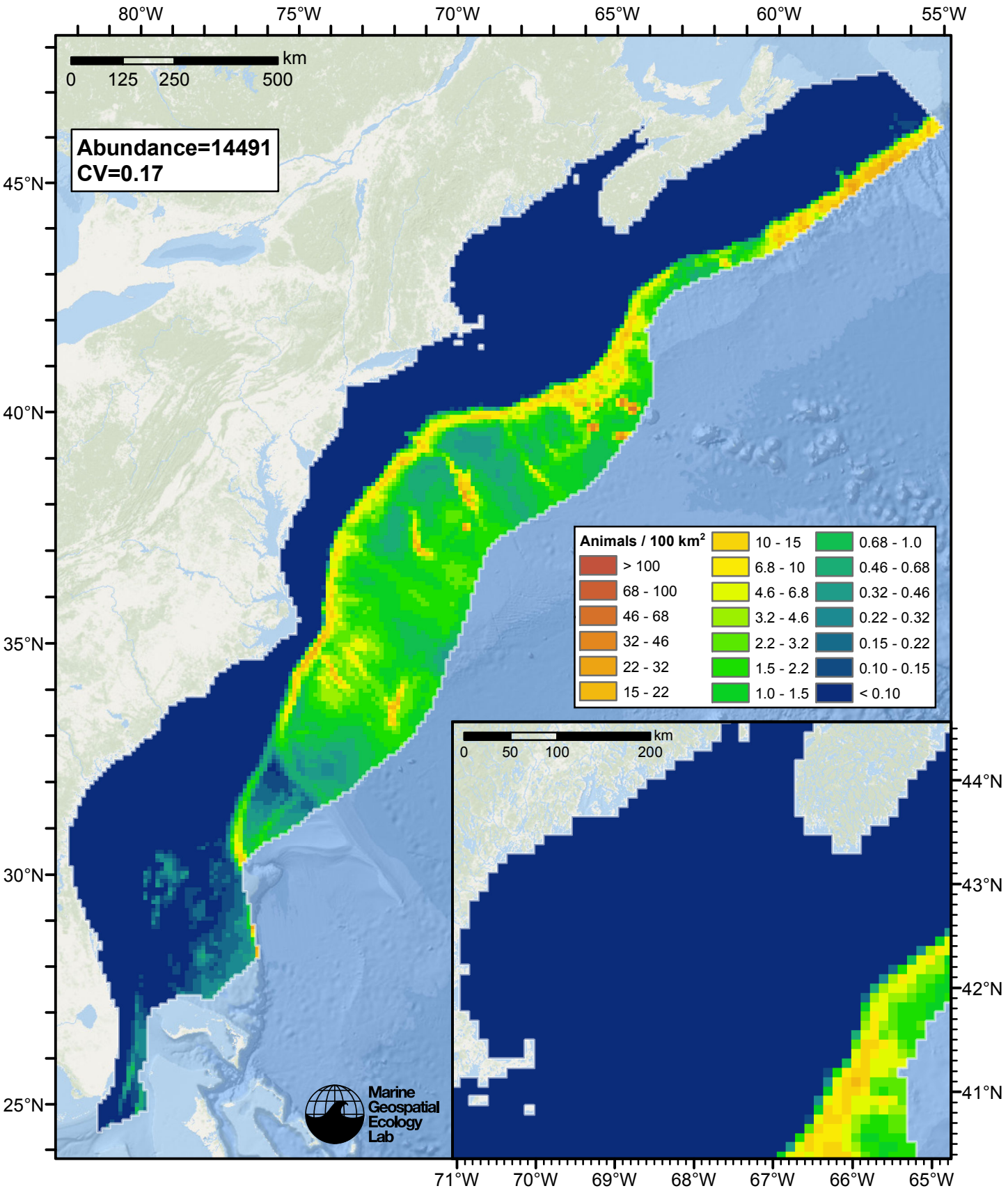

Figure 57: Beaked whales density and abundance predicted by the contemporaneous model that explained the most deviance. Regions inside the study area (white line) where the background map is visible are areas we did not model (see text).

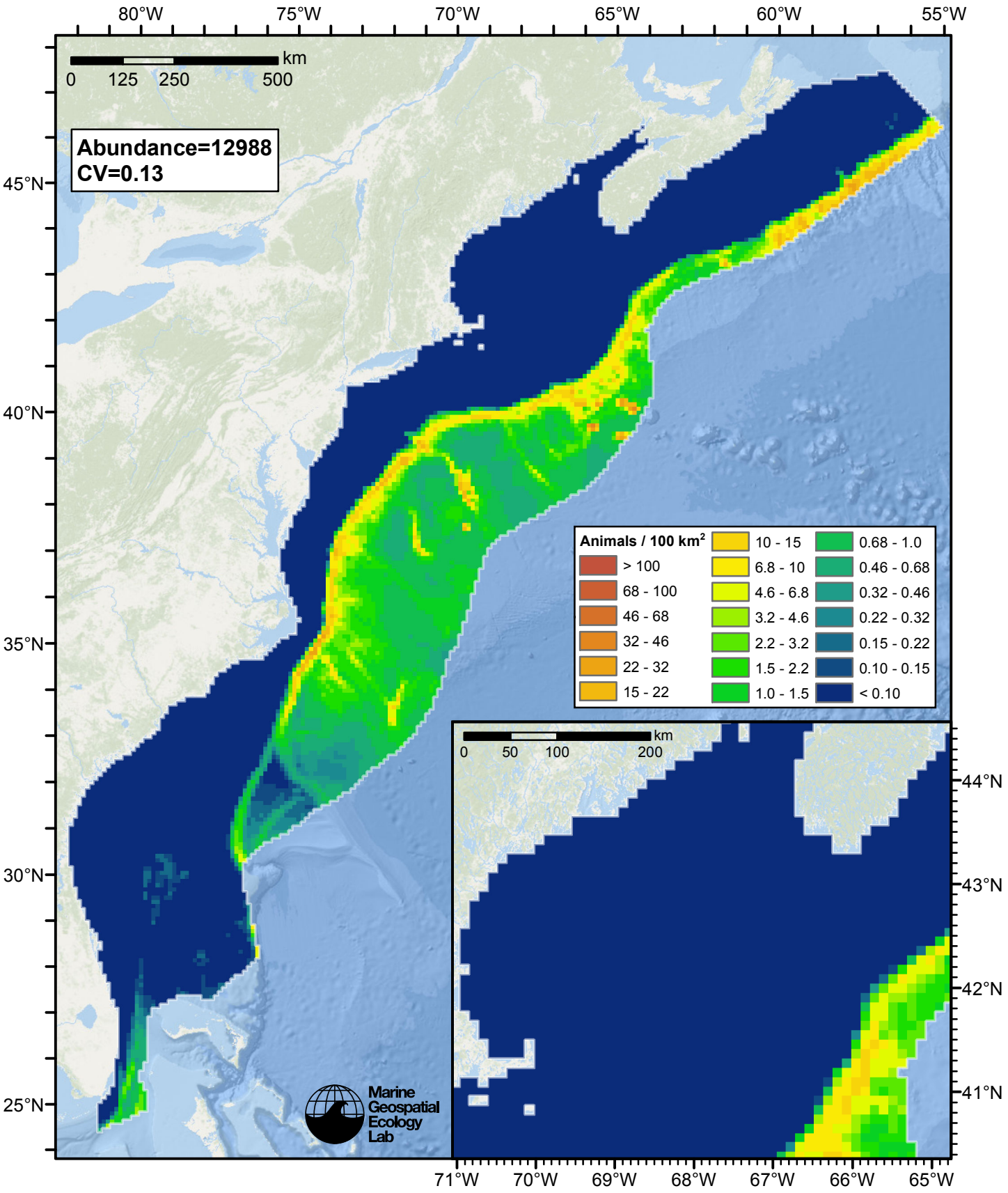

Figure 58: Beaked whales density and abundance predicted by the climatological same segments model that explained the most deviance. Regions inside the study area (white line) where the background map is visible are areas we did not model (see text).

Temporal Variability

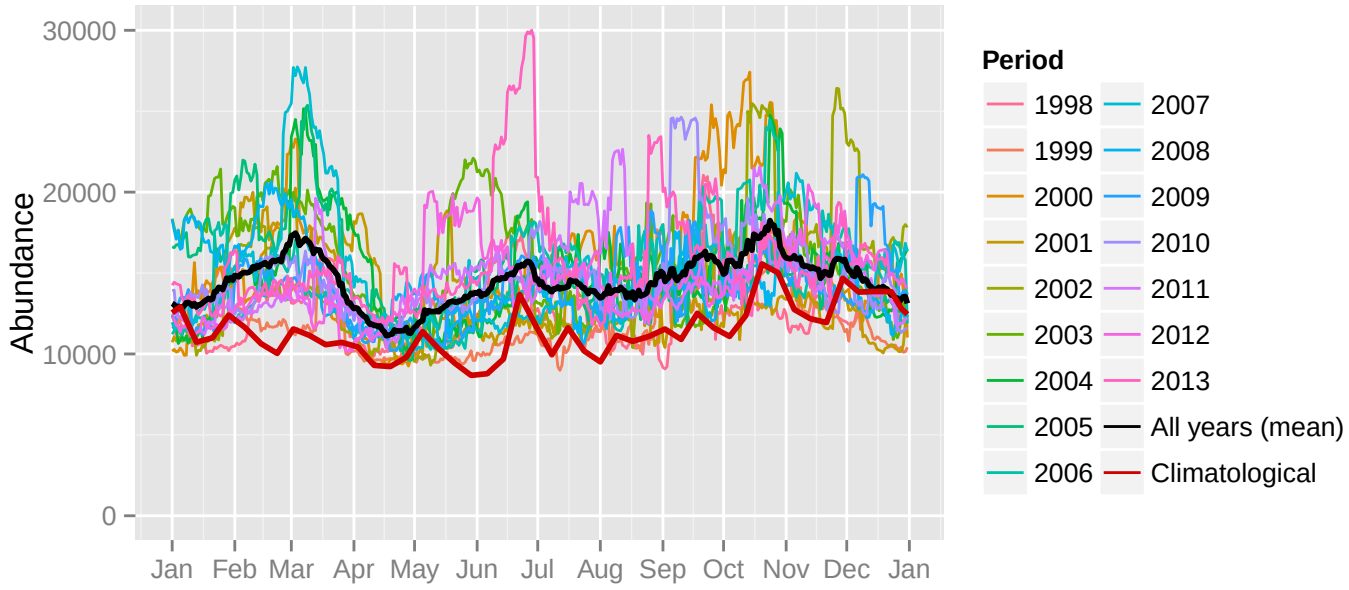

Figure 59: Comparison of Beaked whales abundance predicted at a daily time step for different time periods. Individual years were predicted using contemporaneous models. "All years (mean)" averages the individual years, giving the mean annual abundance of the contemporaneous model. "Climatological" was predicted using the climatological model. The results for the climatological same segments model are not shown.

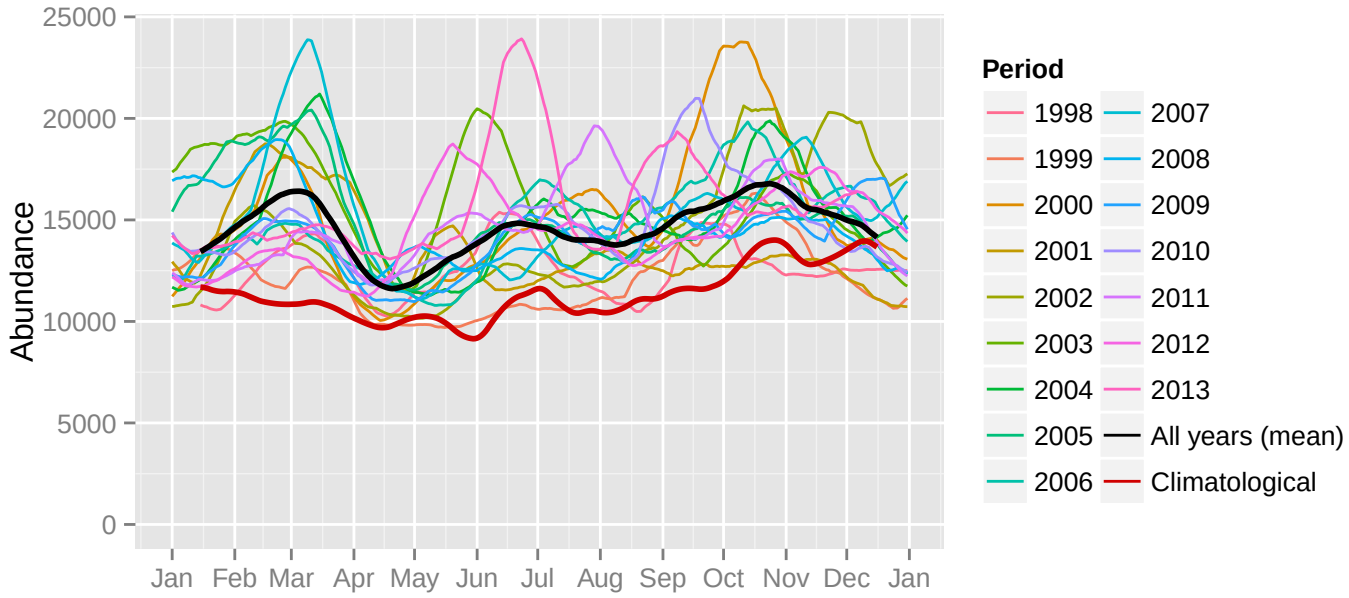

Figure 60: The same data as the preceding figure, but with a 30-day moving average applied.

Climatological Model

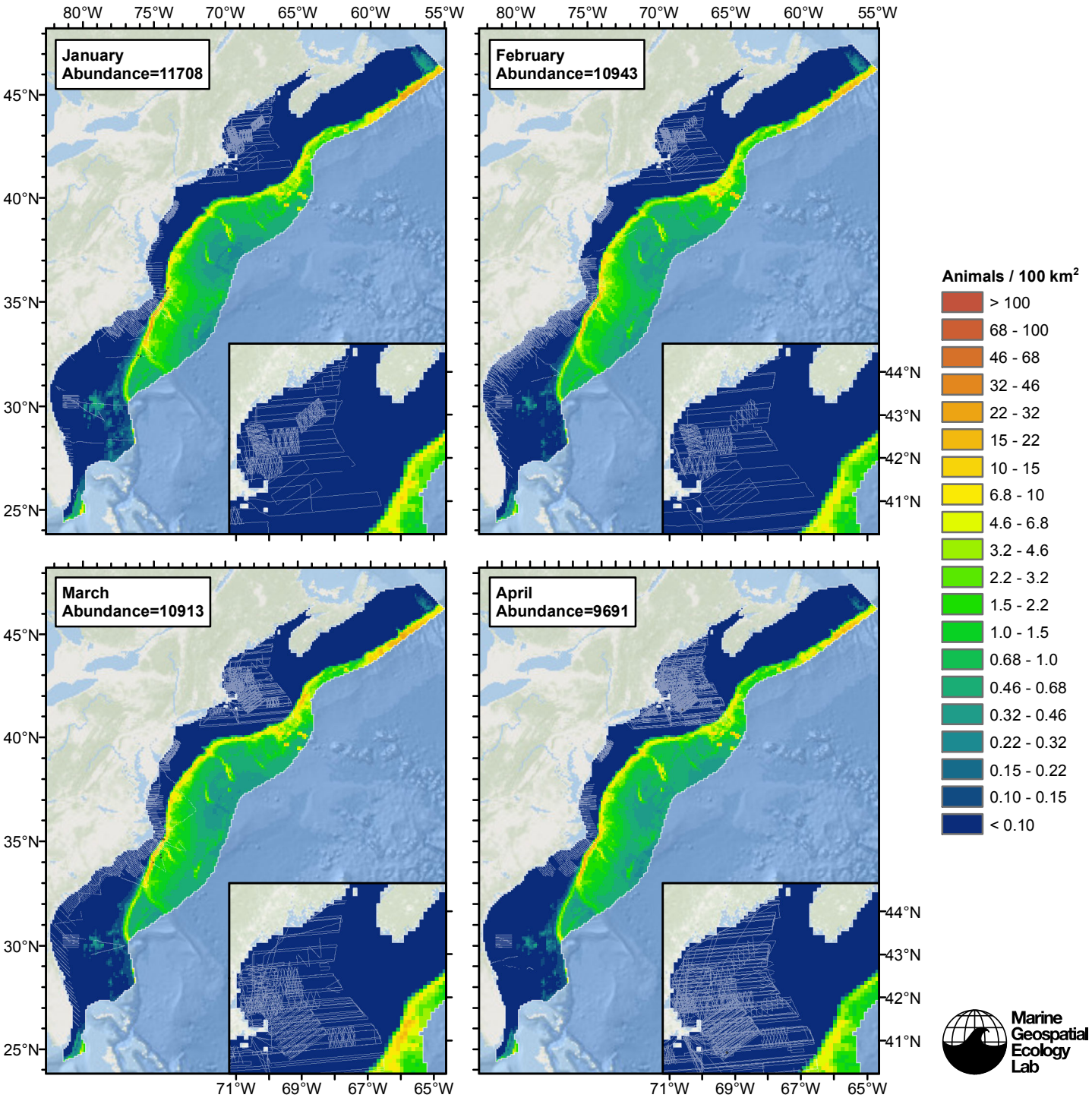

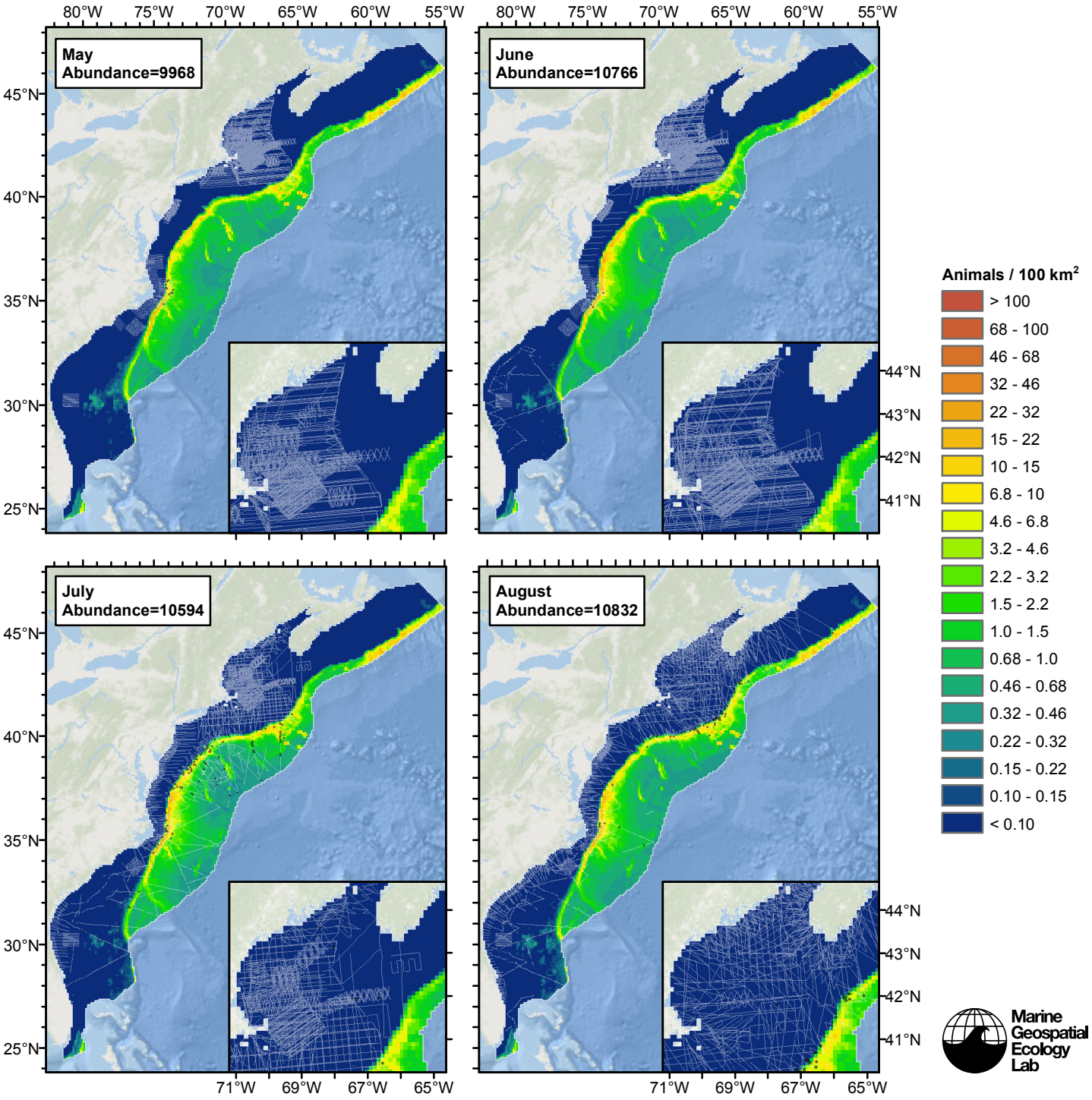
May
Abundance=9968
June
Abundance=10766
July
Abundance=10594
August
Abundance=10832
80°W
75°W
70°W
65°W
60°W
55°W
45°N
40°N
35°N
30°N
25°N
44°N
43°N
42°N
41°N
71°W
69°W
67°W
65°W
Animals / 100 km²
> 100
68 - 100
46 - 68
32 - 46
22 - 32
15 - 22
10 - 15
6.8 - 10
4.6 - 6.8
3.2 - 4.6
2.2 - 3.2
1.5 - 2.2
1.0 - 1.5
0.68 - 1.0
0.46 - 0.68
0.32 - 0.46
0.22 - 0.32
0.15 - 0.22
0.10 - 0.15
< 0.10
Marine
Geospatial
Ecology
Lab

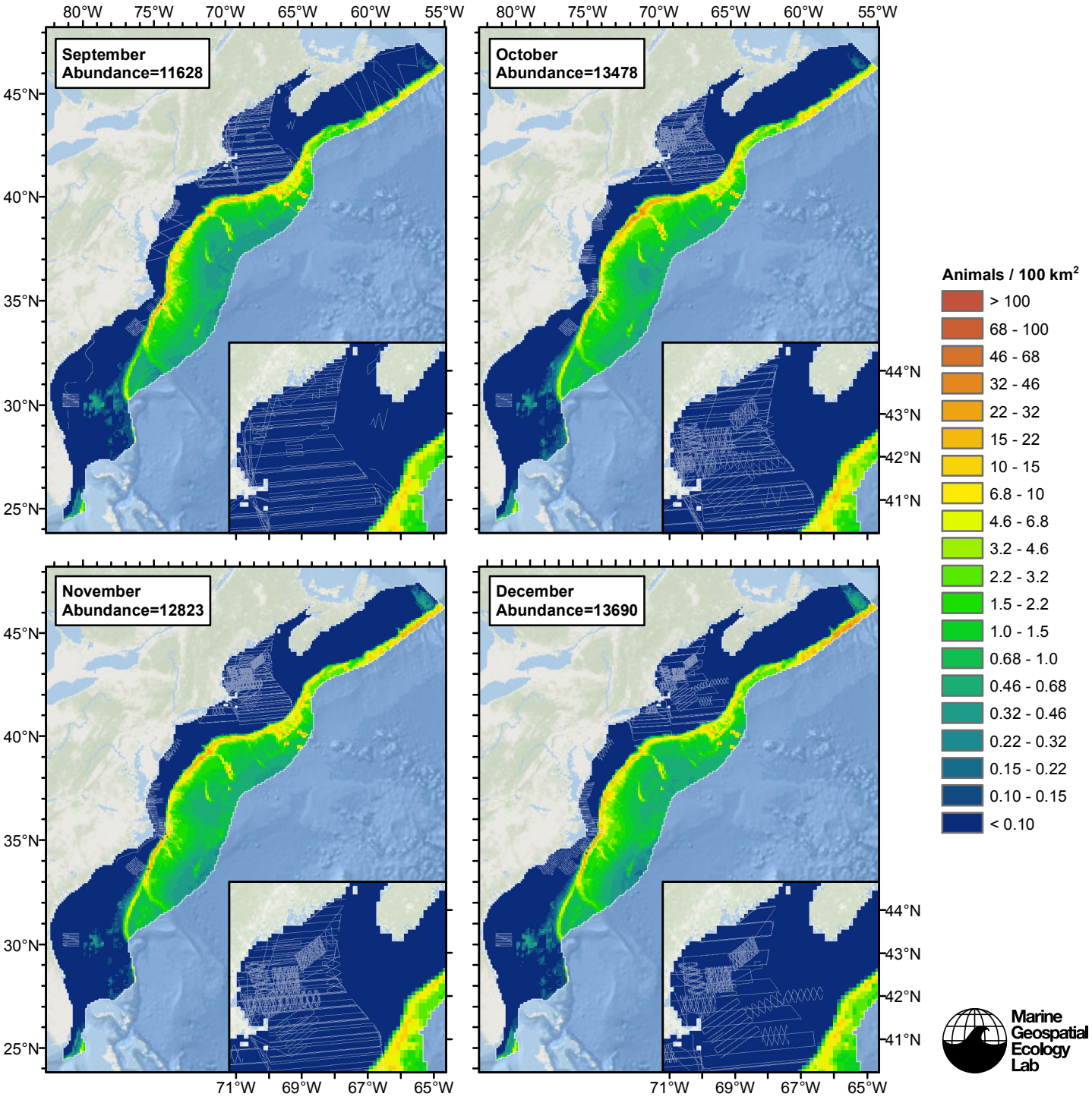
September
Abundance=11628
October
Abundance=13478
November
Abundance=12823
December
Abundance=13690
80°W
75°W
70°W
65°W
60°W
55°W
45°N
40°N
35°N
30°N
25°N
44°N
43°N
42°N
41°N
71°W
69°W
67°W
65°W
Animals / 100 km²
> 100
68 - 100
46 - 68
32 - 46
22 - 32
15 - 22
10 - 15
6.8 - 10
4.6 - 6.8
3.2 - 4.6
2.2 - 3.2
1.5 - 2.2
1.0 - 1.5
0.68 - 1.0
0.46 - 0.68
0.32 - 0.46
0.22 - 0.32
0.15 - 0.22
0.10 - 0.15
< 0.10
Marine
Geospatial
Ecology
Lab

Contemporaneous Model

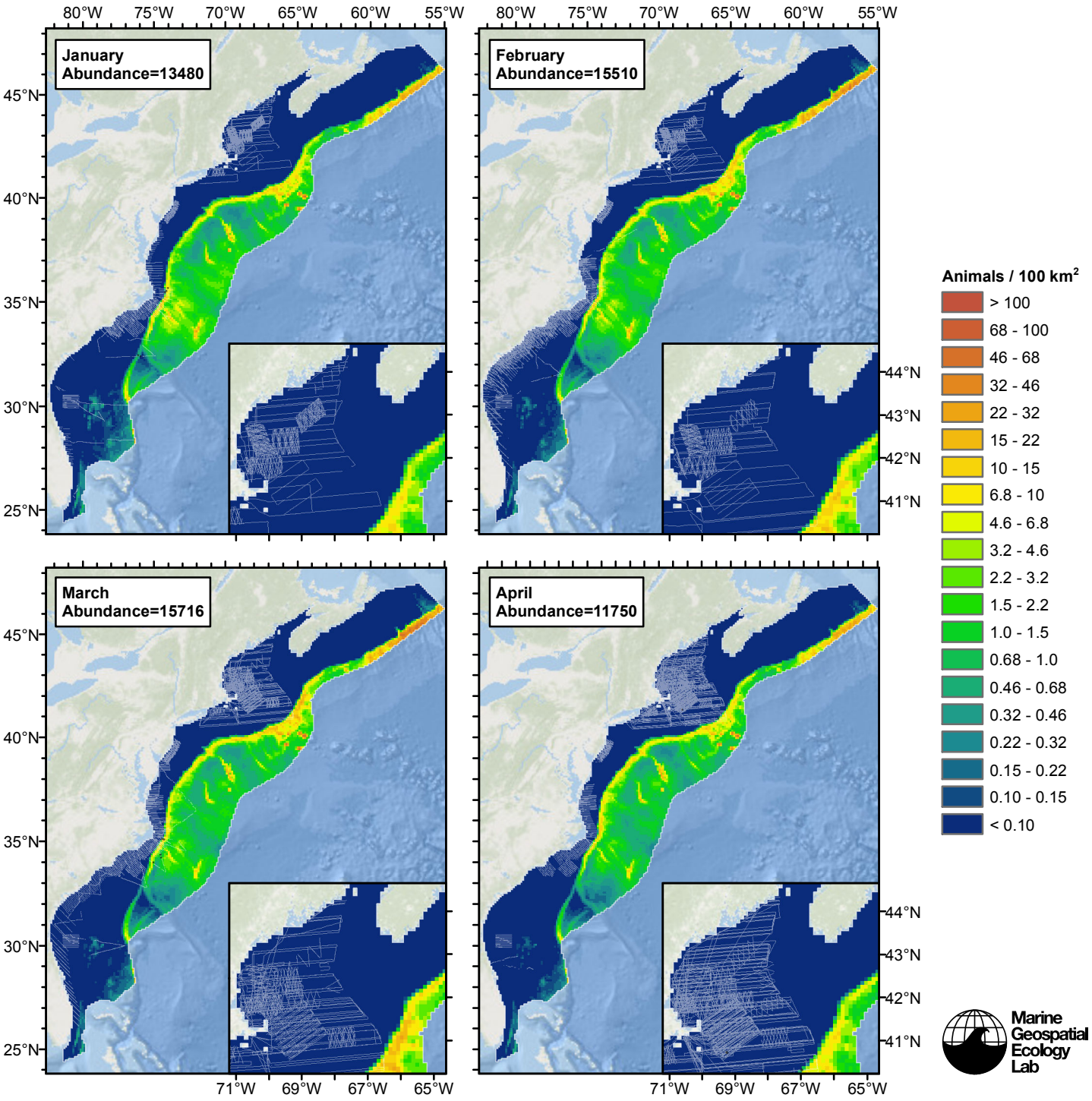

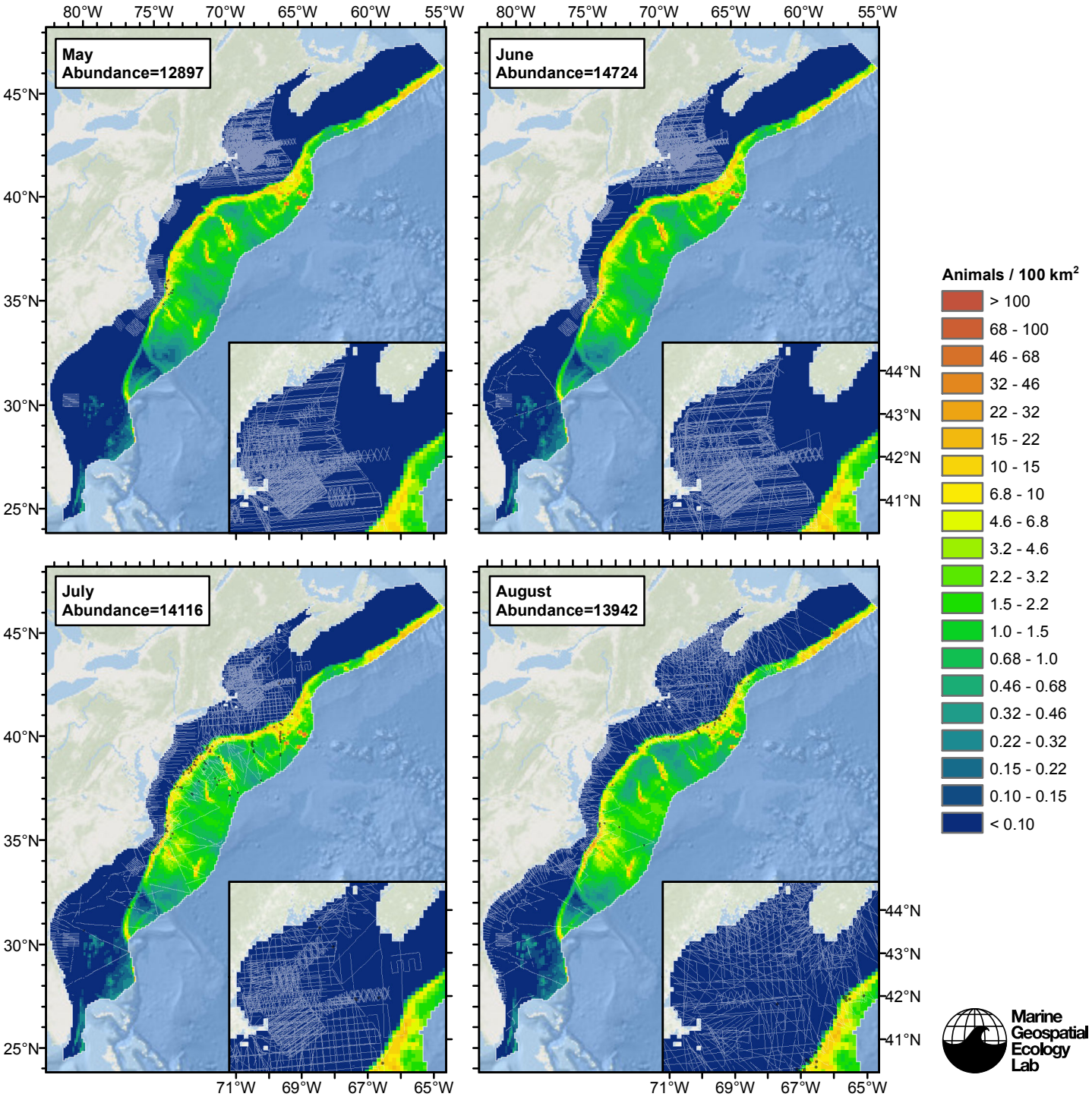
May
Abundance=12897
June
Abundance=14724
July
Abundance=14116
August
Abundance=13942
80°W
75°W
70°W
65°W
60°W
55°W
45°N
40°N
35°N
30°N
25°N
44°N
43°N
42°N
41°N
71°W
69°W
67°W
65°W
Animals / 100 km²
> 100
68 - 100
46 - 68
32 - 46
22 - 32
15 - 22
10 - 15
6.8 - 10
4.6 - 6.8
3.2 - 4.6
2.2 - 3.2
1.5 - 2.2
1.0 - 1.5
0.68 - 1.0
0.46 - 0.68
0.32 - 0.46
0.22 - 0.32
0.15 - 0.22
0.10 - 0.15
< 0.10
Marine
Geospatial
Ecology
Lab

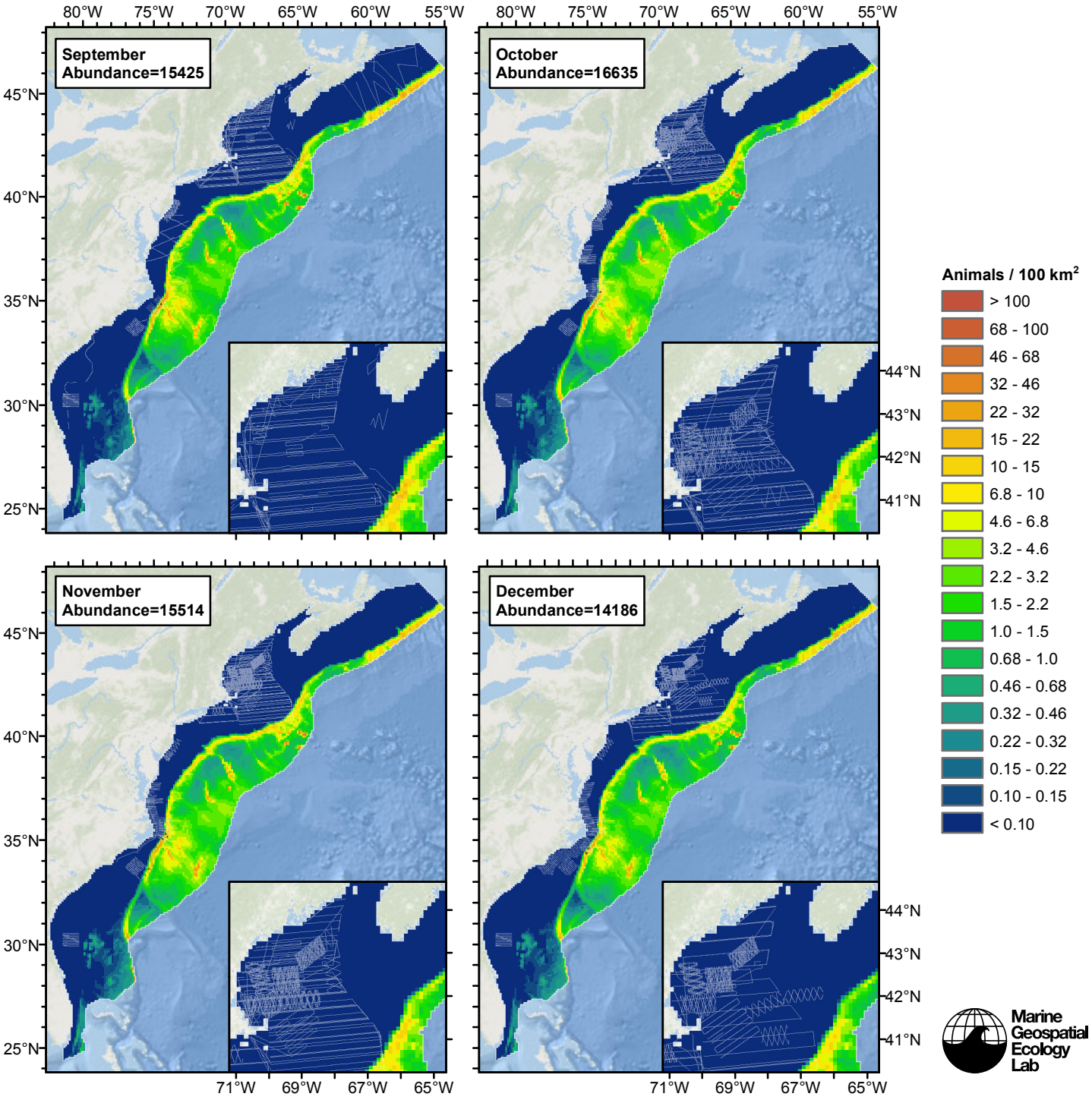
September
Abundance=15425
October
Abundance=16635
November
Abundance=15514
December
Abundance=14186
80°W
75°W
70°W
65°W
60°W
55°W
45°N
40°N
35°N
30°N
25°N
44°N
43°N
42°N
41°N
71°W
69°W
67°W
65°W
Animals / 100 km²
> 100
68 - 100
46 - 68
32 - 46
22 - 32
15 - 22
10 - 15
6.8 - 10
4.6 - 6.8
3.2 - 4.6
2.2 - 3.2
1.5 - 2.2
1.0 - 1.5
0.68 - 1.0
0.46 - 0.68
0.32 - 0.46
0.22 - 0.32
0.15 - 0.22
0.10 - 0.15
< 0.10
Marine
Geospatial
Ecology
Lab

Climatological Same Segments Model

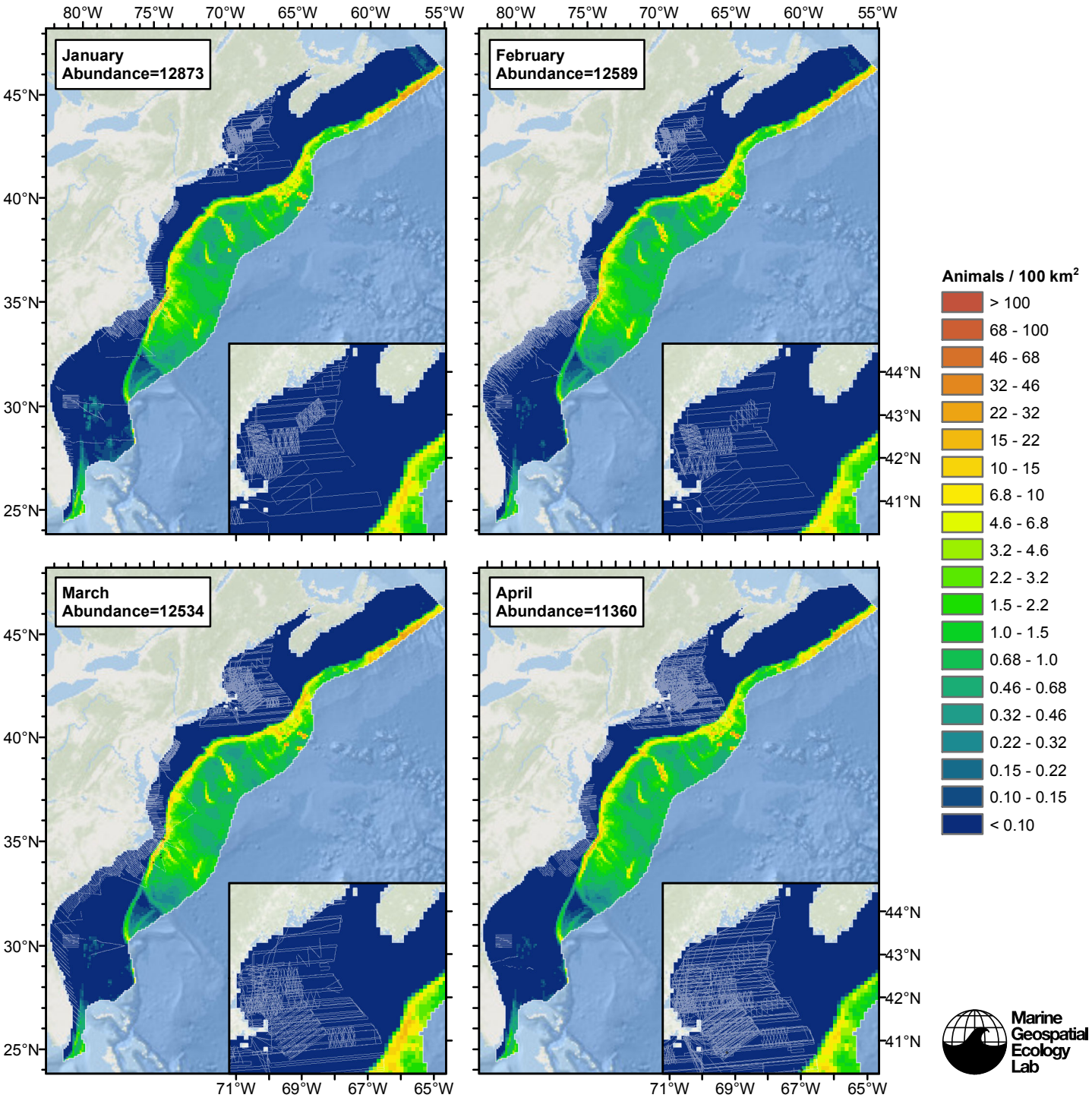

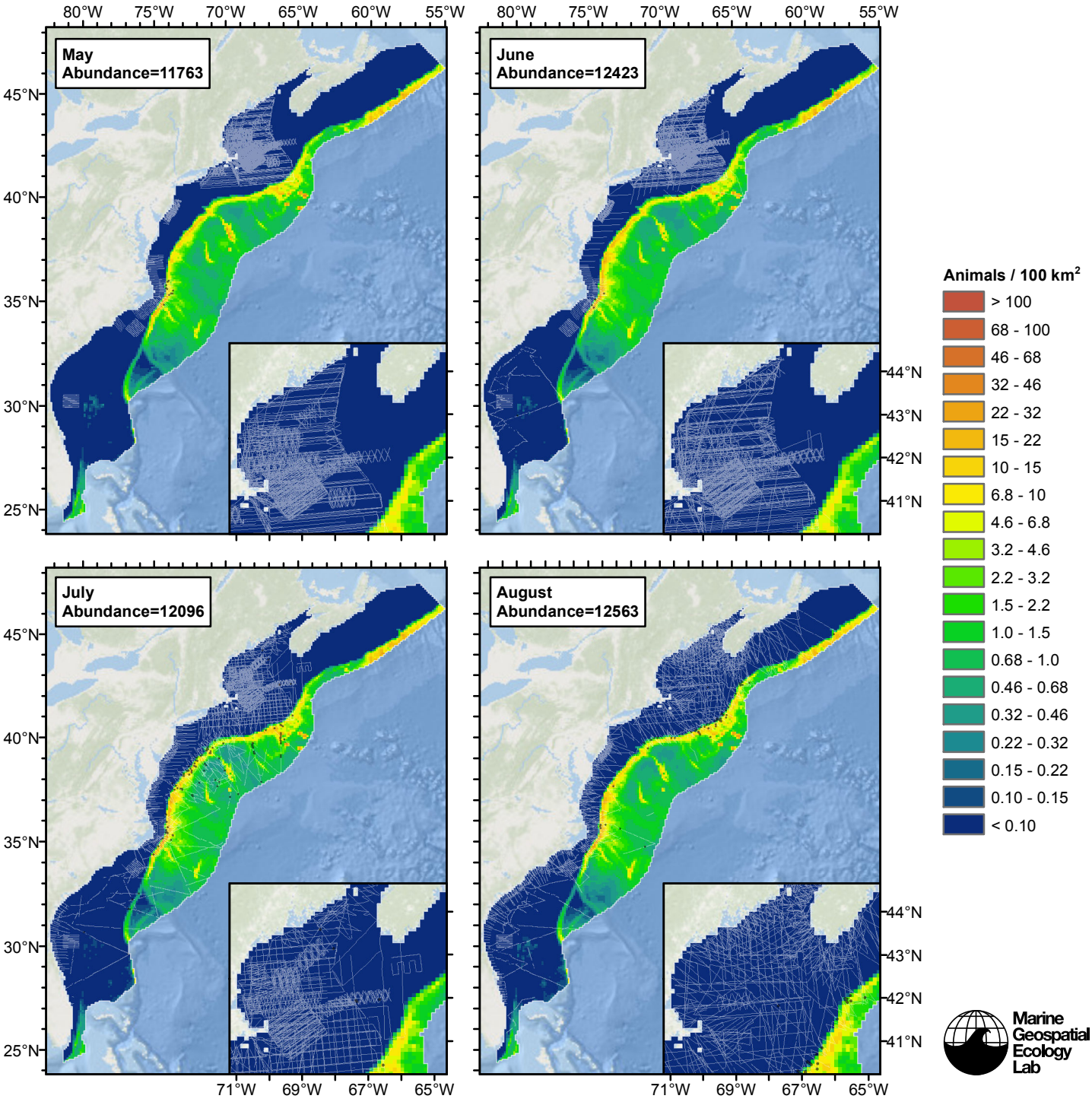
May
Abundance=11763
June
Abundance=12423
July
Abundance=12096
August
Abundance=12563
80°W
75°W
70°W
65°W
60°W
55°W
45°N
40°N
35°N
30°N
25°N
44°N
43°N
42°N
41°N
71°W
69°W
67°W
65°W
Animals / 100 km²
> 100
68 - 100
46 - 68
32 - 46
22 - 32
15 - 22
10 - 15
6.8 - 10
4.6 - 6.8
3.2 - 4.6
2.2 - 3.2
1.5 - 2.2
1.0 - 1.5
0.68 - 1.0
0.46 - 0.68
0.32 - 0.46
0.22 - 0.32
0.15 - 0.22
0.10 - 0.15
< 0.10
Marine
Geospatial
Ecology
Lab

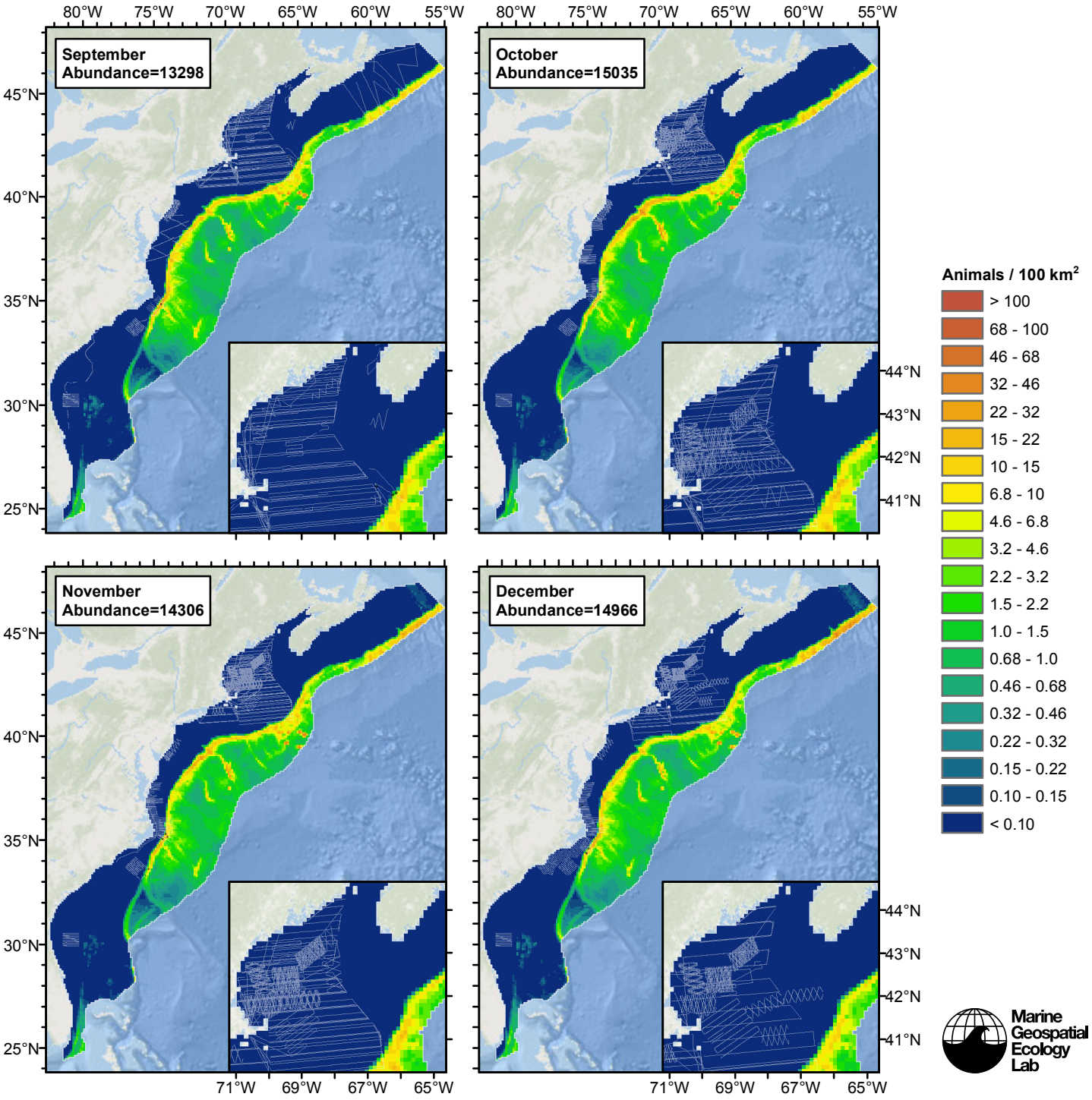

Discussion

Models built with contemporaneous predictors explained more deviance than models built with climatological predictors. On this basis, we selected the contemporaneous predictor model as our as our best estimate of beaked whale density and abundance.

When predicted at a short time step (see Temporal Variability section above) the model predicted relatively stable year-round abundance, compared to species that are known to undertake large seasonal migrations, such as baleen whales. Three of the four most important predictors (ranked by F-score) retained by the model selection procedure were physiographic (and thus static, unchanging with time), reflecting the affinity of these species for high-relief bathymetric features such as slopes, canyons, and escarpments (MacLeod and D'Amico 2006). Of the three dynamic predictors that were retained, two of of them, distance

to SST front and distance to anticyclonic eddy core, are related to mesoscale physical activity that does not exhibit as strong seasonal variability as predictors that are driven directly by solar activity, such as SST or primary productivity. The third dynamic predictor that was retained, primary productivity, does exhibit strong seasonal variability, but the model selection procedure retained a formulation of it that was heavily smoothed in the time dimension (a 90-day running cumulative sum). This heavy smoothing, as well as the fact that this predictor was ranked next to last in importance, limited its influence.

This result suggests that these species do not undertake large seasonal migrations, and our literature review did not yield any descriptions of seasonal movements for these species. We caution, however, that this species is found mainly in deep waters beyond the continental shelf break that have been surveyed relatively poorly except in summer. In light of the model's suggestion of non-seasonality and the lack of non-summer survey effort, we recommend that our year-round prediction of beaked whale density be utilized in management applications, rather than the monthly predictions.

Our total abundance estimate (14491) is relatively similar to NOAA's most recent estimate (13642, from June-August 2011, Central Florida to lower Bay of Fundy, combined, all species). However, it is important to note that our estimate accounted for availability bias, while NOAA's did not (Palka 2012), resulting in an underestimate. Simulation results suggest that the degree of underestimation may depend on diving behavior. Barlow (1999) estimated that if observers focused attention continually on the trackline, greatly reducing perception bias, the probability of detecting Mesoplodon species rose from 0.45 to 0.98, while for Ziphius cavirostris, it rose from 0.23 to 0.75. In Barlow's model, Mesoplodon spp. were assumed to undertake long dives lasting 20.4 min, while Z. cavirostris undertook long dives lasting 28.6 min, resulting in a reduced probability of detection. Palka (2012) modeled the abundance of Mesoplodon spp. and Z. cavirostris separately. Barlow's results suggest that availability bias might have produced a greater underestimation of abundance in Palka's Z. cavirostris model than Palka's Mesoplodon spp. model. In any case, to obtain results that are more directly comparable to Palka's, we hope to produce separate Mesoplodon spp. and Z. cavirostris models, once we are able to incorporate additional modern surveys for which observers produced definitive species identifications.

References

Baird RW, Webster DL, McSweeney DJ, Ligon AD, Schorr GS, Barlow J (2006) Diving behaviour of Cuvier's (Ziphius cavirostris) and Blainville's (Mesoplodon densirostris) beaked whales in Hawai'i. Can J Zool 84: 1120-1128.

Barlow J (1999) Trackline detection probability for long diving whales. In: Marine Mammal Survey and Assessment Methods (Garner GW, Amstrup SC, Laake JL, Manly BFJ, McDonald LL, Robertson DG, eds.). Balkema, Rotterdam, pp. 209-221.

Barlow J, Oliver CW, Jackson TD, Taylor BL (1988) Harbor Porpoise, Phocoena phocoena, Abundance Estimation for California, Oregon, and Washington: II. Aerial Surveys. Fishery Bulletin 86: 433-444.

Carretta JV, Lowry MS, Stinchcomb CE, Lynn MS, Cosgrove RE (2000) Distribution and abundance of marine mammals at San Clemente Island and surrounding offshore waters: results from aerial and ground surveys in 1998 and 1999. Administrative Report LJ-00-02, available from Southwest Fisheries Science Center, P.O. Box 271, La Jolla, CA USA 92038. 44 p.

MacLeod CD, D'Amico A (2006) A review of beaked whale behaviour and ecology in relation to assessing and mitigating impacts of anthropogenic noise. Journal of Cetacean Research and Management 7: 211-221.

Madsen PT, Aguilar de Soto N, Tyack PL, Johnson M (2014) Beaked whales. Current Biology 24: R728-R730.

Moors-Murphy HB (2014) Submarine canyons as important habitat for cetaceans, with special reference to the Gully: A review. Deep Sea Research Part II: Topical Studies in Oceanography 104: 6-19.

Palka DL (2006) Summer Abundance Estimates of Cetaceans in US North Atlantic Navy Operating Areas. US Dept Commer, Northeast Fish Sci Cent Ref Doc. 06-03: 41 p.

Palka DL (2012) Cetacean abundance estimates in US northwestern Atlantic Ocean waters from summer 2011 line transect survey. US Dept Commer, Northeast Fish Sci Cent Ref Doc. 12-29. 37 p.

Schorr GS, Falcone EA, Moretti DJ, Andrews RD (2014) First Long-Term Behavioral Records from Cuvier's Beaked Whales (Ziphius cavirostris) Reveal Record-Breaking Dives. PLoS ONE. 9: e92633.

Tyack PL, Johnson M, Soto NA, Sturlese A, Madsen PT (2006) Extreme diving of beaked whales. Journal of Experimental Biology 209: 4238-4253.

Waring GT, Josephson E, Fairfield CP, Maze-Foley K, ds. (2006) U.S. Atlantic and Gulf of Mexico Marine Mammal Stock Assessments – 2005. NOAA Tech Memo 194.

Waring GT, Josephson E, Maze-Foley K, Rosel PE, eds. (2013) U.S. Atlantic and Gulf of Mexico Marine Mammal Stock Assessments – 2012. NOAA Tech Memo NMFS NE 223; 419 p.

Waring GT, Josephson E, Maze-Foley K, Rosel PE, eds. (2014) U.S. Atlantic and Gulf of Mexico Marine Mammal Stock Assessments – 2013. NOAA Tech Memo NMFS NE 228; 464 p.